GROUP ON
EARTH OBSERVATIONS

Crafting geoinformation

The art and science of Earth observation

Crafting geoinformation

The art and science of Earth observation

GEO GROUP ON EARTH OBSERVATIONS

The Group on Earth Observations is coordinating efforts to build a Global Earth Observation System of Systems, or GEOSS. It was launched in response to calls for action by the 2002 World Summit on Sustainable Development and by the G8 (Group of Eight) leading industrialized countries. These high-level meetings recognized that international collaboration is essential for exploiting the growing potential of Earth observations to support decision making in an increasingly complex and environmentally stressed world.

GEO is a voluntary partnership of governments and international organizations. It provides a framework within which these partners can develop new projects and coordinate their strategies and investments. As of June 2010, GEO's members include 81 governments and the European Commission. In addition, 58 intergovernmental, international and regional organizations with a mandate in Earth observation or related issues have been recognized as participating organizations.

GEO is constructing GEOSS on the basis of a 10-year implementation plan for the period 2005 to 2015. The plan defines a vision statement for GEOSS, its purpose and scope, expected benefits, and the nine "Societal Benefit Areas" of disasters, health, energy, climate, water, weather, ecosystems, agriculture and biodiversity.

Cover photo: The EIGEN-CG01C geoid. The NASA/DLR GRACE mission (Gravity Recovery And Climate Experiment) provides highly accurate data on Earth's gravity field. Using these data, models such as this 'EIGEN-CG01C' geoid can be created. The geoid is a reference surface in the gravity field of Earth for the measurement and description of the planet's shape. The data come from both GRACE and the satellite CHAMP.

CONTENTS

Producing geoinformation is a science, and an art. Like every creative human endeavour, it requires a sense of purpose, plus fortitude, ingenuity, training and talent.

Forecasting next week's weather, next winter's snow cover, this year's global soy production, or long-term changes in forest cover all require an impressive combination of technology, hard work and expertise. The production chain for generating such forecasts and assessments, from the conception of an Earth monitoring instrument for gathering the necessary data to the final delivery of useful information, is a long one.

Compelling photos of the cloud-wreathed Earth from space, or highly processed, multi-coloured images of its surface, are familiar sights today. What people do not always realize is just how much work goes into making these observations available. Designing, building, launching, testing, processing and delivering data from an observation system takes a minimum of five years, often 10 years for space-based instruments. Even more time, technology, expertise and collaboration are required to transform these data into information products and services that can support decision making. This endeavour can be compared to making fine wine or preparing a great meal: although the diner rarely peeks into the kitchen to see how the ingredients are being assembled and processed, he can only enjoy the gourmet dishes and vintage bottles thanks to the intensive labour, technology, creativity and skills of highly trained teams.

This book is dedicated to the engineers, technicians, scientists, computer geeks and practitioners – the wine makers and chefs who are serving up the feast that is GEOSS, the Global Earth Observation System of Systems. They are the individuals standing behind the multitude of observation systems, models, computers and information services that are increasingly essential to helping humanity mitigate natural disasters and disease epidemics, predict severe weather events, sustainably manage natural resources and maintain our ecological balance.

Crafting geoinformation seeks to inspire greater appreciation of the art and science of Earth observation by taking the reader behind the scenes and revealing the secrets of the kitchen where geoinformation is made.

OBSERVING OUR PLANET

GEOSS interconnects the Earth observation systems that are owned and maintained by the member governments and participating organizations of the Group on Earth Observations (GEO). Investments in environmental monitoring and forecasting have now reached a critical mass, resulting in a vast and expanding array of observation systems. These include ocean buoys, meteorological stations and balloons, sonar and radar systems, seismic and Global Positioning System (GPS) stations, more than 60 high-tech environmental satellites and a large number of powerful computerized models. GEO seeks to make these systems fully interoperable and accessible.

Crafting geoinformation describes a small sample of the observing instruments and systems that monitor the Earth from space, the atmosphere, the oceans and the land. Each instrument provides a unique vantage point on some aspect of the Earth system; together, they offer a comprehensive picture of the planet.

Many of these instruments are arrayed in regional networks, while others are contained in global networks maintained by international partnerships. The examples given here are of radars for tracking rain, flux towers for measuring carbon dioxide levels, ocean buoys for monitoring currents and heat transport, and seismographs for recording earthquakes. Also featured are the high-powered drills used to obtain ice cores for reconstructing past climates.

In addition to these instruments based on or near the Earth's surface, more and more instruments are being flown by satellites. The ones described in this book are used to measure atmospheric levels of carbon dioxide and methane; to image the Earth's surface, topography and tectonic deformation; and to monitor the Earth's gravity field in order to gain insight into the thickness of the polar ice caps and changes in the subsurface water table.

To date, one of GEO's greatest accomplishments has been to advance the full and open sharing of Earth observation data. Several examples are offered that highlight the importance of such openness and collaboration. The concept of virtual constellations, whereby space agencies coordinate the missions and outputs of their satellites in order to compensate for the long time it takes individual instruments to revisit the same site, is illustrated by complementary images of central Beijing.

Lidars (LIght Detection And Ranging) have enormous potential for measuring forests, polar ice, clouds, aerosols, gases, wind and many other parameters. The need to track the ash cloud that Iceland's Eyjafjallajökull volcano emitted in early 2010, causing chaos for air travellers in Europe, provides a superb example of data sharing and collaboration.

One should not forget human observers with their pens and notebooks, perhaps the most sophisticated Earth observation instrument of all. The

Geo-Wiki project provides an innovative example of how the internet can be used to network people and ensure the *in situ* validation of remote observations; it invites individuals around the world to share their personal knowledge and observations to help validate regional and global land cover maps.

INFORMING DECISION MAKERS

The bulk of this book is dedicated to nine stories that picture GEOSS-based decision making in the nine GEO societal benefit areas, thus illustrating the range of highly topical issues that Earth observation helps to address. We have deliberately chosen not to provide the technical details of how each system works. Instead, the stories simply outline the process for gathering data and images, processing and combining them, and then presenting the resulting information to decision makers.

For example, earthquakes were big news in 2010. The days and weeks following the quake that struck Port-au-Prince in January 2010 revealed that the rapid provision of information was critical in enabling emergency responders to take rapid action.

The case study on meningitis epidemics in Africa provides further evidence of how collaboration amongst data providers and analysts from different communities – in this case health experts and climate researchers – can generate information and answers that can save human lives.

Also in 2010, observations from satellites, ocean vessels and other carriers were critical to the early and near-real time assessments of, and responses to, the Deepwater Horizon oil spill in the Gulf of Mexico.

The prediction of extreme weather events clearly requires rapid and collaborative efforts to gather and analyse observations. The case of

Typhoon Lupit, which threatened the Philippines in October 2009, confirms that space agencies, meteorological offices and analysts are well practised at sharing data and forecasts. Together they are now generating more accurate probabilistic forecasts to help communities anticipate and prepare for destructive storms.

Collaboration is also essential for predicting the availability of water resources for agriculture, energy and domestic use, as well as for forecasting the risk of floods and droughts. Such work requires the engagement of many different teams and systems for gathering wide-ranging data and analyses on a diverse range of variables, such as precipitation, soils and topography.

Yet another example looks at the provision of information on forest cover and, more importantly, deforestation rates. This is vital for estimating the capacity of forests to store carbon, preserve biodiversity and provide other ecosystem services.

Environmental information products are also valuable tools for making longer-term decisions. Examples of how information is generated to support biodiversity conservation planning in Africa, and of how mapping is used to evaluate global ecosystems, further demonstrate the power of Earth observation. An ambitious effort to build a comprehensive global monitoring system for agriculture and food security offers similar insights into the increasing potential of geoinformation to promote human well-being.

Crafting geoinformation concludes with a series of global images of the Earth that provide snapshots of the state of the planet in 2010. Some of the parameters shown do not change substantially over time. Other variables change continuously. These snapshots constitute a baseline against which we will be able to assess global change over the coming years and decades.

All of the stories featured here confirm the key message that capturing observations and producing information is a complex and challenging process. It requires heavy investment and long-term planning by governments and organizations, innovative design and construction by engineers and technicians, sophisticated modelling and analysis by scientists and experts, and the coordinated creativity and commitment of many individuals, institutions and governments. It is our hope that, after exploring this book, the reader will gain a better understanding of the value of Earth observation and the critical importance of sustaining our global monitoring and information systems.

José Achache
Secretariat Director
Group on Earth Observations

THE FOLLOWING AGENCIES AND ORGANIZATIONS ARE THE PROVIDERS OF THE INFORMATION SYSTEMS, SERVICES AND PRODUCTS DESCRIBED IN THIS BOOK

African Center of Meteorological Applications for Development (ACMAD)

Argo

AsiaFlux

BirdLife International

Brazil National Institute for Space Research (INPE)

China Center for Resources Satellite Data and Application (CRESDA)

China Meteorological Administration (CMA)

China National Space Administration (CNSA)

Chinese Academy of Sciences

Committee on Earth Observation Satellites (CEOS)

Consortium for Small-scale Modelling (COSMO)

Disaster Monitoring Constellation (DMC)

EARLINET

European Civil Protection

European Commission (EC)

European Commission Joint Research Centre (JRC)

European Centre for Medium-range Weather Forecasts (ECMWF)

European Space Agency (ESA)

e-GEOS

Famine Early Warning System Network (FEWS-NET)

FluxNet

Food and Agriculture Organization of the United Nations (FAO)

French Space Agency (CNES)

GeoEye

Geo-Wiki

German Aerospace Center (DLR)

German Weather Service (DWD)

Global Atmosphere Watch (GAW)

Global Biodiversity Information Facility (GBIF)

Global Monitoring for Environment and Security (GMES)

Global Runoff Data Centre (GRDC)

Global Seismographic Network (GSN)

Indian Space Research Organisation (ISRO)

International Charter for Space and Major Disasters

International Institute for Applied Systems Analysis (IIASA)

Meningitis Environmental Risk Information Technologies (MERIT) Project

Italian Space Agency (ASI)

Open Geospatial Consortium, Inc. (OGC)

Japan Aerospace Exploration Agency (JAXA)

OneGeology

Japan Meteorological Agency (JMA)

Regional Service of Image Treatment and Remote Sensing (SERTIT)

Japan Ministry of Economy, Trade and Industry (METI)

SarVision

Japan National Institute of Advanced Industrial Science and Technology (AIST)

South Africa Council for Scientific and Industrial Research (CSIR)

Japan National Institute of Informatics (NII)

UK Met Office

JapanFlux

United Nations Environment Programme World Conservation Monitoring Centre (UNEP-WCMC)

University of Maryland

US National Oceanic and Atmospheric Administration (NOAA)

University of Miami

Wageningen University

University of Tokyo

World Meteorological Organization (WMO)

UNAVCO

United Nations Institute for Training and Research (UNITAR)

US Department of Agriculture (USDA)

US Environmental Protection Agency (EPA)

US Geological Survey (USGS)

US National Aeronautics and Space Administration (NASA)

Information for
decision making
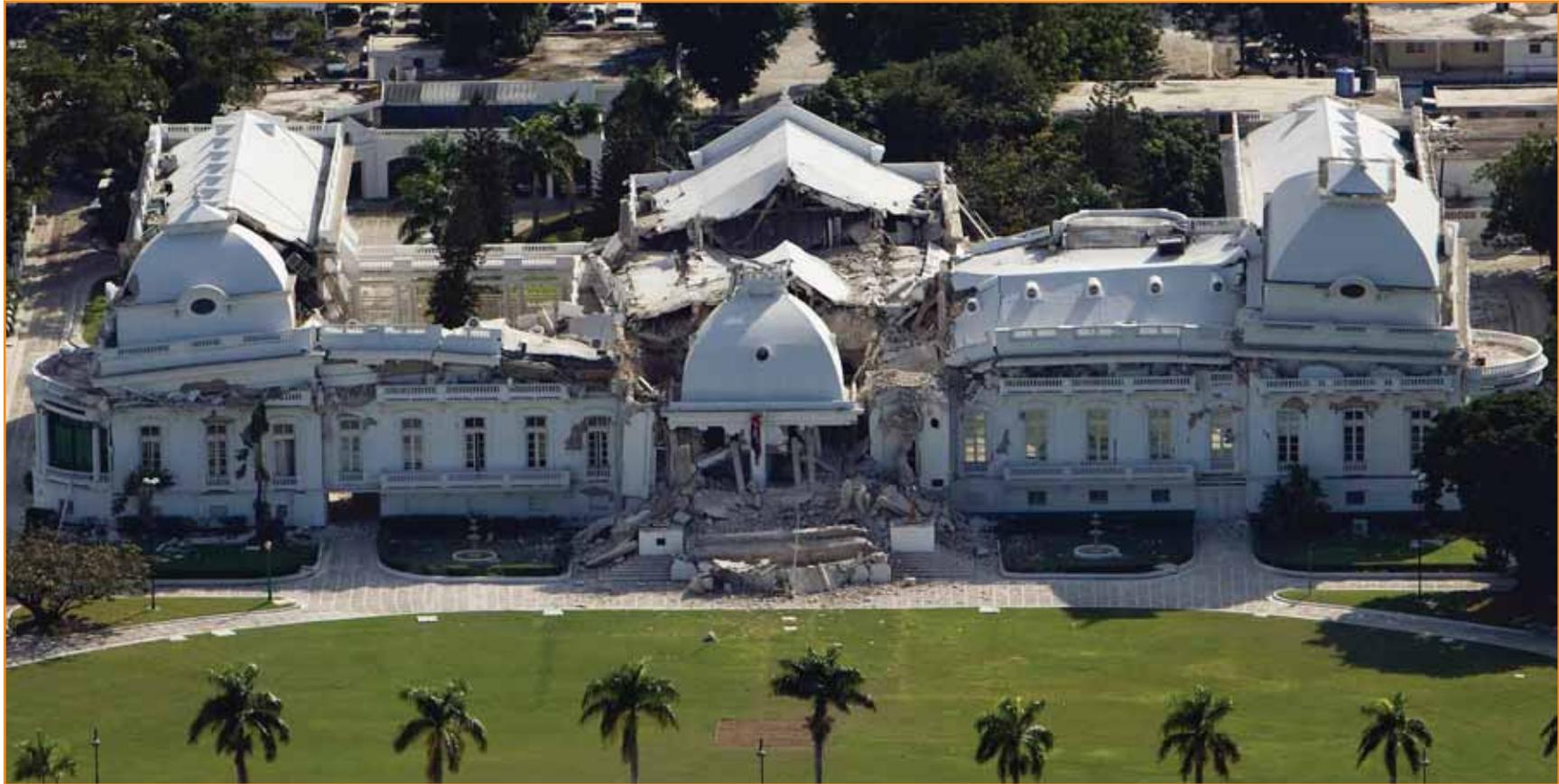
THE HAITI EARTHQUAKE

On 12 January 2010, a magnitude 7.0 earthquake struck the Haitian capital of Port-au-Prince, killing almost 250,000 people, injuring hundreds of thousands and leaving another million homeless. In the immediate wake of the disaster, the United Nations and various national emergency response agencies obtained satellite data via the International Charter on Space and Major Disasters. These satellite images were provided by Canada, China, France, Japan, the United States of America and the European Space Agency. Within 24 hours they were processed using up-to-date cartographic material to create situation maps for helping rescuers locate damaged areas and at-risk people.

In parallel, scientists benefited from the rapid availability of satellite images of the Haitian earthquake via the GEO Supersites web site. This allowed them to analyse the fault that caused the disaster, predict the potential for further seismic events, and provide advice to policy makers and relief teams.

Source: UNDP.

Haiti: before the earthquake

This multi-spectral image was captured by Landsat, a series of Earth observation satellites operated by the United States since 1973. Multi-spectral images consist of a limited number of specific wavelengths, including frequencies invisible to the human eye, that are particularly effective in revealing information about landforms. The clouds, distortions caused by the camera lens and other irregularities have been removed and corrected to process the present image. The epicentre (yellow star) and fault line (red line) have been added.

Source: COMET Centre for the Observation and
Modelling of Earthquakes, Volcanoes and Tectonics, UK.

Port-au-Prince

Enriquillo Fault

Port-au-Prince: 12 January 2010

This map uses various symbols and colours to indicate informal Internally Displaced Persons (IDP) sites as well as bridges and road obstacles using GeoEye-1 satellite imagery from 12 January. The Operational Satellite Applications Programme UNOSAT, hosted by the UN Institute for Training and Research (UNITAR), has produced several such post-earthquake maps of Haiti to illustrate damage assessments, pre- and post-disaster comparisons, and much more.

UPDATE 1: ANALYSIS SUMMARY WITHIN PORT-AU-PRINCE:

- 123 informal IDP shelters identified;
- 77 bridges and culverts were identified: four appeared to be partially damaged or blocked with building debris;
- 449 road obstacles were identified, almost all resulting from building debris; of this total 125 were severe, likely blocking all vehicle transport, and 231 were partial road obstructions, restricting vehicle access.

Legend:
- Airfield
- Port
- Bridge
- Culvert
- Foot bridge
- Primary road
- Secondary road
- Unpaved/minor road
- Railroad
- Likely informal IDP site
- Likely closed by debris
- Likely restricted by debris

Operational Analysis with GeoEYE-1 Data Acquired 13 January 2010 and QuickBird data aquired 4 March 2008

Map Data © 2009 Google

The depiction and use of boundaries, geographic names and related data shown here are not warranted to be error-free nor do they imply official endorsement or acceptance by the United Nations. UNOSAT is a program of the United Nations Institute for Training and Research (UNITAR), providing satellite imagery and related geographic information, research and analysis to UN humanitarian & development agencies & their implementing partners.

Source: UNITAR/UNOSAT.

Port-au-Prince: 13 January 2010

This map product classifies the level of building damage in each 250-metre grid on the basis of an expert visual interpretation of a satellite image acquired on 13 January.

Source: GeoEye.
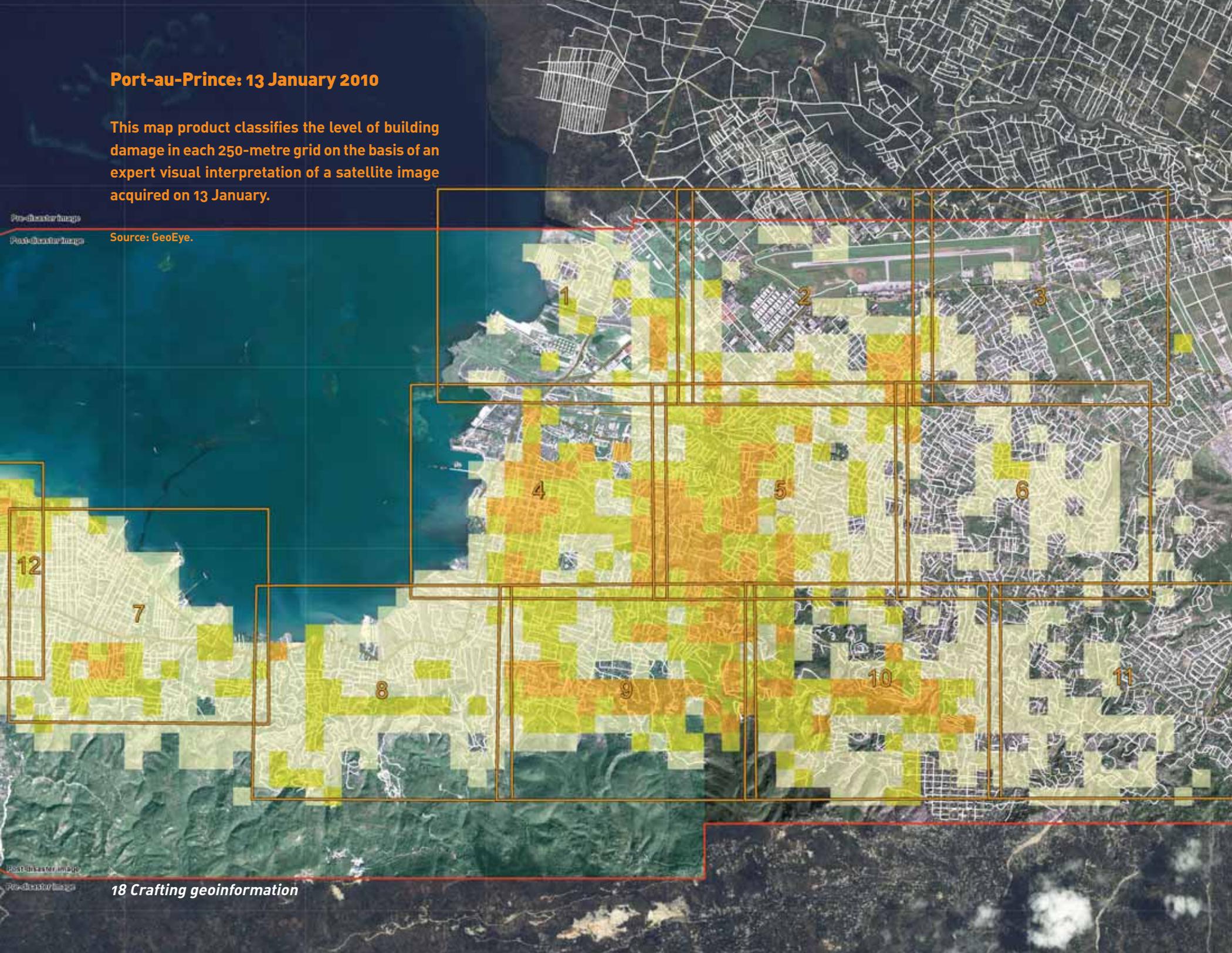
Port-au-Prince: recovery planning and reconstruction

A comprehensive atlas of damage caused in Haiti has been produced to help recovery planning and reconstruction measures. The maps, based on the comparison between pre-disaster satellite imagery and post-disaster aerial photos, provide an overview of building damage in the main affected cities. They reveal that almost 60,000 buildings were destroyed or very heavily damaged, including a number of critical infrastructures such as government premises, educational buildings and hospitals.

Information for decision making: disasters 19

Port-au-Prince: 48 hours on

The first radar satellite high-resolution images available for Port-au-Prince were dated 14 January, only 48 hours after the event. Using these images along with reference images acquired during previous campaigns, it was possible to rapidly assess the effects of the earthquake on the affected area. The ILU (Interferometric Land Use modified) map of the Port-au-Prince area produced by the Italian Space Agency using COSMO-Skymed images reports areas where there is a big difference in the back-scattering between the pre- and the post-event images (red elements), highlighting the zones more affected by the quake.

Source: ASI/COSMO-Skymed.

Developing elevation maps

Digital Elevation Models use optical and radar space observations to map the elevation and contours of the Earth's surface, highlighting features such as mountains and rivers. They are used for a wide range of purposes, such as creating relief maps, modelling water flow to anticipate flooding impacts, predicting landslides and planning new infrastructure. In this image, the long horizontal line is the earthquake's fault line; Port-au-Prince and its harbour can be seen just above.

Source: NASA Shuttle Radar Topography Mission (SRTM).
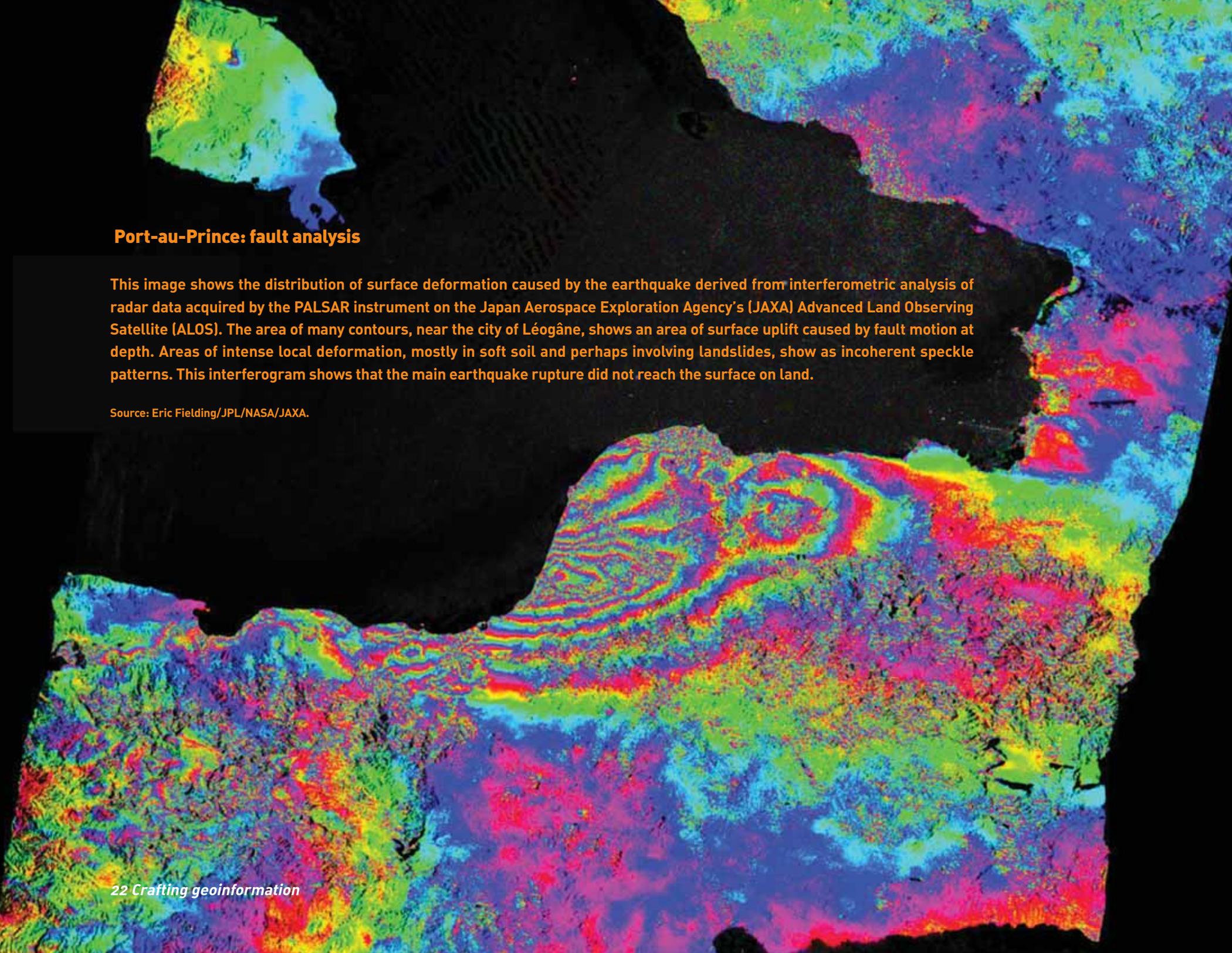
Port-au-Prince: fault analysis

This image shows the distribution of surface deformation caused by the earthquake derived from interferometric analysis of radar data acquired by the PALSAR instrument on the Japan Aerospace Exploration Agency's (JAXA) Advanced Land Observing Satellite (ALOS). The area of many contours, near the city of Léogâne, shows an area of surface uplift caused by fault motion at depth. Areas of intense local deformation, mostly in soft soil and perhaps involving landslides, show as incoherent speckle patterns. This interferogram shows that the main earthquake rupture did not reach the surface on land.

Source: Eric Fielding/JPL/NASA/JAXA.

20 cm →

GONAVE PLATE

Port-au-Prince

Enriquillo fault

USGS CMT

Harvard CMT

■ GPS site

○ Aftershocks (USGS/NEIC)

CARIBBEAN PLATE

m

0.0   0.5   1.0   1.5   2.0   2.5   3.0   3.5   4.0   4.5   5.0

Slip distribution from A. Sladen (Caltech)

cm

-11.8   0.0   11.8

Range change
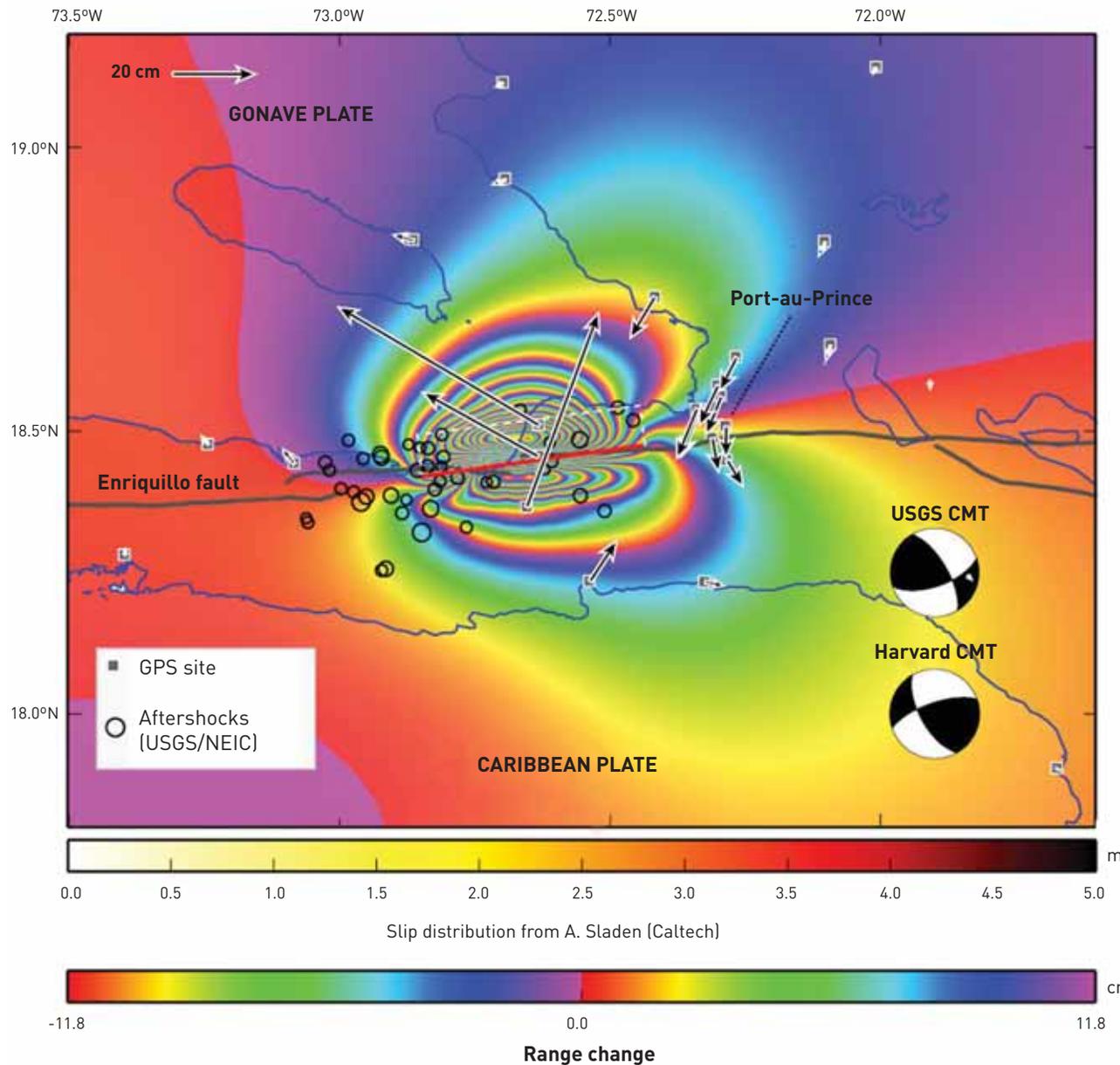
Fault analysis

To model the potential for future earthquakes, researchers simulated the coseismic ground motion based on the finite fault model of Caltech. Black arrows show expected displacements at Global Positioning System (GPS) sites, while the background colour shows interferometric fringes.

Through an iterative process, a model is built and then gradually improved until it corresponds more fully with observations (including both aps and interferometric analysis of radar images). The model is a vital aid for understanding and predicting the probability of future shocks.

Fault analysis

In this image scientists have sought to model the redistribution of stress along the fault line resulting from the earthquake.

The model reveals that the greatest area of concern for a large triggered shock is immediately to the east of the 12 January 2010 rupture of the Enriquillo fault, where stress is calculated to have risen. Typically, stress increases of this magnitude are associated with aftershocks (white dots). The next most likely site for a subsequent fault rupture lies to the west of the 12 January rupture where, interestingly, aftershocks are observed.
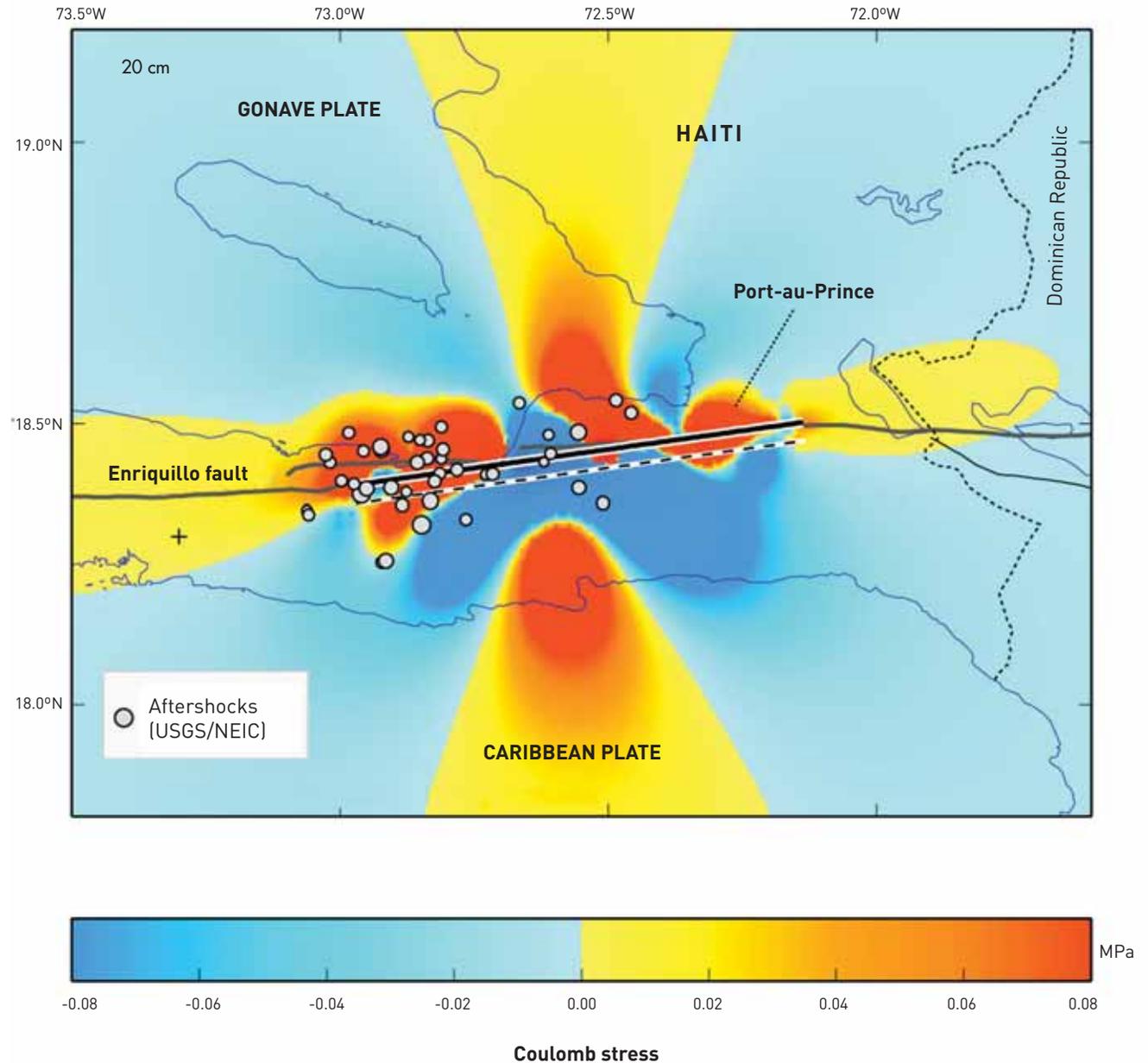
Source: E. Calais, Purdue University.
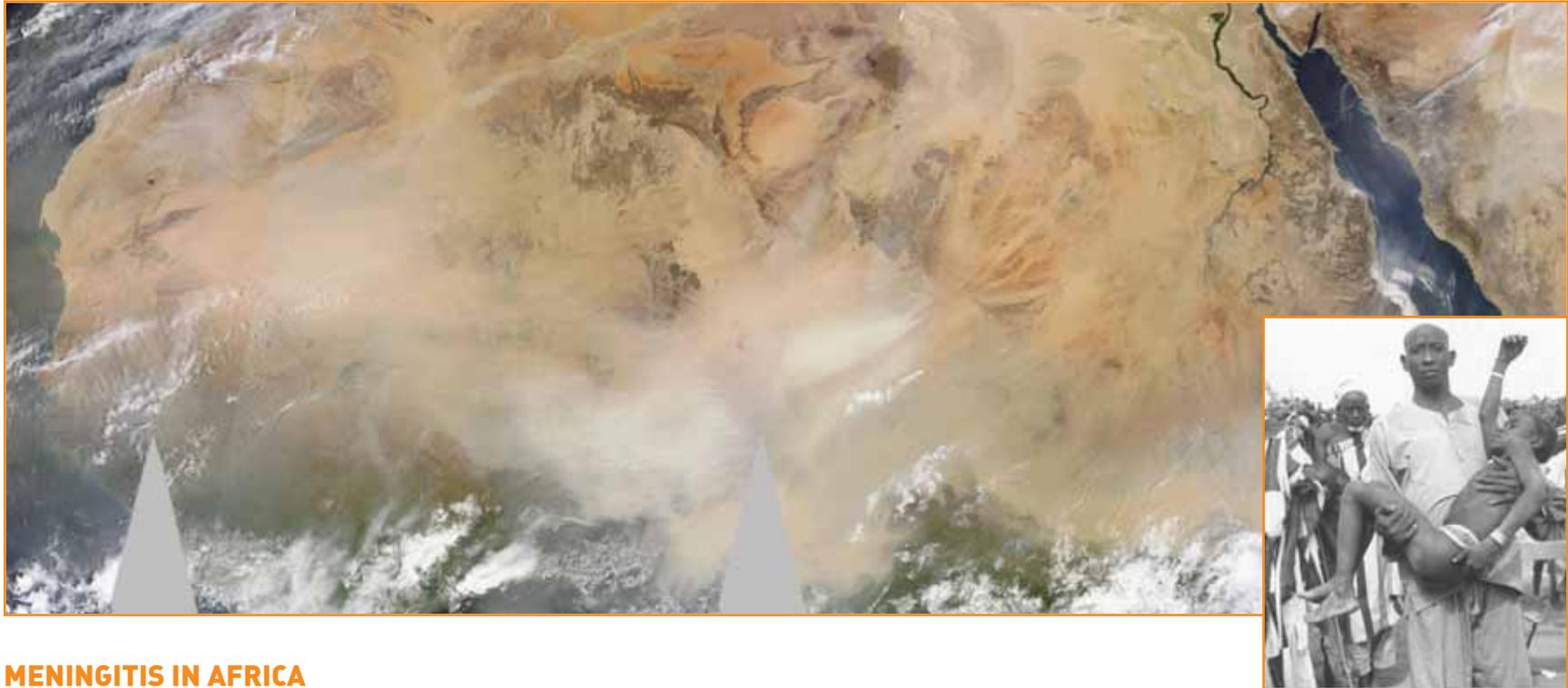
MENINGITIS IN AFRICA

Many different factors have been known to contribute to disease outbreaks, and over the past several years the health sector has increasingly recognized that the environment may be one of the factors for climate-sensitive illnesses. The Meningitis Environmental Risk Information Technologies (MERIT) project illustrates how the health and climate communities are cooperating to support decision making. MERIT is demonstrating how combining data, information and models on demographics, health resources, past outbreaks, vaccination campaigns, environmental changes and other variables can support public-health interventions. The decision by the World Health Organization and the other MERIT partners to model meningitis disease outbreaks is a step towards developing an early warning system. It is hoped that they will help to guide the implementation of a new vaccine campaign under way in 2010.

The main image above is of a massive dust storm sweeping across the southern Sahara Desert on 19 March 2010. This image is made up of seven separate satellite overpasses acquired by the Moderate Resolution Imaging Spectroradiometer (MODIS) on NASA's Terra and Aqua satellites throughout the morning and early afternoon. Grey triangles indicate areas where the satellites did not collect data. The image spans more than 10,000 kilometres (6,000 miles). The smaller picture shows a meningitis victim.

Source (main image): MODIS Rapid Response Team at NASA GSFC; (inset) WHO.

Aerosols in the atmosphere

Suspended particles in the atmosphere known as aerosols can affect weather and climate as well as people. This diagram of the global distribution of atmospheric aerosols shows that dust from Northern Africa and Asia is a major component of the atmosphere over much of the world.

The map was generated by combining data from six satellites operating for limited periods between 1979 and 2004; the data were validated using ground-based observations. The blue box over Africa highlights the approximate location of the meningitis belt, home to 350 million people. The very dry air and high levels of suspended dust particles observed during the meningitis season are thought to be among the factors leading to disease outbreaks.

Aerosol optical depth
(a measurement of particle density in the air)

0.0

0.2

0.4

0.6

Meningitis belt

Source: Kinne, S., "Remote sensing data combinations-superior global maps for aerosol optical depth" in *Satellite Aerosol Remote Sensing Over Land,* A. Kokhanovsky and G. de Leeuw eds., Springer, 2009.

Humidity

Specific humidity Jan-Feb 2008
(kg/kg)
0.008
0.001
Source: NASA GLDAS.

Meningitis outbreaks 2008

Mali
Niger
Chad
Burkina Faso
Guinea
Côte d'Ivoire
Benin
Togo
Ghana
Nigeria
Central African Rep.
Cameroon
Ethiopia
Dem. Rep. of Congo

☐ Country

Attack rate
☐ No data
▦ Acceptable
☐ Reached the alarm threshold
☐ Reached the epidemic threshold

©Multi Disease Surveillance Centre (MD SC)/
World Health Organization/African Region
Source: Ministries of Health

These two sets of paired map images represent (left) specific humidity data for January-February gathered by the NASA Global Land Data Assimilation System (GLDAS) and (right) cumulative meningitis attack rates during the first 39 weeks of 2008 (above) and 2009 (below). Note the strong correlation between the dark blue areas in the humidity maps and the red and yellow areas in the meningitis outbreak maps.

Specific humidity Jan-Feb 2009
(kg/kg)
0.008
0.001
Source: NASA GLDAS.

Meningitis outbreaks 2009

Mali
Niger
Chad
Burkina Faso
Guinea
Côte d'Ivoire
Benin
Togo
Ghana
Nigeria
Central African Rep.
Cameroon
Ethiopia
Dem. Rep. of Congo

☐ Country

Attack rate
☐ No data
▦ Acceptable
☐ Reached the alarm threshold
☐ Reached the epidemic threshold

©Multi Disease Surveillance Centre (MD SC)/
World Health Organization/African Region
Source: Ministries of Health

Information for decision making: health 27

Wind direction

The Inter-Tropical Discontinuity, or ITD, is the demarcation line between the dry and dusty north/northeasterly winds from the Sahara and the moist and humid south/southwesterly winds from the ocean. It moves gradually northwards from its extreme southern position in January to its extreme northern position in August, and southwards again from late August to early January. The ITD's position during the year influences disease risk. When areas to its north experience the dry and dusty Harmattan winds, meningitis and acute respiratory diseases tend to increase.

Source: ACMAD.

ITD DEKAD 1 March 2010 MEAN: 07-10 FORECAST
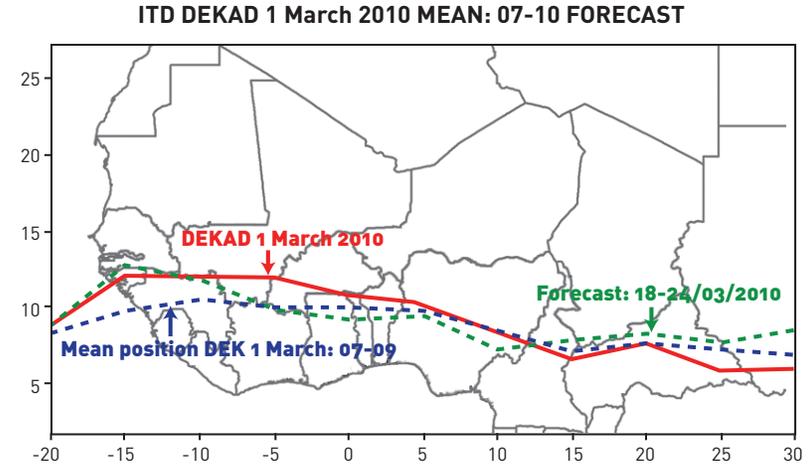
Population density

In order to incorporate demographic risk factors as predictors when modelling epidemic outbreaks, demographic information about relevant population aspects (such as counts, density, distribution, and age and sex structure) is combined with climate data. The result is frequently presented in raster format (a grid of pixels or points). The Center for International Earth Science Information Network (CIESIN) uses their Gridded Population of the World (GPW) version 3 and Global Rural Urban Mapping Project (GRUMP) global population surfaces to integrate demographic data with remote-sensing products.

Source: CIESIN.

Predicted probability of meningitis epidemics

- Very high risk (p >= 0.80)
- High risk (0.60 <= p < 0.80)
- Moderate risk (0.40 <= p < 0.60)
- Low risk (p < 0.40)
- No data

Population density (people per km²)

High: 140,000

Low: 0

500 km
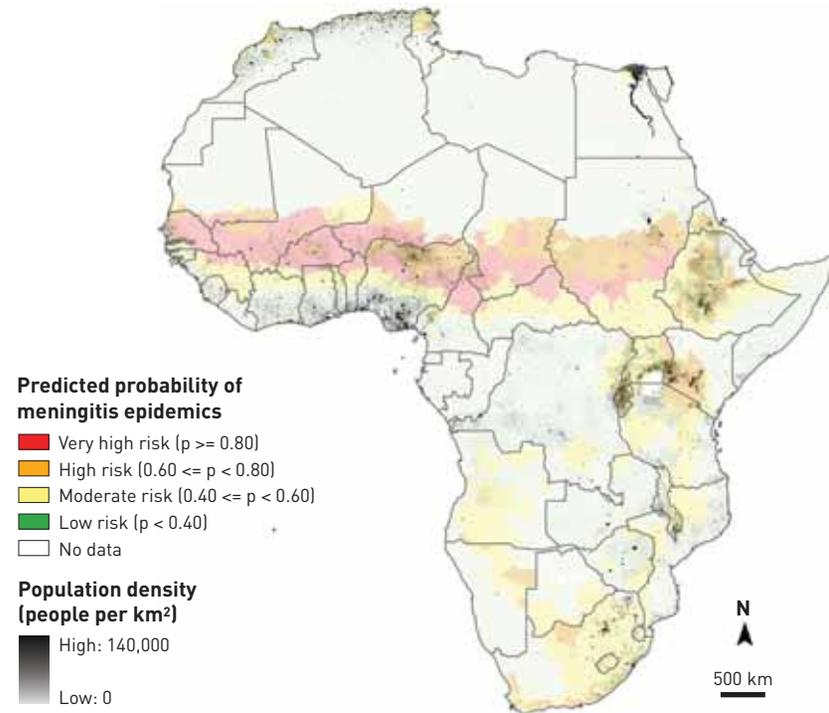
Precipitation, pressure and dust concentration

**BSC-DREAM8b 12h acc. Precipitation and MSL pressure
12h forecast for 00z 22 MAR 10**

Source: BSC.

Forecasts of sand and dust and basic meteorological variables for periods of 10 days are currently being made available to health practitioners. While such Earth observation-based information products cannot yet be used operationally, they do help increase the health community's understanding of, and sensitivity to, the role of the environment in disease outbreaks.

**BSC-DREAM8b Lowest model level dust conc. (ug / m~3)
12h forecast for 00z 22 MAR 10**

Source: BSC.

Meningitis Environmental Risk Information Technologies is a partnership of international organizations led by the World Health Organization in collaboration with governments, academia and the private sector. MERIT website: http://merit.hc-foundation.org/

Contributors to this section include the World Health Organization; International Research Institute for Climate and Society, Columbia University; Center for International Earth Science Information Network, Columbia University; Health and Climate Foundation; African Centre of Meteorological Applications for Development; World Meteorological Organization; Barcelona Supercomputing Center (BSC); and US National Aeronautics and Space Administration (NASA) Goddard Institute for Space Studies.

THE DEEPWATER HORIZON OIL SPILL

On 20 April 2010, an explosion occurred on the semi-submersible offshore drilling rig Deepwater Horizon in the Gulf of Mexico. In the weeks that followed, approximately 35,000-60,000 barrels (5,600-9,500 cubic metres) of crude oil a day leaked into the Gulf.

From day one, US agencies such as the National Oceanic and Atmospheric Administration, the US Geological Survey and the National Aeronautics and Space Administration used Earth observations from satellites, aeroplanes, ships, underwater gliders and scientists on the ground and on the water to track every aspect of the spill. These data were used to derive information and forecasting products that proved invaluable for emergency response teams, coastal communities, wildlife managers and many others affected by the spill.

Source: US Coast Guard.

Mississippi Delta: 24 May 2010

The Moderate-Resolution Imaging Spectro-radiometer (MODIS) on NASA's Terra satellite captured this image of sunlight illuminating the lingering oil slick off the Mississippi Delta on 24 May. Oil smoothes the ocean surface, making the oil slick appear brighter than the surrounding water in some places (image centre) and darker in others (lower right). A small, dark plume along the edge of the slick, not far from the original location of the Deepwater Horizon rig, indicates a possible controlled burn of oil on the ocean surface.

Source: NASA.

Information for decision making: energy 31

Tracking surface oil

Gulfport Mobile Pensacola

New Orleans

★ Deepwater Horizon

Tampa

Miami

NOAA's Satellite Analysis Branch obtained data from a variety of high-resolution visible and synthetic aperture radar satellites from NOAA's Earth observation partners to document the latest extent of the surface oil (in red). Satellite data used in this daily analysis include NASA's Aqua and Terra MODIS, the Canadian Space Agency's RADARSAT-1 and -2 SAR, the Italian Space Agency's COSMO-SkyMed, the German Aerospace Center's TerraSAR-X, the Japan Aerospace Exploration Agency's Advanced Land Observing Satellite, Satellite Imaging Corporation's SPOT-5, the Disaster Monitoring Constellation's multispectral imagery and the European Space Agency's ENVISAT SAR.

Source: NOAA.

Surface ocean currents

Surface current forecast for 8pm EDT Friday 14 May 2010

Surface horizontal current (m/s)
120-hour forecast
valid 00Z 15 May 2010

Strong current headed towards Texas

Spill location

Loop current

Max. 2.11 at 29.3°N 75.1°W
Min: 0.00 at 17.1°N 76.5°W
NCEP/EMC/MMAB 10 May 2010

Surface horizontal current (m/s)

Source: NOAA.

Space-based and *in situ* observations of weather, ocean currents and the state of the sea are vital for crafting the forecasts and information products needed for decision making.

Trajectory mapping

This forecast of the spill's future trajectory is based on the US National Weather Service spot forecast from the morning of 12 May. Currents were obtained from several models (NOAA Gulf of Mexico, West Florida Shelf/USF, Texas A&M/TGLO, NAVO/NRL) and High Frequency Resistance (HFR) measurements. The model was initialized from a combination of satellite imagery analysis (NOAA/NESDIS) and overflight observations.

**Trajectory Forecast
Mississippi Canyon 252**

NOAA/NOS/OR&R
Estimate for: 0600 CDT, Thursday, 5/13/10
Date Prepared: 1300 CDT, Wednesday, 5/12/10

Forecast location for oil on 13 May 10 at 0600 CDT

Mississippi Canyon 252 Incident Location

Winds are forecast to be persistently from the SE throughout the week. These moderately-strong onshore winds (up to 15 kts) have the potential to move new oil onshore. The Mississippi Delta, Breton Sound, the Chandeleur Islands and areas directly north have a potential for shoreline contacts throughout the forecast period. Oil observed to the west of the Delta offshore of Timbalier Bay could threaten shorelines as far west as Atchafalaya Bay by Thursday.

Trajectory
☐ Uncertainty
■ Light
■ Medium
■ Heavy
✕ Potential beached oil

This scale bar shows the meaning of the distribution at the current time.

Next Forecast: May 13 AM

Source: NOAA.

Tropical storm

- High tide + surge + waves (yellow)
- High tide + surge (orange)
- High tide (dark red)
- Elevations not affected (grey)

Grand Isle

N

Kilometres
0   1   2

Miles
0   1   2

Developing scenarios

As the oil moved towards the coast, there was a clear potential for deposition on sandy beaches and in marshes. Weather scenarios were used as an input for making inundation and overwash predictions. These scenarios were based on recent and forecasted weather patterns, as well as larger events that could be expected based on historical records. For each scenario, representative values for tide, wave height, wave period and surge were obtained from NOAA models. The total water level, including wave runup, was compared to Lidar elevation data collected by USGS and the Joint Airborne Lidar Bathymetry Technical Center of Expertise (JALBTCX) to identify barrier-island locations where oil was most likely to be transported and deposited.

Source: USGS.

Providing information to local communities

The dynamic nature of the Deep-water Horizon oil spill was a challenge for local communities, from hotel operators and fishermen to local community leaders.

GeoPlatform.gov established a customizable and interactive map providing near real-time information about the response effort (http://www.geoplatform.gov/gulf response). Developed by NOAA with the US Environmental Protection Agency, the US Coast Guard and the US Department of Interior, the site integrates the latest data the US federal responders have about the oil spill's trajectory. It also features information on fishery area closures and sightings of sea turtles (dead or alive) and other wildlife.

Source: NOAA.
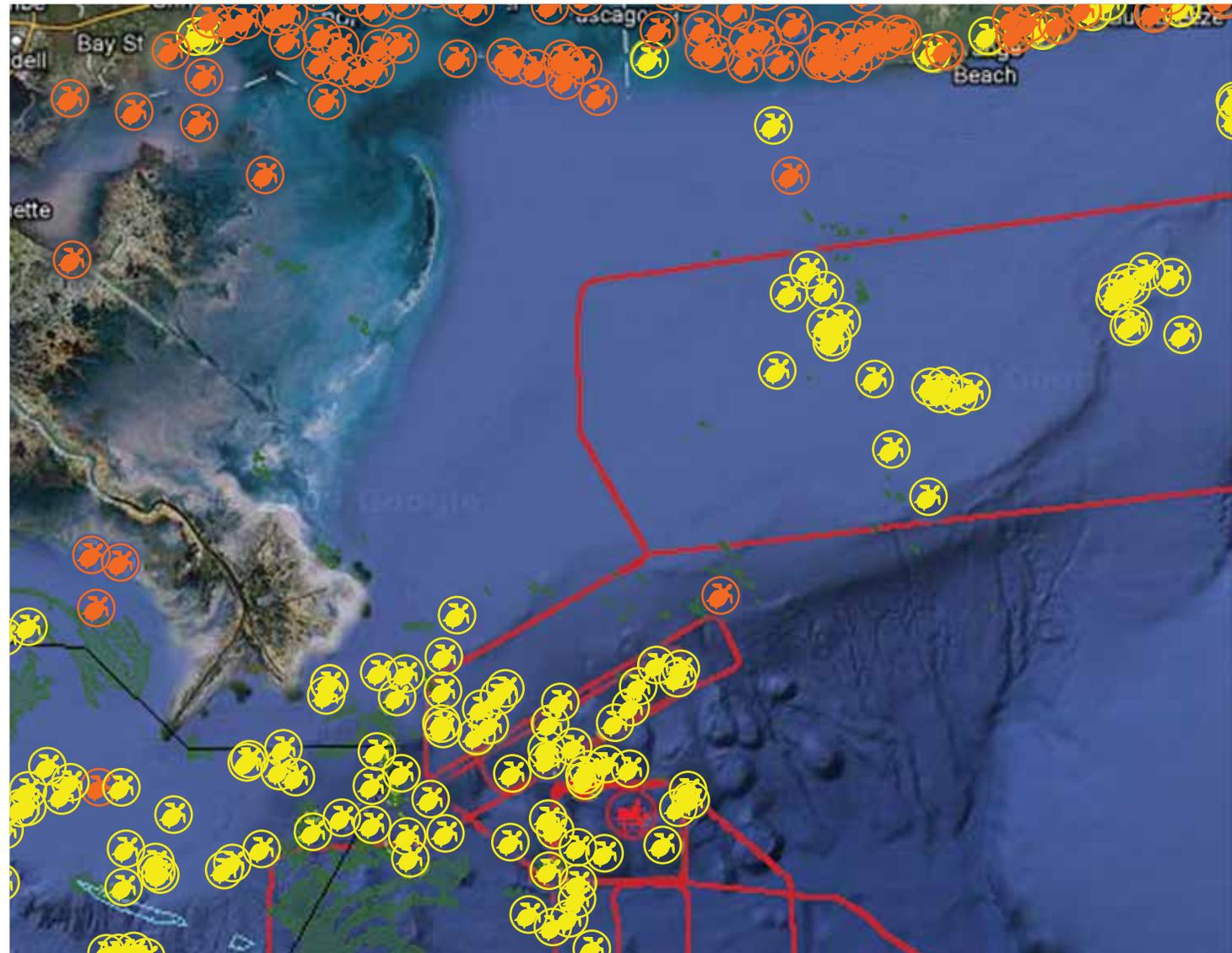
FORESTS AND CARBON

Forests play a vital role in regulating climate, storing carbon and providing many other ecosystem services. Policy makers and managers therefore need timely information on changes in the extent and density of the world's forests. This information can be provided by combining optical and radar data from satellites with on-the-ground observations.

Coordinating data

June 1975

Monitoring trends in forest cover requires obtaining data periodically over many years.

    These optical images of deforestation in Rondonia, Brazil were taken from the US's Landsat satellite over a period of 26 years.

Source: USGS-Landsat.

July 1989

September 2001

Trained observers take *in situ* measurements to provide "ground truth" in order to validate and calibrate satellite measurements. They typically record tree diameter and height; species composition (trees, crops and other plants); soil and water quality; and indicators of land degradation. Sample observations taken from each unit of a regular grid make it possible to extrapolate the results to the entire forest or region.

Using satellite radar sensors ...

A time series of processed images showing the removal of a Malaysian mangrove forest over several years. These images were taken from an L-band radar sensor on Japan's Advanced Land Observing Satellite (ALOS). Radar has the advantage of being able to penetrate clouds as well as the nighttime dark.

Source: JAXA/METI.

2006

2008

2010

... to monitor mangrove clearance

The three previous images have been combined into this composite image. The different colours represent the years in which the forest was cut.

Source: JAXA/METI.

Scenes acquired
June-September 2009

173	Landsat
507	ALOS PALSAR
161	Radarsat 2
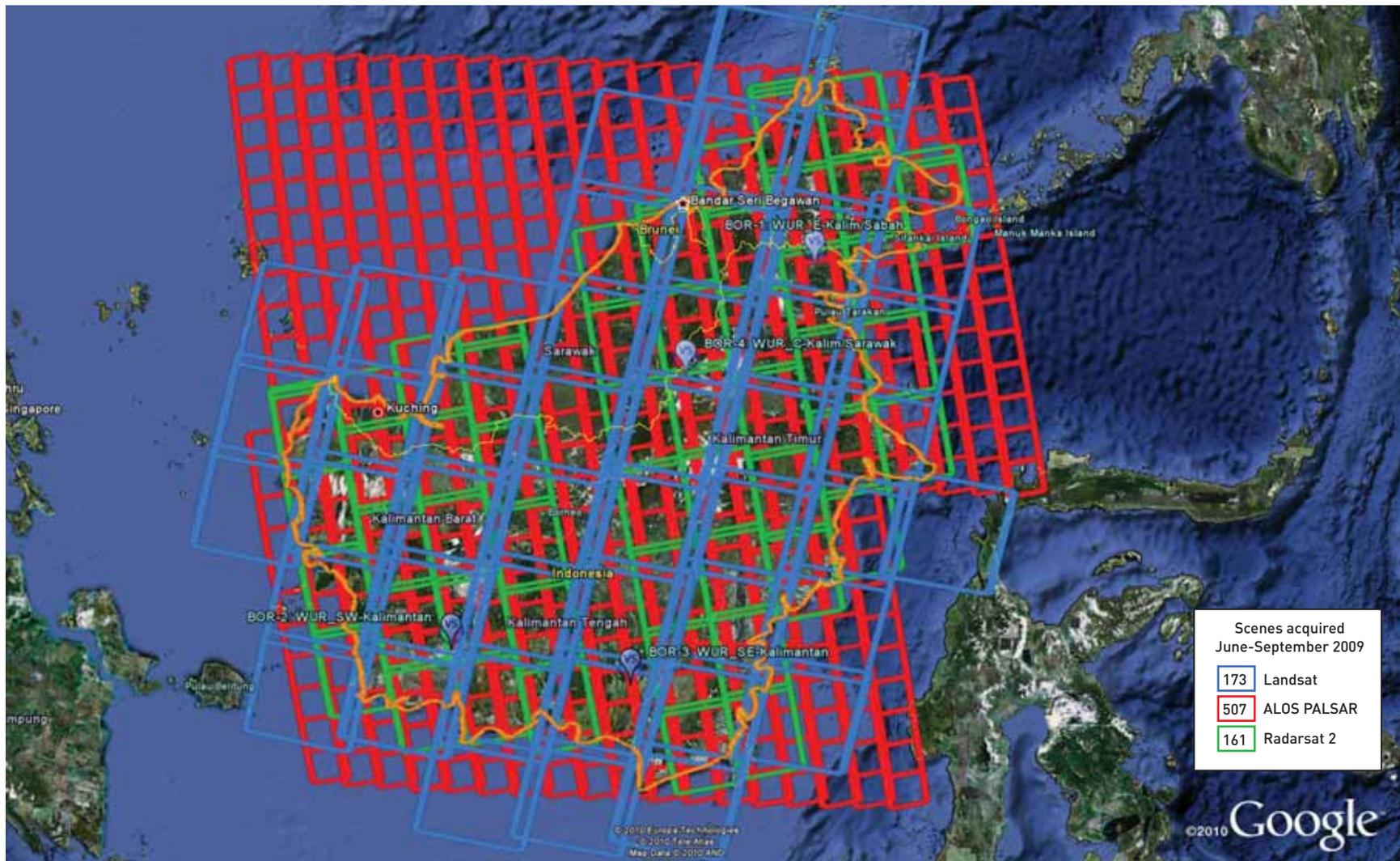
Combining multiple images over Borneo

By coordinating data acquisition from various satellite missions, it is possible to ensure that forests are monitored consistently by a variety of radar and optical sensors. Filling gaps in coverage, establishing baselines and building time series from regular observations are essential for tracking changes.

42 Crafting geoinformation

Legend:
- Tropical lowland forest
- Tropical mountain forest
- Riverine forest
- Swamp forest
- Mangrove forest
- Nipah mangrove forest
- Peat swamp (pole) forest
- Peat swamp (padang) forest
- Riverine shrubland
- Forest mosaics/fragmented or degraded forest
- High shrub
- Medium shrub
- Ferns/grass
- Grassland
- Cropland (upland)
- Cropland (irrigated)
- Plantations
- Tree cover, burnt
- Water body
- No data

Land cover and land use

Time series of processed images are combined to produce information in the form of a map of land cover and land use. The accuracy of the classifications listed in the legend is improved by using complementary data from different sensors. The map is validated using *in situ* and airborne observations as well as very high resolution satellite data.

Land cover and land use

The Amazon Deforestation Monitoring Program (PRODES) of Brazil's National Institute for Space Research (INPE) is an operational system for monitoring forest change. It provides yearly forest/non-forest maps based on regular satellite and *in situ* observations in order to identify the incremental deforestation occurring over time.


Source: INPE.

▦ Deforestation 1997	▦ Deforestation 2003	▦ Deforestation 2007	▦ Residual
▦ Deforestation 2000	▦ Deforestation 2004	▦ Deforestation 2008	▦ Not observed
▦ Deforestation 2001	▦ Deforestation 2005	▦ Non forest	▦ Hydrography
▦ Deforestation 2002	▦ Deforestation 2006	▦ Forest	▦ Clouds
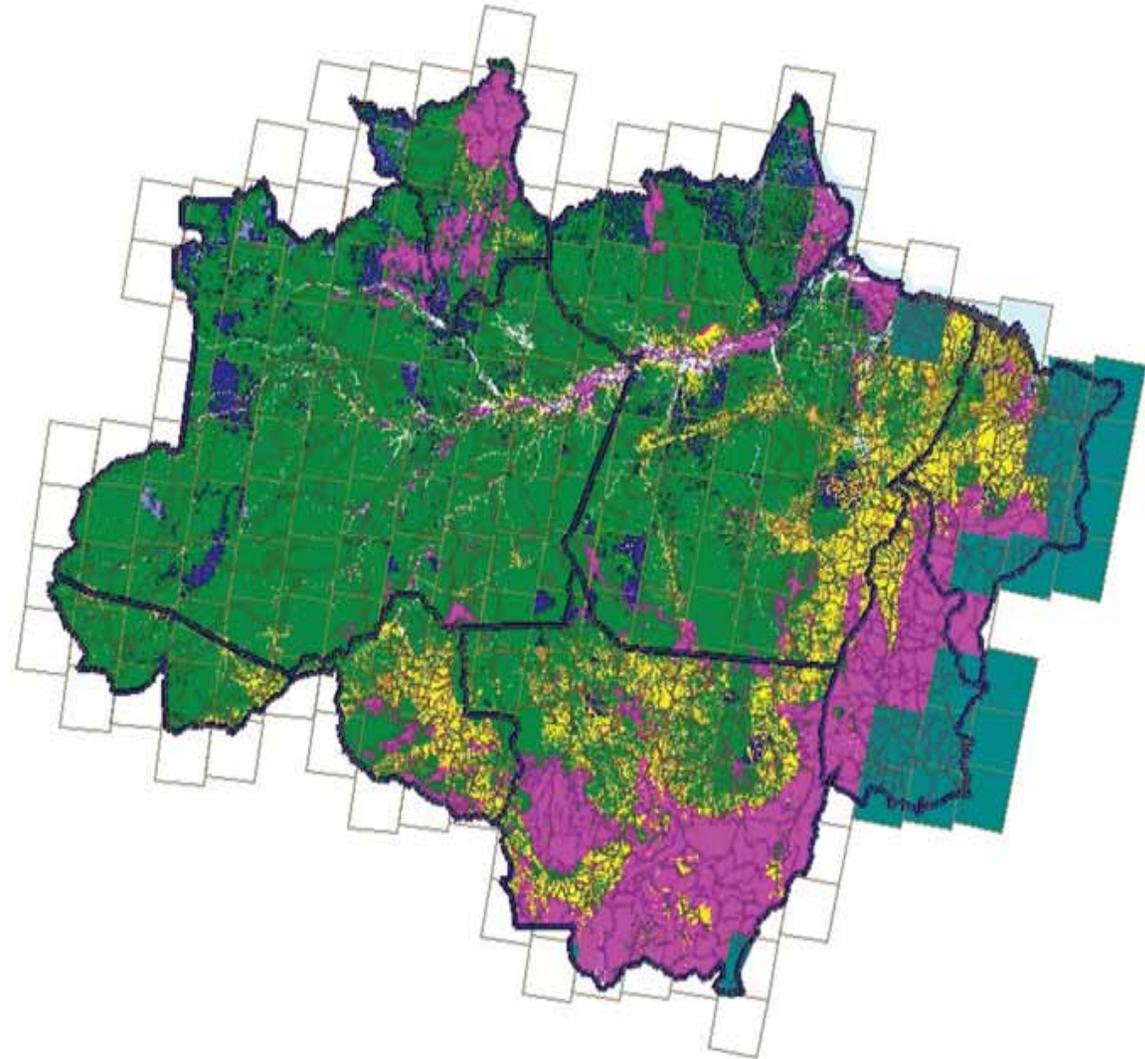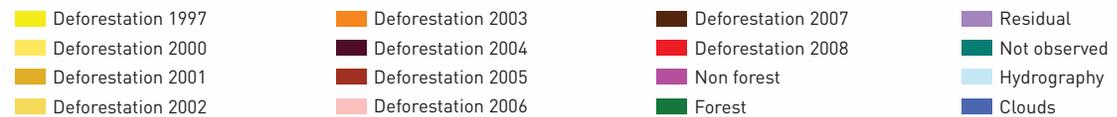
WATER RESOURCES

Water-flow forecasting systems in individual catchments provide essential information for managing the water resources needed for agriculture, industry and households. They also produce and share information for flood alert systems in order to provide longer lead-times for warning people about impending disasters.

Source: UNEP.

Land cover codes

Land cover classification

The European Flood Alert System (EFAS) geographic information system (GIS) land cover layer contains 44 categories, including urban, agriculture, coniferous/deciduous forest, wetlands and bare soil. Information on the type of land cover is compiled from space and *in situ* observations. It is critical for determining runoff characteristics in the hydrological model.

Source: European Landcover 2000.
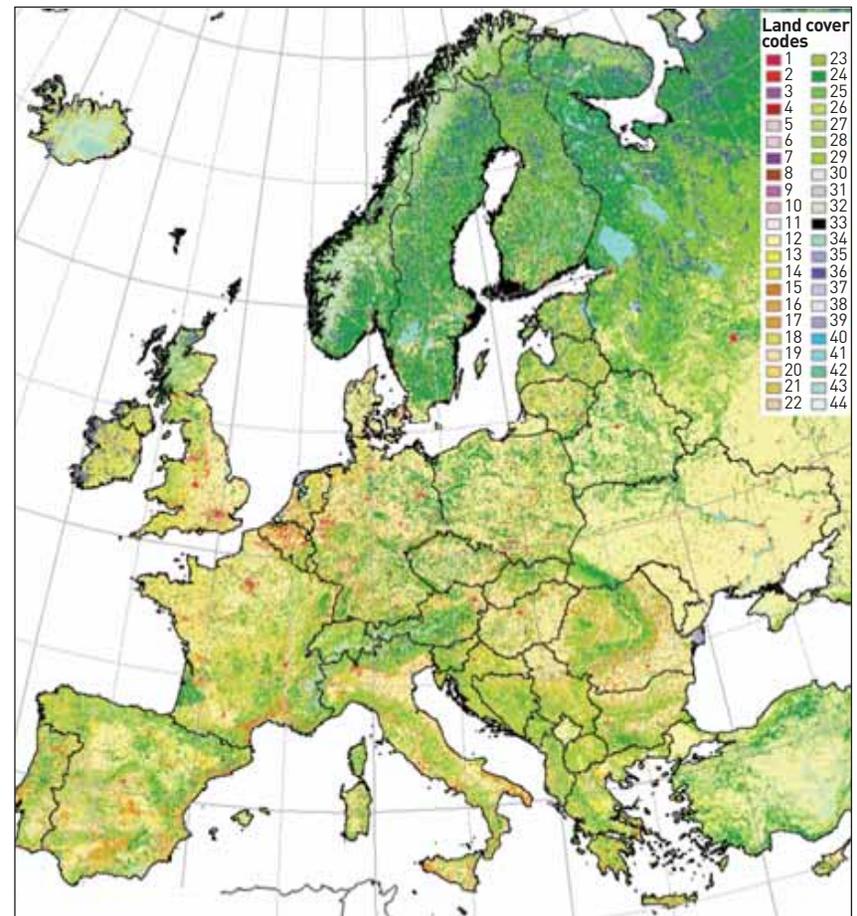
European Terrestrial Network for River Discharge

The monitoring stations that constitute the European Terrestrial Network for River Discharge (ETN-R) gather near real-time river discharge and water level data from 30 European national and trans-boundary river basins in 35 countries. This network in turn supplies EFAS with *in situ* river observations.

Source: EFAS.

Soil texture classifications

Geographic information system (GIS) layers for topsoil (below left) and subsoil (right) are each divided into six categories. Soil information is important for determining percolation, runoff and erosion characteristics in the hydrological model.

Source: EFAS.

Elevation
Height in metres
< -20
-20-200
200-500
500-750
750-1,000
1,000-1,500
1,500-2,000
2,000-2,500
2,500-3,000
3,000-4,536
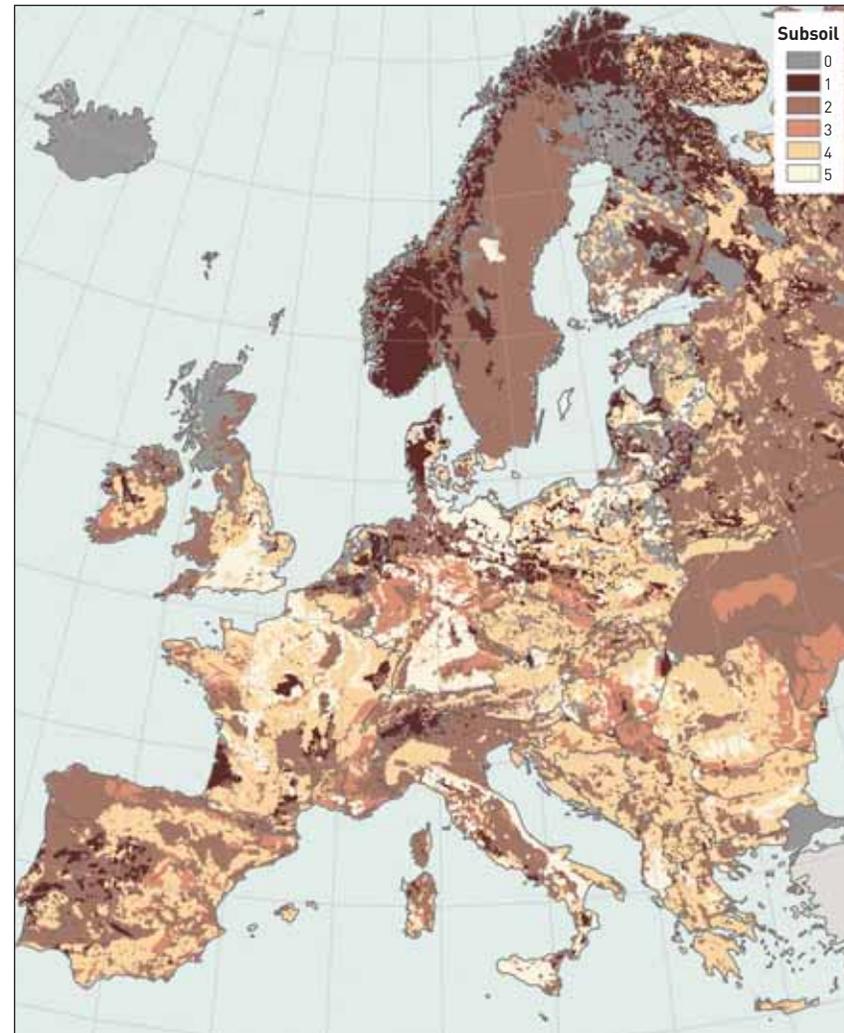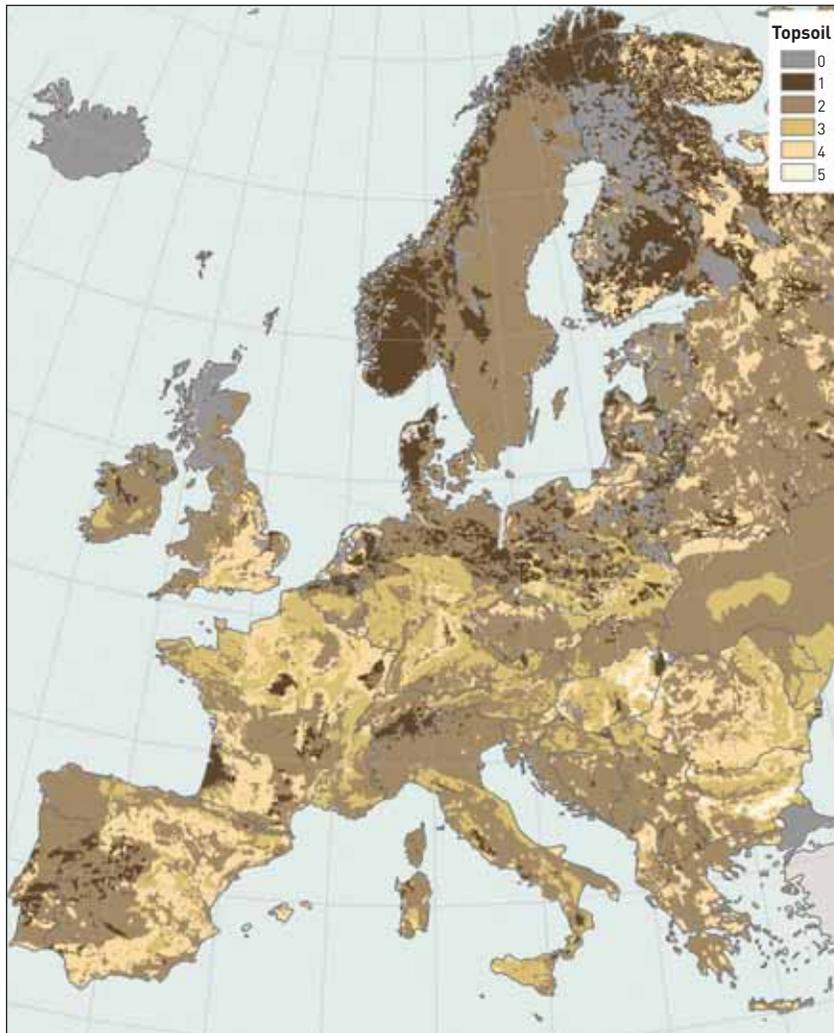
Topography

A 1-kilometre resolution Digital Elevation Model (DEM) of Europe derived from the Shuttle Radar Topography Mission (SRTM) is used by the EFAS hydrological model (colours indicate elevation). A DEM is critical for establishing the slope of terrain in river catchments, which in turn has implications for runoff intensity and the potential for erosion.

Source: EFAS.

Slope and hypsometry

Intermediate landform products derived from the DEM include slope classification (steepness intensity, below upper) and hypsometry (elevation categories, below lower). Flood alert systems need these products in order to determine the channelling of precipitation runoff and river flow.
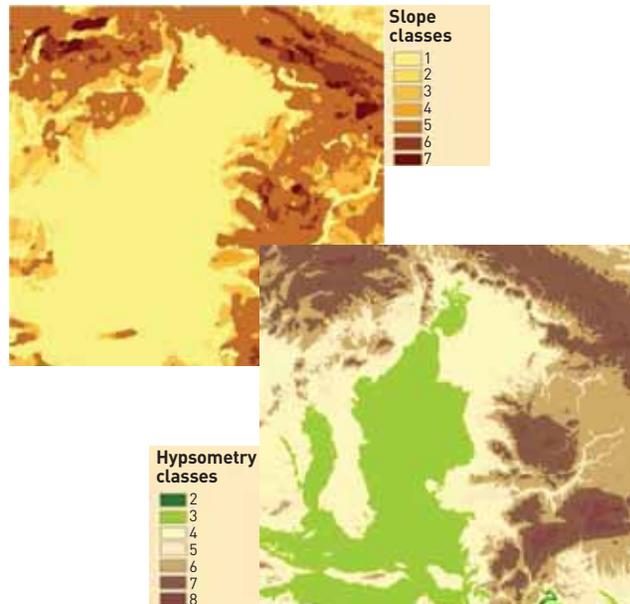

Source: GISCO LAEA.
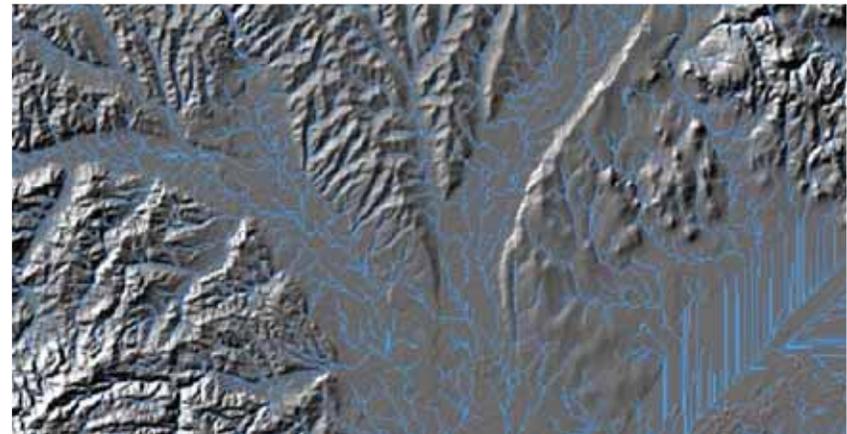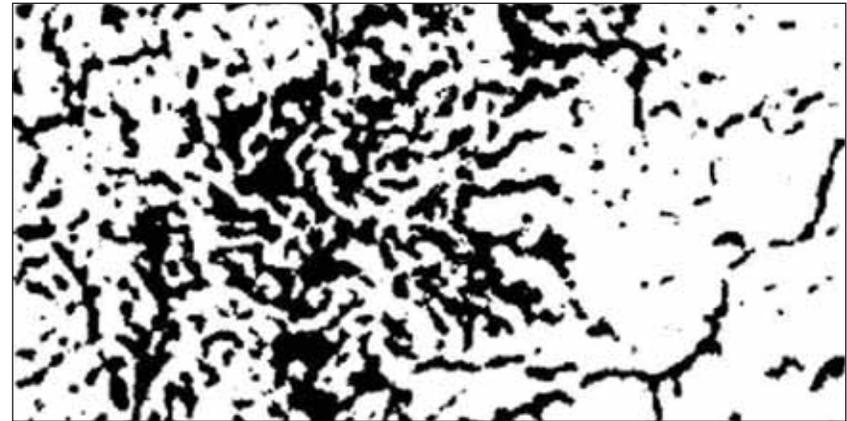
Intermediate landform products

Intermediate landform products derived from the slope and hypsometry classifications include the probability drainage density, the likelihood of water collecting into an area (upper), and ultimately the river channel network (lower), for which the hydrological model computes water flux in the river basins.

Precipitation forecast

Deterministic precipitation forecasts are used as inputs into the hydrological model. In the case of Europe, forecasts for up to 10 days are supplied by the European Centre for Medium-Range Weather Forecasting (ECWMF), and for up to seven days by the German Weather Service (Deutsche Wetter Dienst – DWD).

To increase the robustness of medium-range forecasts, Ensemble Prediction Systems (EPS) are used to provide an average forecast computed from several dozen numerical weather model runs. This average forecast is then compared with the deterministic forecasts as a precipitation input to the hydrological model.


Wednesday 21 July 2010 00UTC. Forecast probability t+038-080 VT: Thursday 22 July 2010 12 UTC. Surface: Total precipitation of at least 10 mm.
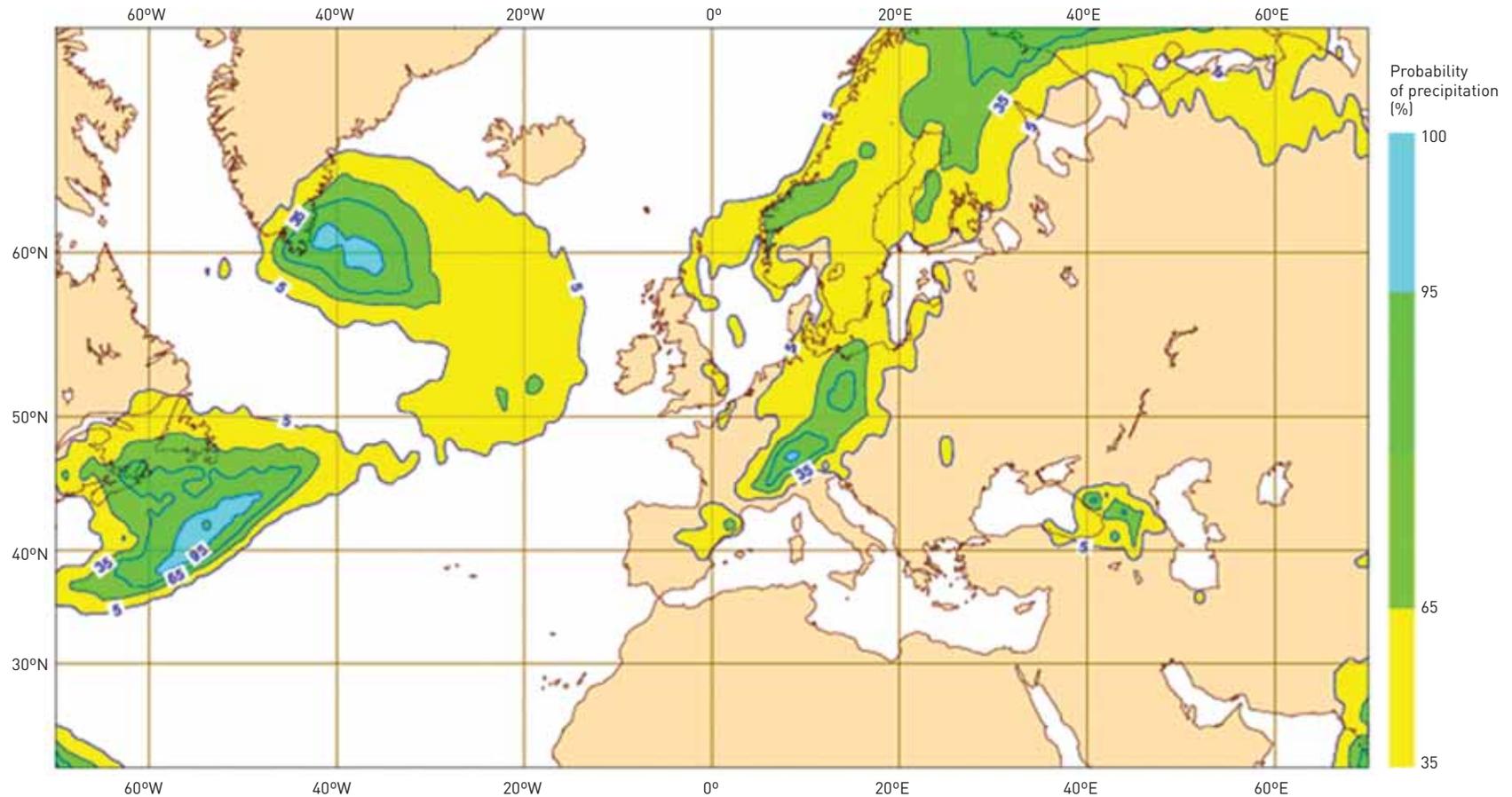
Source: ECMWF.

Annual run-off

The global distribution of mean annual runoff (mm/year) indicates the maximum available renewable freshwater resource. The amount of water that is actually usable depends also on consumption and water pollution, in addition to the infrastructure for supporting stable water supply.

Source: Oki and Kanae, *Science*, 2006.
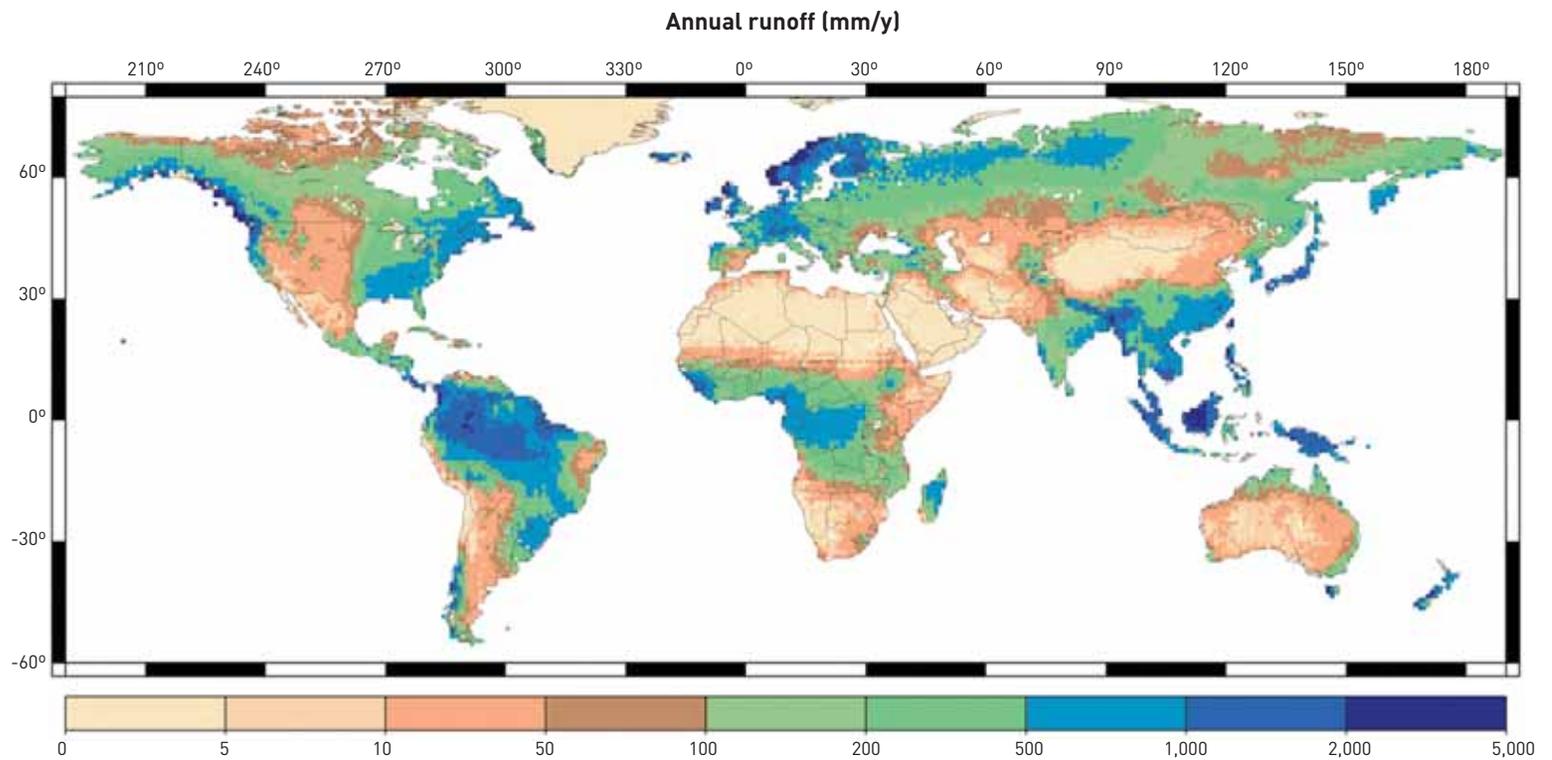
Annual runoff (mm/y)

The water scarcity index reflects the balance between the annual water withdrawal and the maximum available renewable freshwater resource. Water stress is high for regions with a high index.

Source: Oki and Kanae, *Science*, 2006.

Water scarcity index
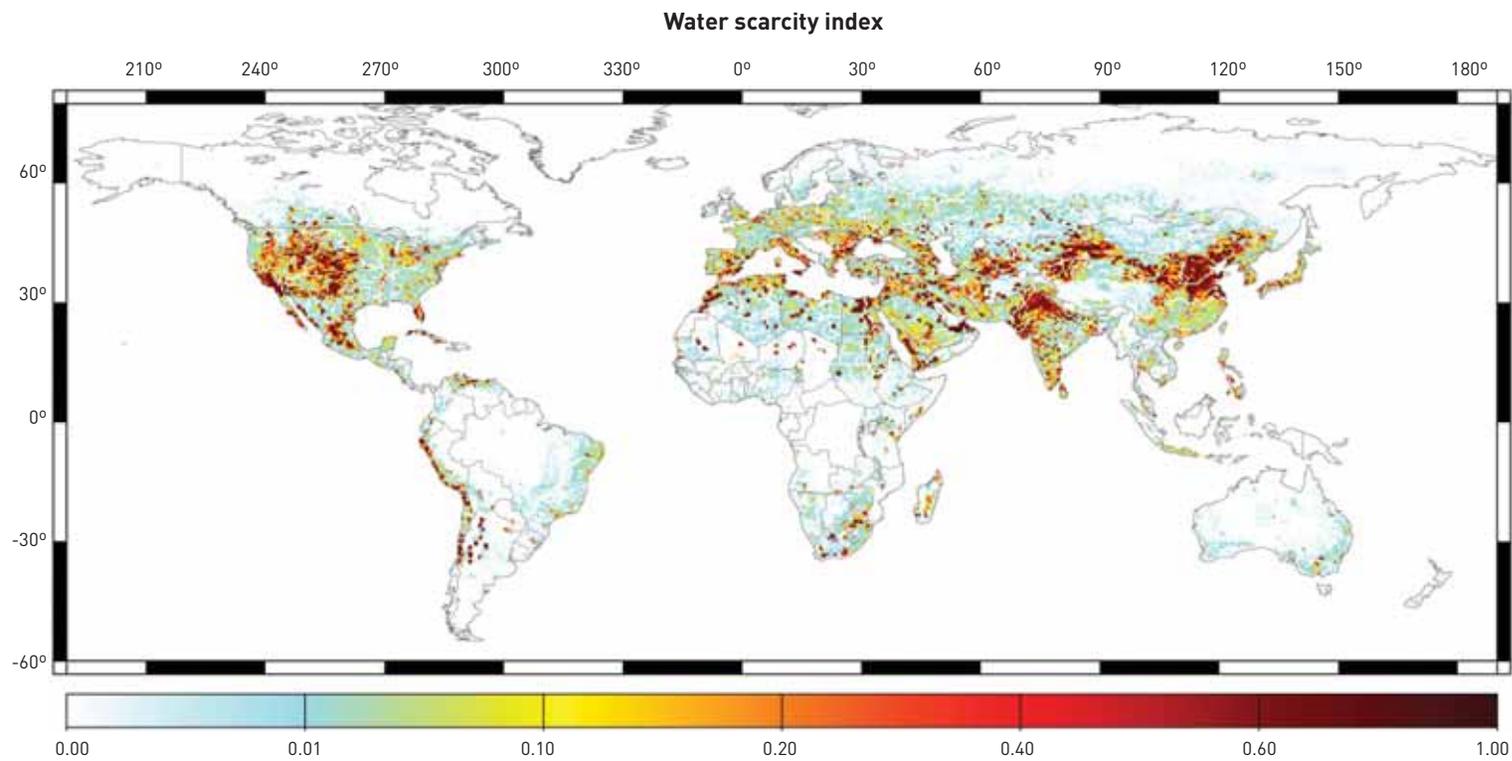
Near real-time flood monitoring

Near real-time flood monitoring information provided by EFAS: the urgency and intensity of warnings is indicated by the symbol and the colour scheme.

Producing data

CARBON DIOXIDE: FLUX TOWERS

FLUX TOWERS are used to measure the exchange, or flux, of carbon dioxide (CO_2), water vapour and energy (heat) between terrestrial ecosystems, such as forests, and the atmosphere. There are currently more than 500 flux towers in the world. Most are part of the FLUXNET network of regional networks.

Observation instruments used on flux towers generally include an ultrasonic anemometer that measures wind speed and an inlet for a CO_2 gas analyser, which are mounted at the top of the tower. Measurements of how much CO_2 or water vapour is moving vertically past the tower are made using a statistical technique known as eddy covariance. The resulting observations are plotted as graphs to show how the flux changes over time.


Source: AIST.

FLUXNET networks

Networks
- ▲ Ameriflux
- ▲ AsiaFlux
- ▲ CARBOAFRICA
- ▲ CarboEurope IP
- ▲ Carbomont
- ▲ ChinaFLUX
- ▲ Canadian CP
- △ Other
- ▲ KoFlux
- ▲ LBA
- ▲ OzFlux
- ▲ Sardinilla Proj
- ▲ TROPI-DRY
- ▲ USCCC
- ▲ Unaffiliated

FLUXNET
March 2010, 502 sites
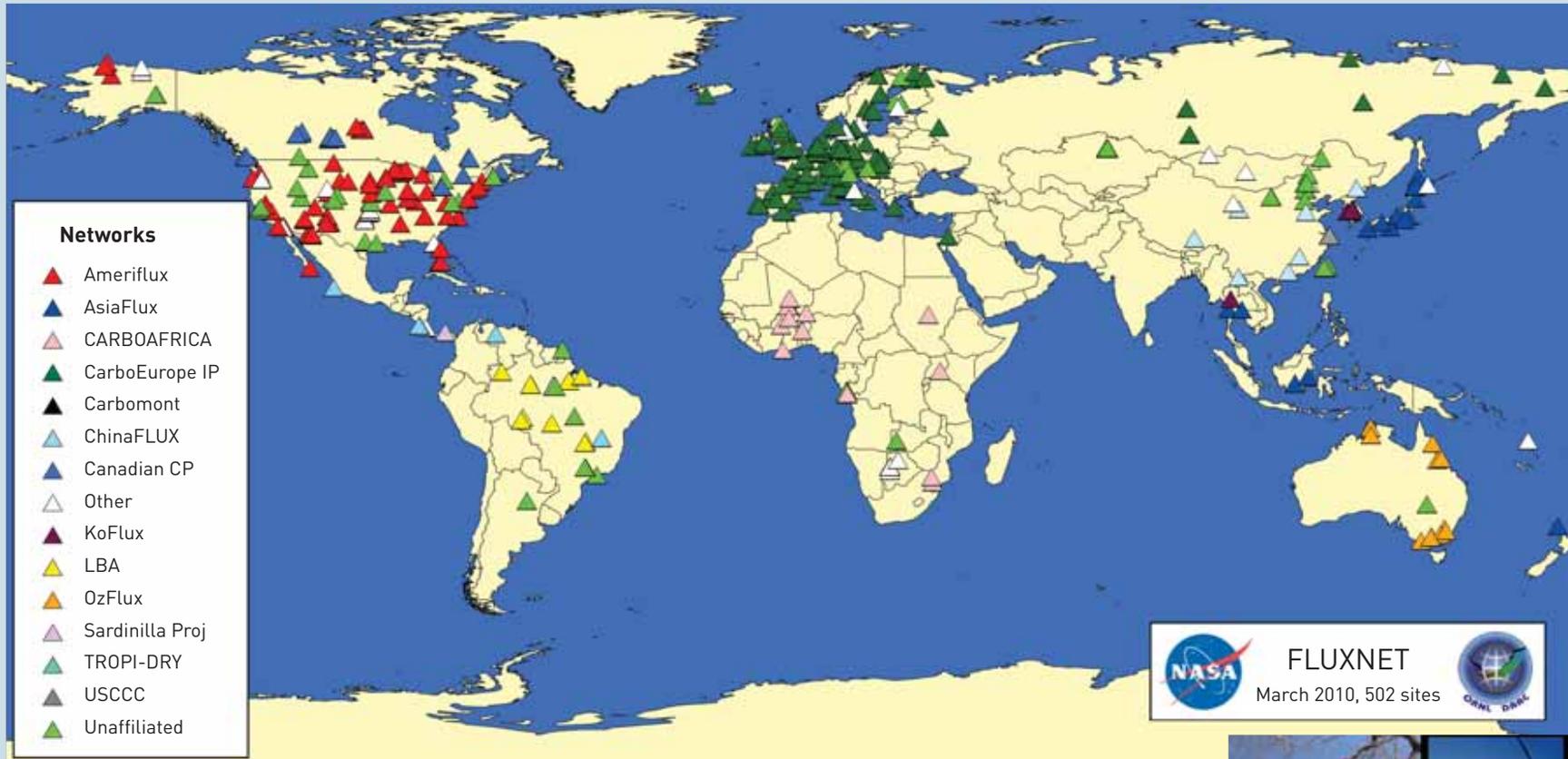
Distribution of tower sites within the global network of networks.
Source: FLUXNET.

The Takayama (TKY) flux tower site is located in a deciduous forest in central Japan (previous page and right, upper); it is part of the AsiaFlux network and started taking observations in 1993, making it the oldest flux tower in Asia. The CO$_2$ analyser Licor 6262 and gases for calibration (right, lower) are placed in a cabin at the foot of the tower.

Source: AIST.

Satellite antenna

Temperature/salinity probe

Circuit boards and satellite transmitter

Gear motor

Stability disk

Single-stroke pump

Battery

Hydraulic pump (piston)

Hydraulic fluid

Bladder
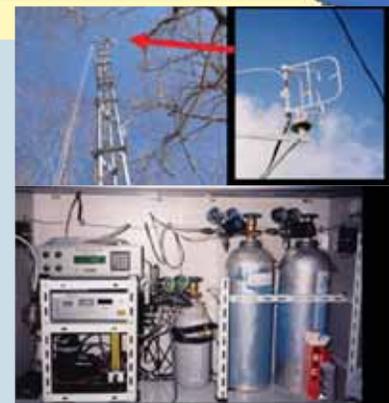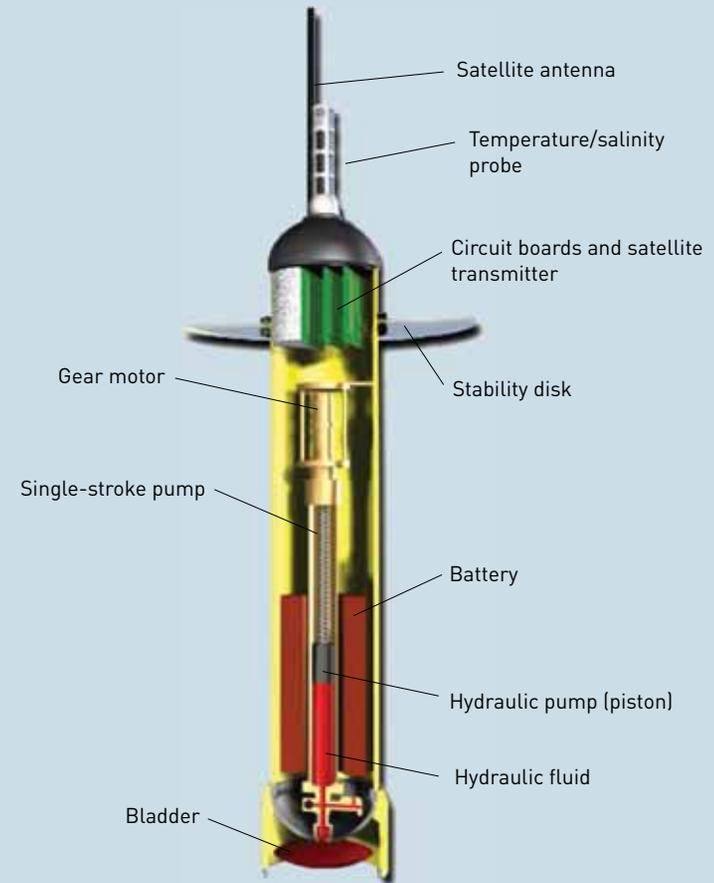
OCEAN TEMPERATURE AND SALINITY: ARGO BUOYS

THE OCEANS play a vital role in shaping weather conditions and driving the climate system. Until recently, however, information on how heat travels through the oceans was limited. To address this problem, governments launched the global system of Argo ocean buoys in the year 2000.

Source: Jcommops.org/ARGO.

1. Buoy deployed by ship or aircraft.

2. Slow descent to 2,000 metres, 6 hours at 10 cm/s.

3. Drift for nine days with ocean currents.

4. Oil pumped from internal reservoir to inflate external bladder causing buoy to rise.

5. Temperature and salinity profile recorded during ascent.

6. Up to 12 hours at surface to transmit data to satellite.

7. Oil pumped back to internal reservoir. New cycle begins.

8. Data sent to weather and climate forecasting centres around the world.

Producing data: Argo buoys 59

Argo buoys around the world
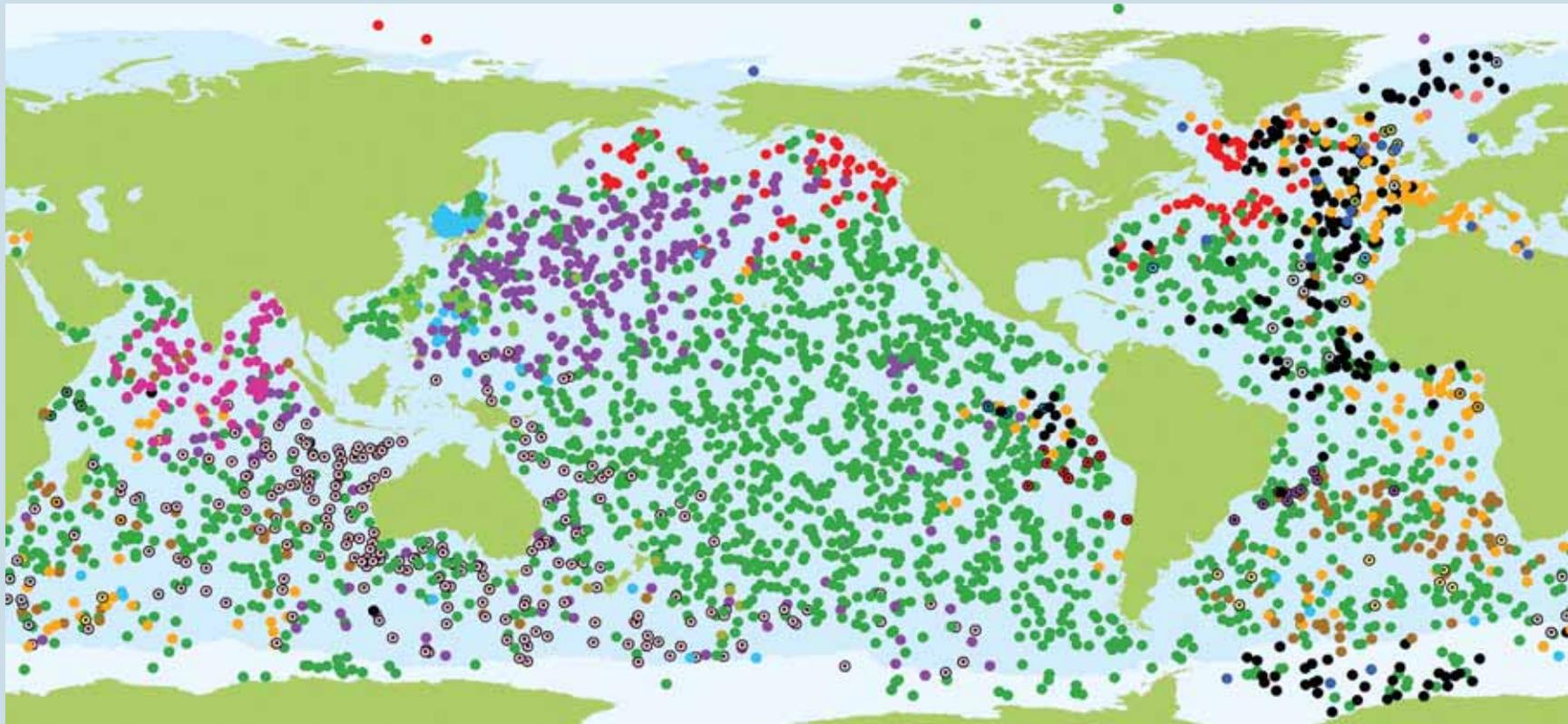
3,621 Argo buoys

⊙ Argentina (11)	● China (31)	● Germany (177)	● Rep. of Korea (90)	⊙ Poland (1)
⊙ Australia (224)	⊙ Ecuador (3)	● India (72)	⊙ Mauritius (2)	● Russian Federation (2)
● Brazil (10)	● European Union (17)	⊙ Ireland (7)	⊙ Netherlands (25)	⊙ Spain (2)
● Canada (118)	● France (156)	● Japan (320)	● New Zealand (9)	● United Kingdom (115)
● Chile (10)	⊙ Gabon (2)	⊙ Kenya (4)	● Norway (4)	● United States (1,849)

Source: Jcommops.org/Argo.

Today a fleet of more than 3,600 of these robotic buoys from 25 countries is measuring ocean temperature and salinity with support from satellite altimetry instruments. The resulting data are essential for weather and climate forecasting, oceanographic studies, fishing management and disaster mitigation. The logistics and costs of deploying this system throughout the world's oceans and in space would have been daunting for any single nation. The project has become feasible because it is being jointly undertaken by many countries for the common good. Ensuring the long-term sustainable operation of such systems will require continued international cooperation.

VOLCANIC ASH CLOUDS: LIDARS

IN APRIL 2010, a plume of tiny particles of ash (right) and smoke emitted by Iceland's Eyjafjallajökull volcano caused havoc to air travel in Europe. Researchers and monitoring agencies around the world spontaneously collaborated on observing and analysing the volcanic plume. Relying in particular on Lidar (Light Detection And Ranging) observations from ground, air and space, they pooled their data and demonstrated the potential for developing operational services in the future.

Source: (main image) Árni Friðriksson/Wikimedia Commons; (ash particles) German Aerospace Center (DLR) Institute of Atmospheric Physics.

Lidar transmits laser pulses into the atmosphere and detects the resulting backscatter. It is used to measure the vertical distribution of aerosols in the atmosphere. Lidar instruments can be positioned at ground stations or carried by aeroplanes or satellites.

Lidar (Light Detection And Ranging)
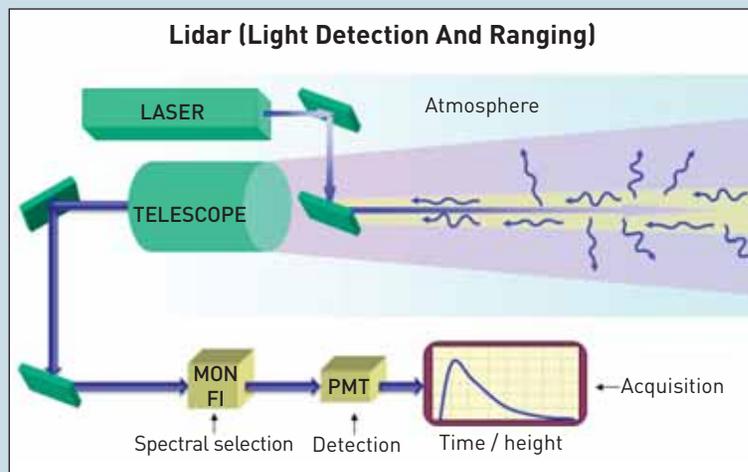
Earth observation data from the European Aerosol Research Lidar NETwork, or EARLINET, were vital for helping scientists to understand and predict the volcano's behaviour. Established in 2000, EARLINET encompasses the 27 advanced Lidar stations on this map and is the first coordinated Lidar network for tropospheric aerosol study to be established on the continental scale. It provided data about the presence, altitude and layering of the volcanic cloud, together with optical information all over Europe. (See www.earlinet.org.)
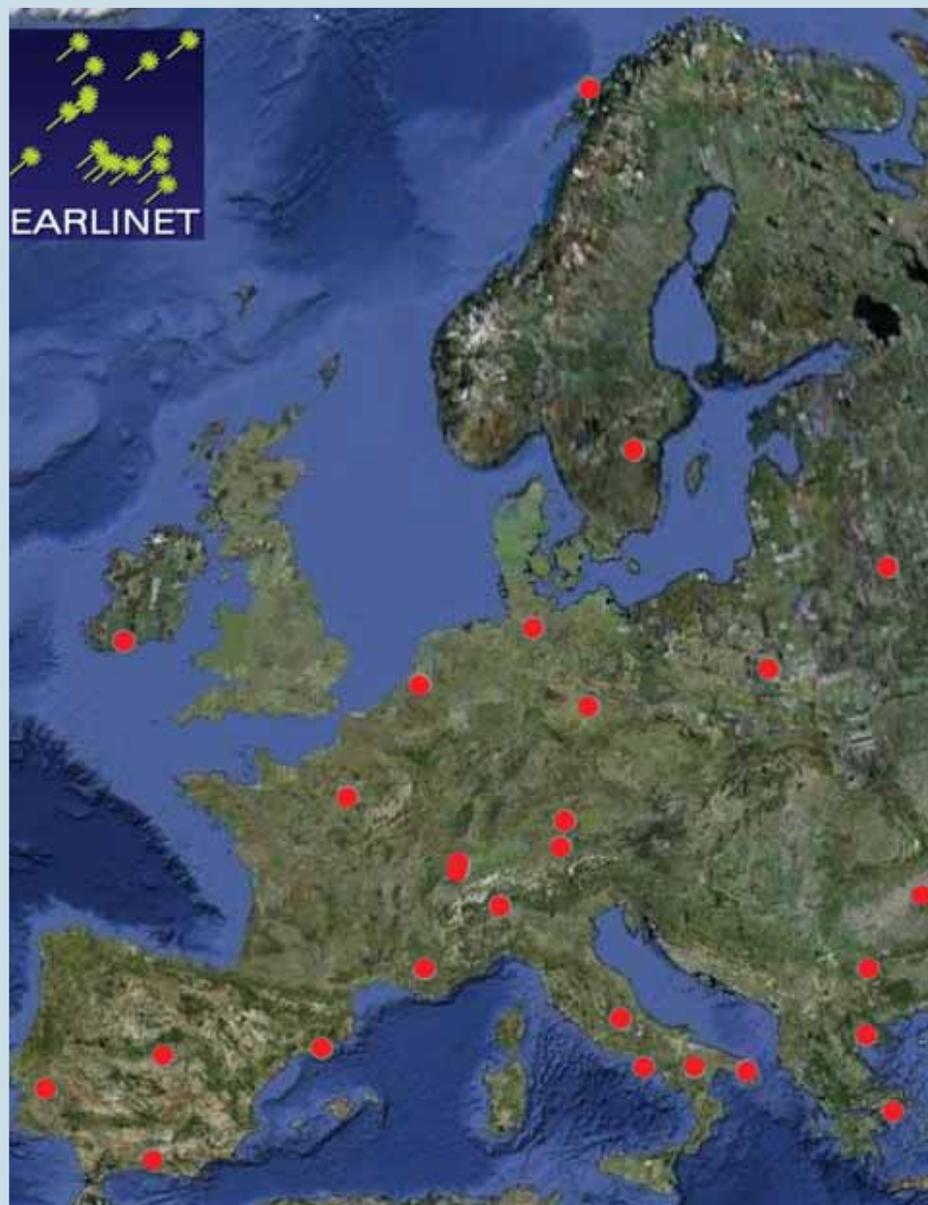
Tracking the plume from the ground: 16-17 April 2010
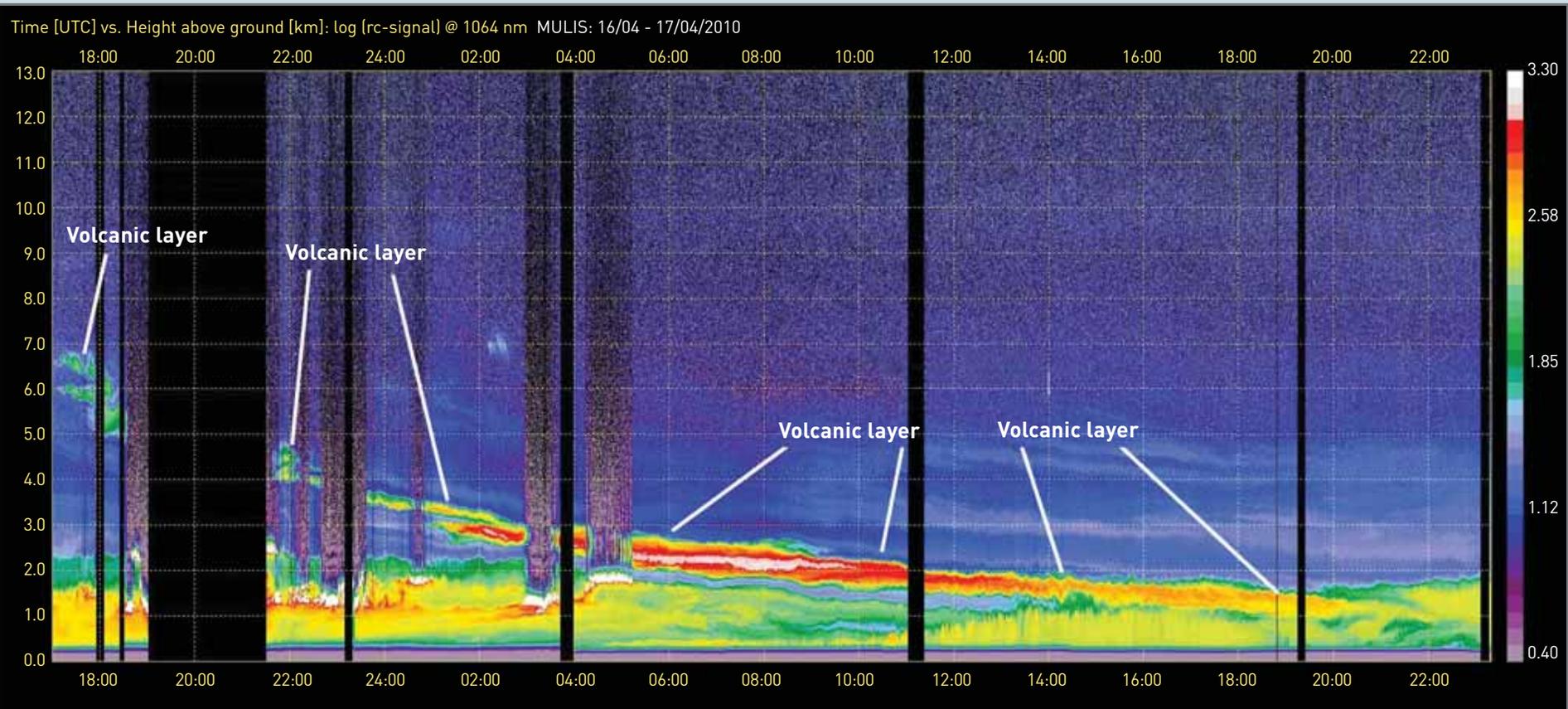
EARLINET performed almost continuous measurements from 15 April in order to follow the evolution of the volcanic plume. The above image from the EARLINET station in Munich graphs the height of the plume against the time of day during the course of 16-17 April. During the morning of 16 April, the ash plume was observed by EARLINET stations over the Netherlands, Germany and France at 5-6 kilometres above sea level and at upper altitudes of around 8 kilometres above sea level over Belarus.

Producing data: Lidars 63

Tracking the plume from the air: 21 June 2010

Plume and Keflavik (Iceland) soundings

Plume sounded 1st time

Range-corrected backscatter signal @ 2 μm

0.10
0.17
0.31
0.53
0.94
1.6
2.9
5.0
8.7
15
26
46
81
142
250

N

Eyjafjallajökull

7.4 km

Cirrus clouds

Stratocumulus clouds

Volcanic ash plume

60 km

Source: DLR.
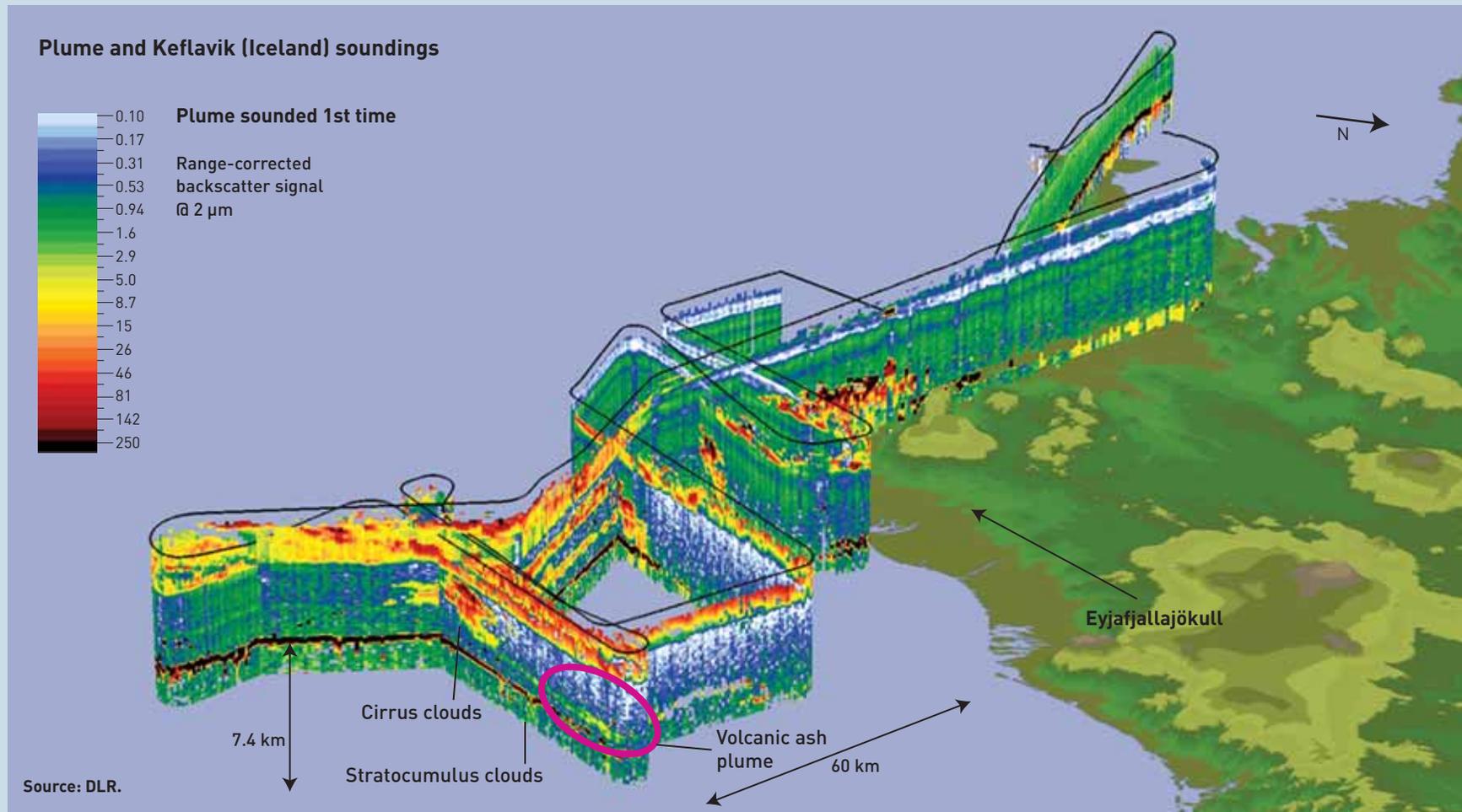
Aerial Lidar monitoring offers the flexibility of choosing the trajectory that will best characterize the volcanic cloud. This image is based on aerial Lidar observations taken by the German Aerospace Center (DLR) on 21 June.

Tracking the plume from space: 17 April 2010

The Cloud-Aerosol Lidar and Infrared Pathfinder Satellite Observations (CALIPSO), a joint mission of the French Space Agency and the US National Aeronautics and Space Administration (NASA), captured this vertical cross-section of the atmosphere. The ash cloud is seen above Paris as a thin, wispy layer of particles ranging in altitude from 1.8 to 6.3 kilometres. The cross-section is displayed on top of an optical map of western Europe.

Source: NASA/Kurt Severance and Tim Marvel.
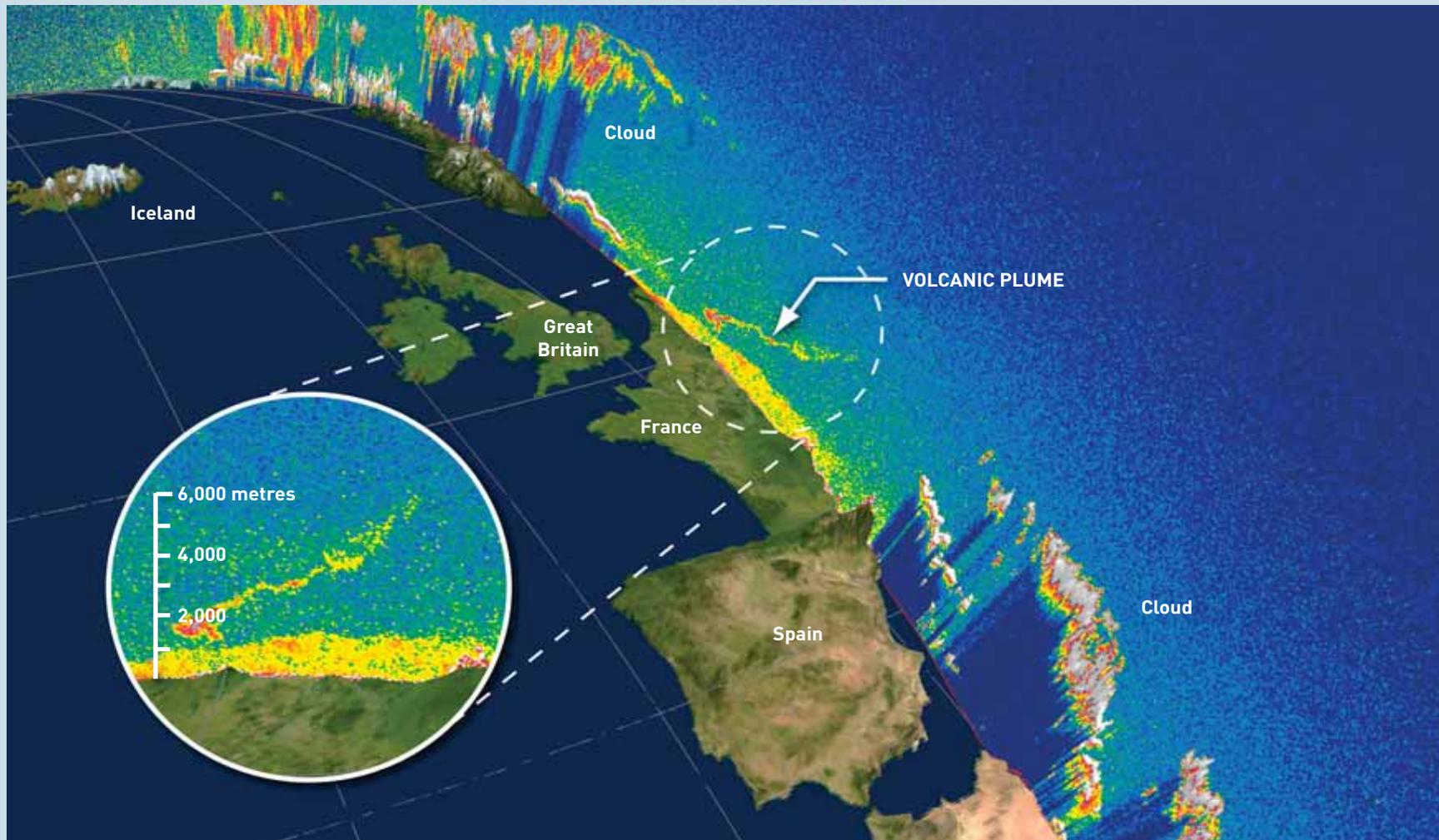
GREENHOUSE GASES: THE "IBUKI" SATELLITE

JAPAN'S GREENHOUSE GASES OBSERVING SATELLITE "IBUKI" (GOSAT) measures atmospheric concentrations of carbon dioxide and methane, the two major greenhouse gases, from space. GOSAT carries two Thermal And Near infrared Sensor for carbon Observation instruments, or TANSO for short. TANSO-FTS is the Fourier Transform Spectrometer, which monitors greenhouse gases. TANSO-CAI is the Cloud and Aerosol Imager; its observations are used to correct those from TANSO-FTS.

Source: GOSAT/JAXA.

Tracking the carbon-dioxide column
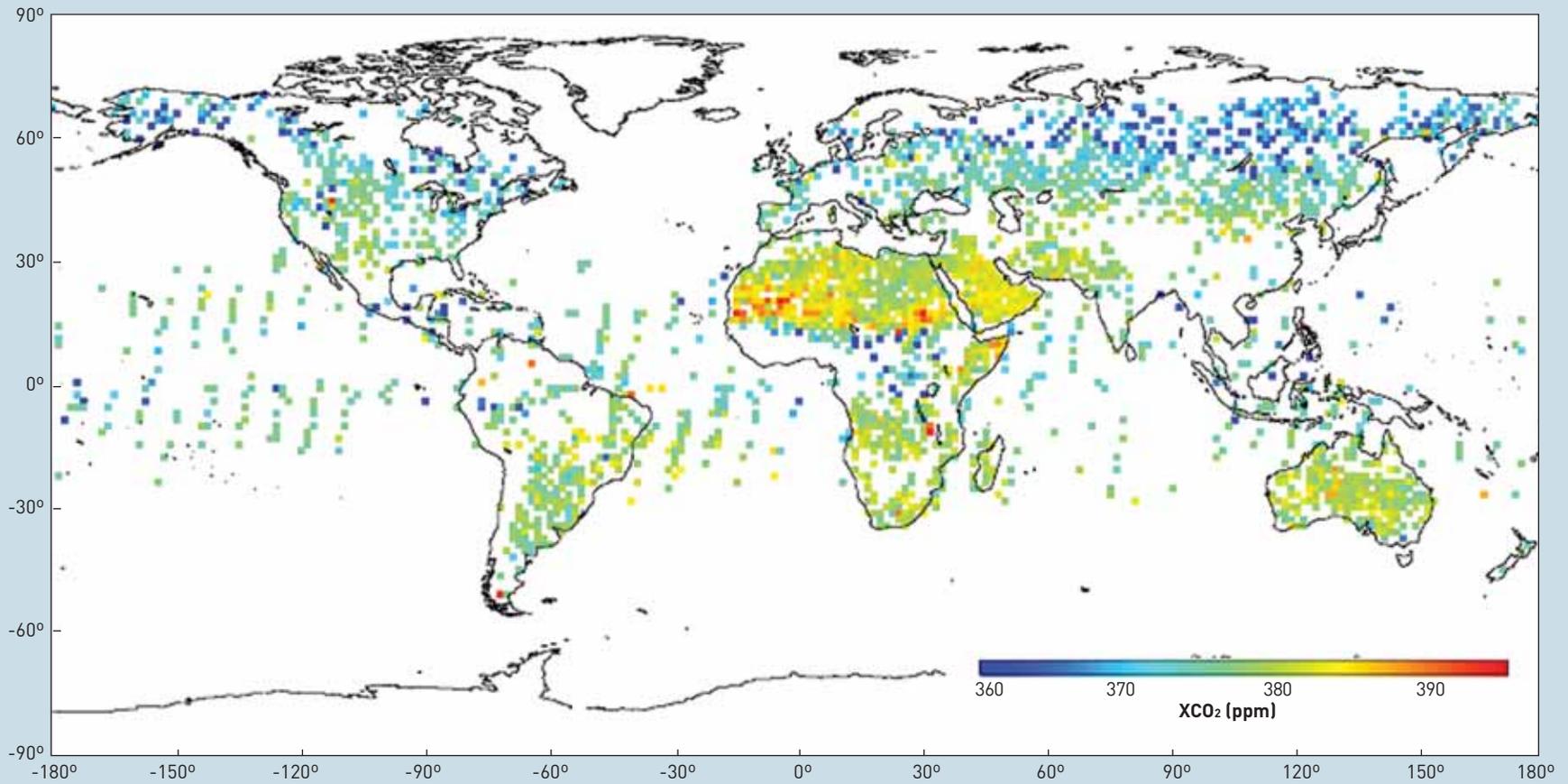
20090901-0930(Ver.00.80)
Source: JAXA/NIES/MOE.

This output is a monthly global map of the CO_2 column-averaged volume mixing ratios (XCO_2) in 1.5 by 1.5 degree mesh in September 2009. The blank area is mainly due to cloud and weak sun reflection.

Producing data: "IBUKI" satellite 67
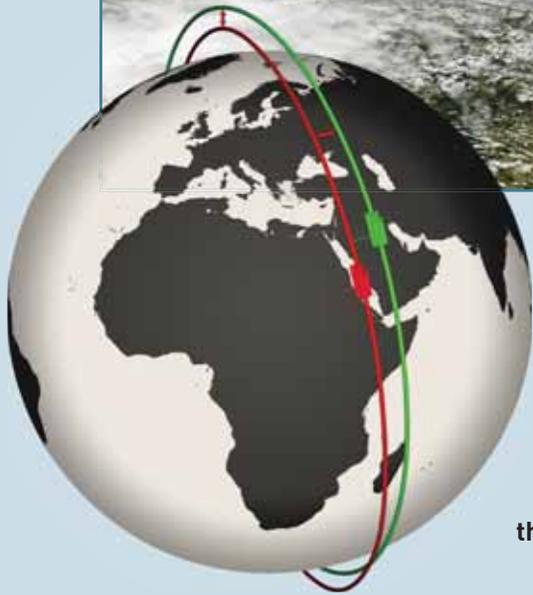
TOPOGRAPHY: RADAR FROM SATELLITES

FLYING IN FORMATION just a few hundred metres apart, the German Aerospace Center's (DLR) two Earth observation satellites, TerraSAR-X and TanDEM-X, are generating a precise digital elevation model (DEM) of the Earth's surface. By working as a huge interferometer allowing flexible baselines, these instruments capture images in the radar spectrum's short-wavelength X band. They are providing highly precise elevation data in a 12-metre grid with a height accuracy of better than 2 metres.

Source: DLR.
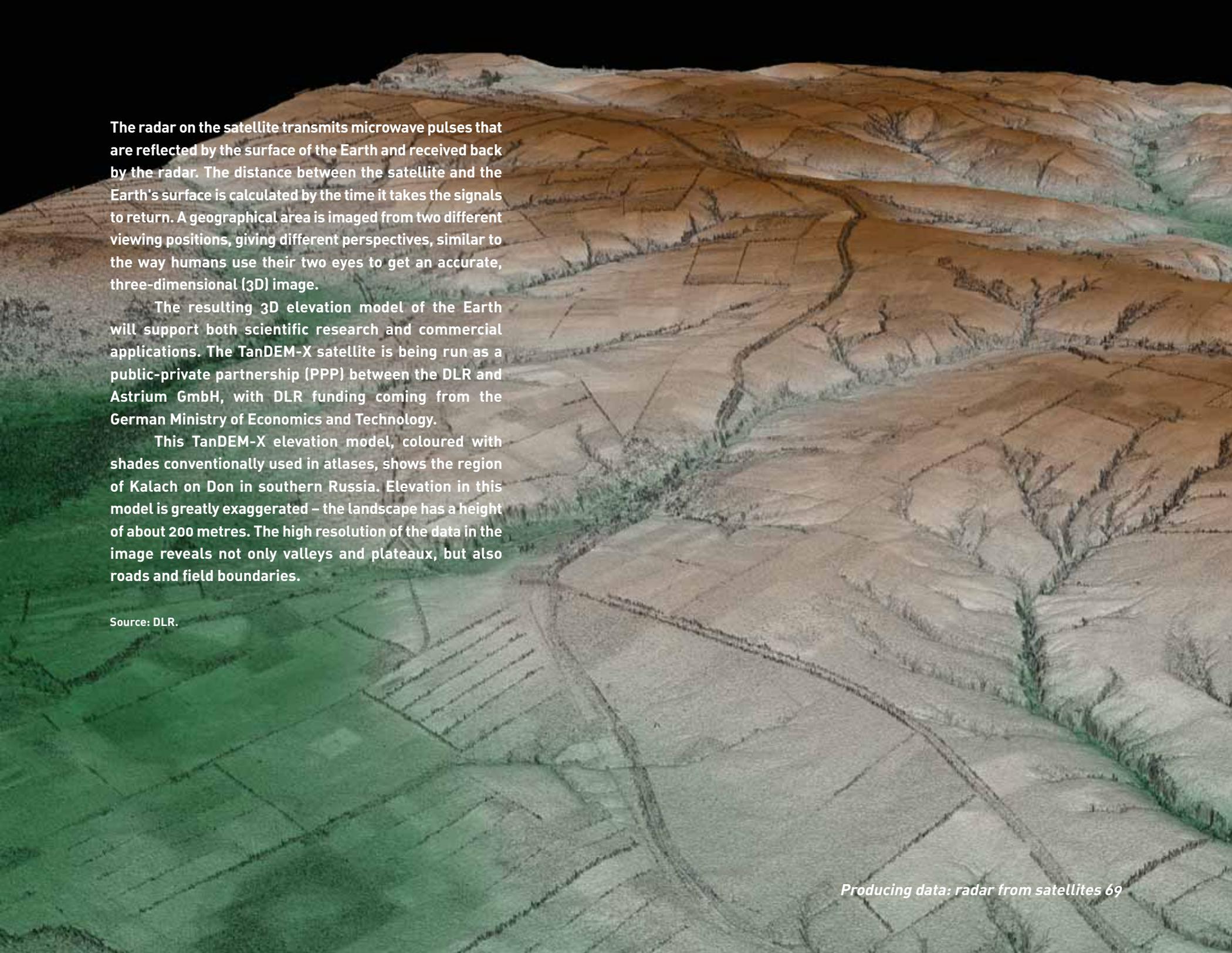
The radar on the satellite transmits microwave pulses that are reflected by the surface of the Earth and received back by the radar. The distance between the satellite and the Earth's surface is calculated by the time it takes the signals to return. A geographical area is imaged from two different viewing positions, giving different perspectives, similar to the way humans use their two eyes to get an accurate, three-dimensional (3D) image.

The resulting 3D elevation model of the Earth will support both scientific research and commercial applications. The TanDEM-X satellite is being run as a public-private partnership (PPP) between the DLR and Astrium GmbH, with DLR funding coming from the German Ministry of Economics and Technology.

This TanDEM-X elevation model, coloured with shades conventionally used in atlases, shows the region of Kalach on Don in southern Russia. Elevation in this model is greatly exaggerated – the landscape has a height of about 200 metres. The high resolution of the data in the image reveals not only valleys and plateaux, but also roads and field boundaries.

Source: DLR.

GRAVITY: THE GRACE SATELLITES

THE GRAVITY RECOVERY and Climate Experiment (GRACE) uses two identical satellites travelling 200 kilometres apart on the same orbital track to provide extremely accurate and high-resolution estimates of the Earth's mean gravity field and a history of how gravity varies over time. Each satellite carries two star cameras (for celestial reference), an accelerometer (for measuring non-gravitational forces due to air drag or solar radiation) and three global positioning system (GPS) antennae. The highly accurate inter-satellite ranging system HAIRS constitutes the core of the instrumentation. It can measure changes in the distance between the twin satellites to an accuracy of 1 micrometre (one millionth of a metre).

GRACE is a joint project between the US National Aeronautics and Space Administration (NASA) and the German Aerospace Center (DLR).
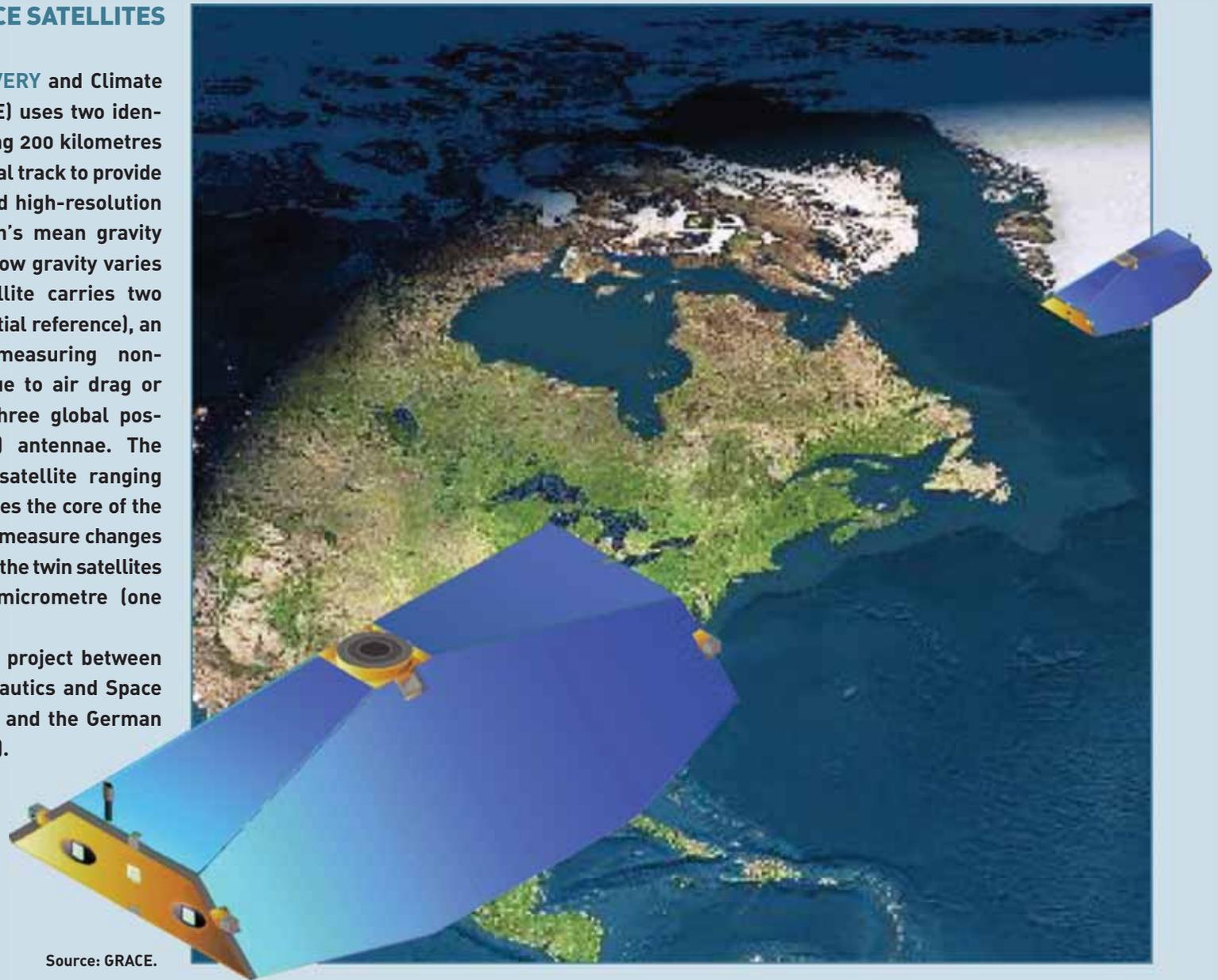
Source: GRACE.

The mean gravity field generated by GRACE, also called the geoid (right and front cover), shows variations in the gravity field caused by movements and heterogeneities inside the Earth; the colours and exaggerated vertical scale make it easier to see the resulting irregularities in the planet's shape. Geodesists and cartographers use it to link together various national height-data systems more precisely, and satellite operators to determine orbits of near-Earth satellites and navigate satellites with much higher accuracy. Solid Earth scientists can infer the Earth's internal structure (crust, mantle and core) more accurately and at a finer resolution. Ocean scientists combine the new gravity models with ocean-height measurements from satellite altimeters to study global surface- and deep-ocean circulation on a finer scale.

GRACE also enables a better understanding of some processes that drive the Earth's dynamic climate system. Monthly snapshots of the Earth's gravity field are used by hydrologists to monitor seasonal and sub-seasonal variations in the continental hydrological cycle (below). Glaciologists use them to study ice-mass loss in Antarctica or Greenland.

Source: DLR.
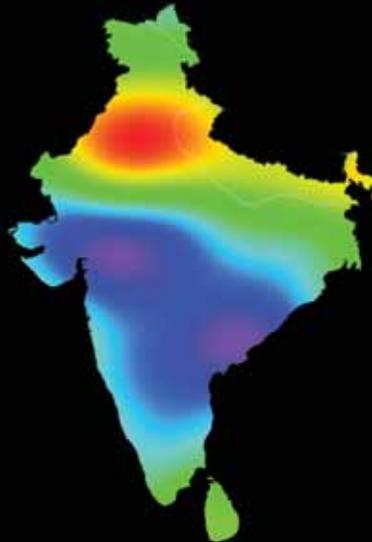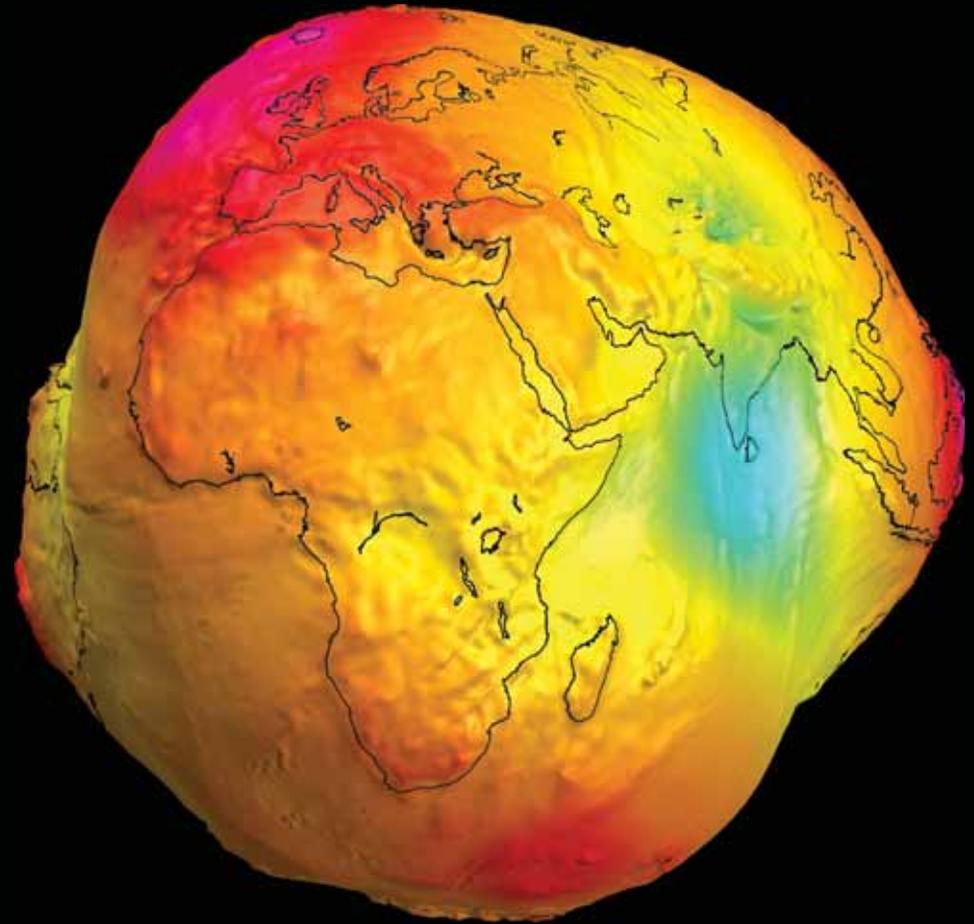
The map (left) shows groundwater changes in India during 2002-08, with losses in red and gains in blue, based on GRACE satellite observations. The estimated rate of depletion of groundwater in northwestern India is 4.0 centimetres per year, equivalent to an annual water-table decline of 33 centimetres per year. Increases in groundwater in southern India are due to recent above-average rainfall, whereas rain in northwestern India was close to normal during the study period.

Source: Velicogna/UC Irvine/NASA.
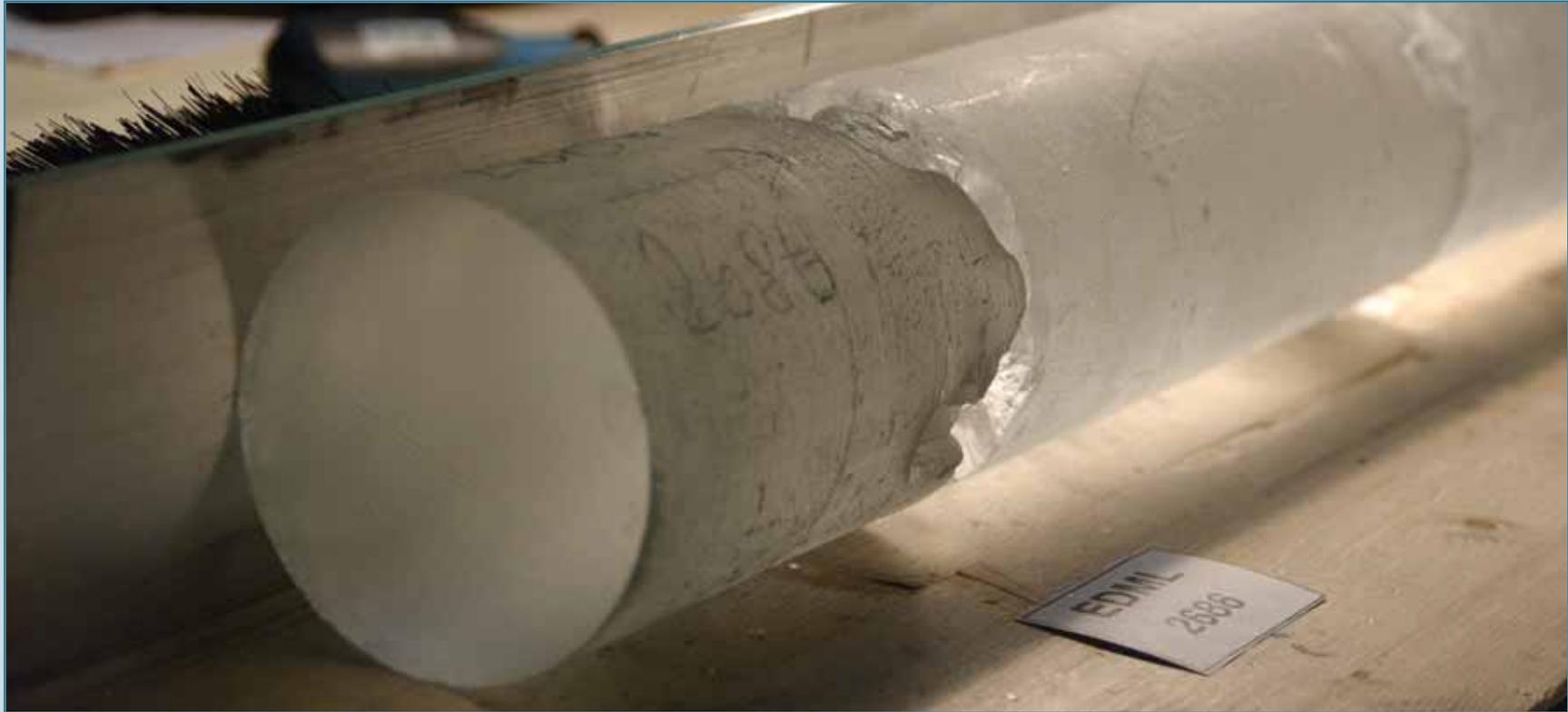
PAST CLIMATES: ICE CORES

ICE CORES are cylinders of compacted snow and ice retrieved by using massive drills to penetrate vertically down through the ice sheets of Greenland and Antarctica. These cores reveal the annual cycles of snowfall, similar to the way in which the rings of a tree trunk reveal annual growth patterns. They also contain wind-blown dust, ash, varying isotopes, and bubbles of atmospheric gas and radioactive substances that provide clues about bygone environmental conditions.

Since ice cores can be several thousand metres in length, they contain an abundance of climate information going back hundreds of thousands of years.

The ice core above was obtained by the European Project for Ice Coring in Antarctica (EPICA), used for comparison with ice cores drilled in the Vostok region of Antarctica.

Source: Alfred-Wegener-Institute for Polar and Sea Research.

Interpreting ice cores

A section of the Greenland Ice Sheet Project (GISP 2) ice core from 1,837–1,838 metres. The clearly visible annual layers result from differences in the size of snow crystals deposited in winter versus summer and the resulting variations in the abundance and size of air bubbles trapped in the ice. This ice was formed around 16,250 years ago during the final stages of the last ice age.

Source: National Ice Core Laboratory/USGS/NSF.

Temperature and CO$_2$ records

Legend:
- Temperature (EPICA Dome C)
- CO$_2$ (Vostok)
- CO$_2$ (EPICA Dome C)
- CO$_2$ (EPICA Dome C)
- CO$_2$ (EPICA Dome C)

Current CO$_2$ level →

Temperature anomaly (°C): 15, 10, 5, 0, -5, -10

Atmospheric CO$_2$ (ppm): 400, 350, 300, 250, 200

Thousands of years ago: 800, 700, 600, 500, 400, 300, 200, 100
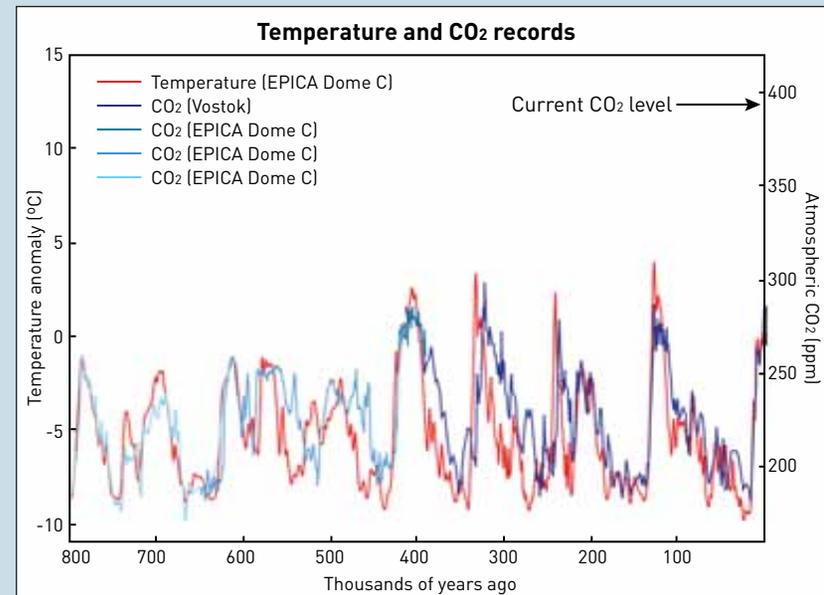
Based on Antarctic ice cores, scientists can estimate atmospheric carbon dioxide levels over the past 800,000 years and reconstruct the temperature levels (indicated here as a difference from the mean temperature for the last 100 years).

Source: Leland McInnes.

RAIN: RADAR STATIONS

RADAR DETECTS RAIN in the atmosphere by emitting pulses of microwave and measuring the signals reflected by the raindrops. In general, the more intense the reflected signals, the more intense is the rain. The distance to the rain is determined by the time it takes for the microwave to travel to and from the rain. Doppler weather radar can even measure the approach or departure speed of raindrops by analysing how the frequency of the returned signal has been altered by the object's motion.

The China Meteorological Administration (CMA) has established a vast national network of 215 Doppler radar instruments, often positioned at the top of hills and tall buildings and structures.

Source: CMA.

● S-band Doppler weather radar
● C-band Doppler weather radar
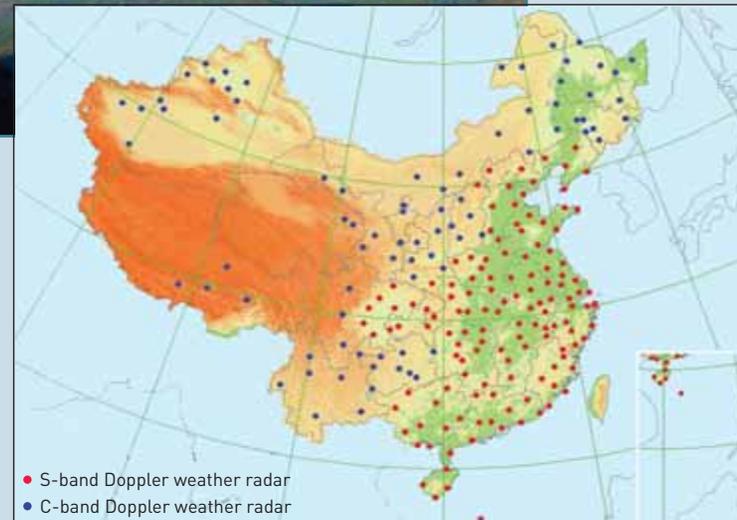
Rain distribution and intensity on 6 September 2010, at 16.50 (Beijing time). Such maps are automatically generated every 15 minutes by the China Meteorological Administration.

Mosaic of rain radar images in China

Hourly
precipitation (mm)

125
100
75
63
50
38
25
10
5

Source: Weather.com.cn/CMA.

Producing data: radar stations 75
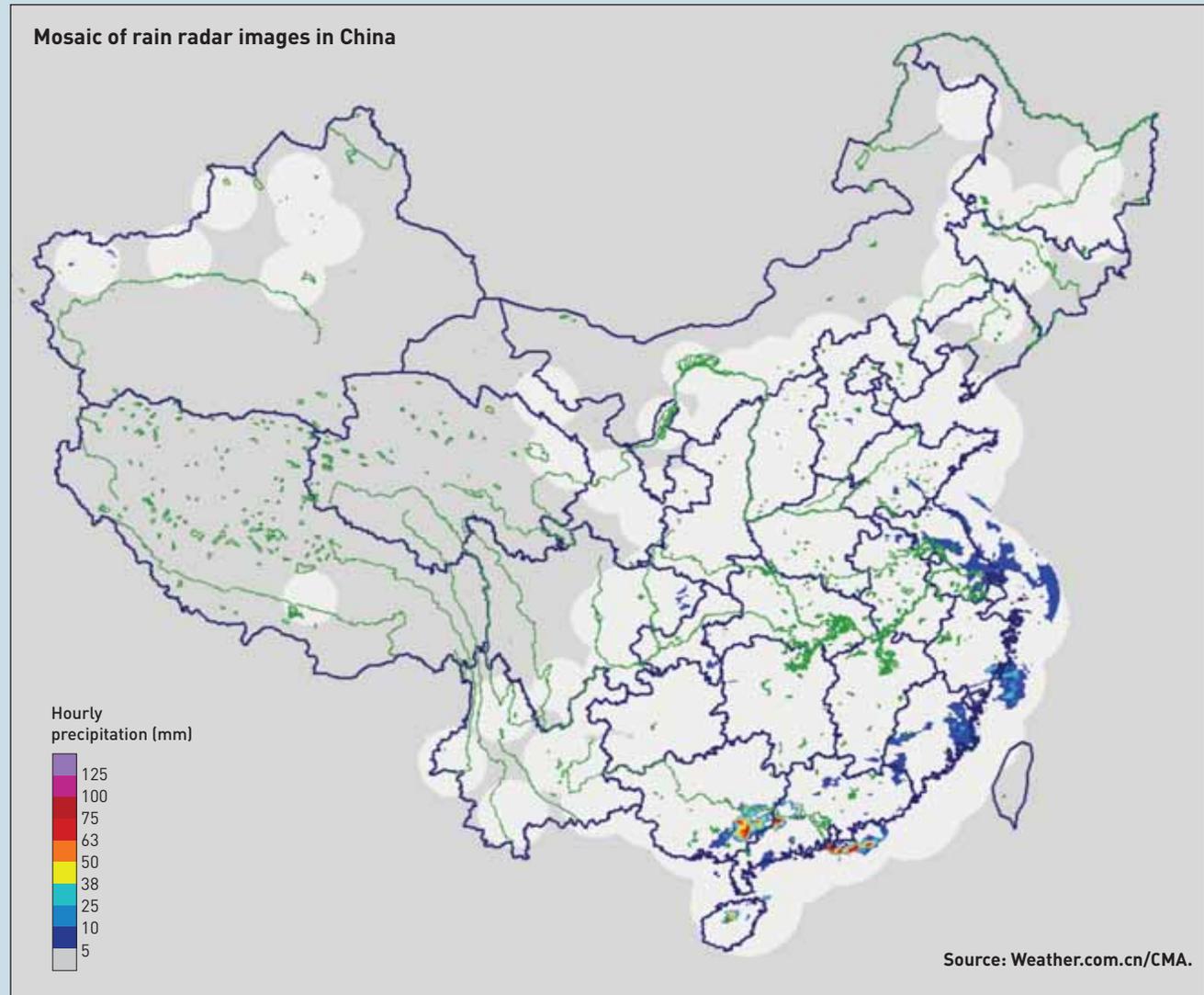
MAPPING THE SURFACE: VIRTUAL SATELLITE CONSTELLATIONS

DECISION MAKERS responsible for crop management, forest surveillance, emergency response, marine safety and other critical activities need to obtain satellite images of the same location every few days or even hours. High-resolution satellites, however, generally take weeks to revisit the same site. To address this problem, the world's space agencies are collaborating through the Committee on Earth Observation Satellites (CEOS) to operate the Land Surface Imaging (LSI) virtual constellation. They coordinate the distribution of images of the Earth's surface from some 20 imaging satellites and inter-calibrate them to ensure comparability despite differences in resolution, spectrum and contrast.

The five images of Beijing were taken by China's HJ1B, the US's Landsat, the China-Brazil Earth Resources Satellite (CBERS), US-Japan's TERRA-ASTER satellite and Japan's ALOS-PRISM. Processed to produce higher resolution images, they show the Forbidden City in central Beijing (facing page).

Actual horizontal distances:
Top left HJ1B - 360 km
Top right Landsat - 185 km
Centre left CBERS - 120 km
Centre right TERRA-ASTER - 60 km
Bottom ALOS-PRISM - 70 km
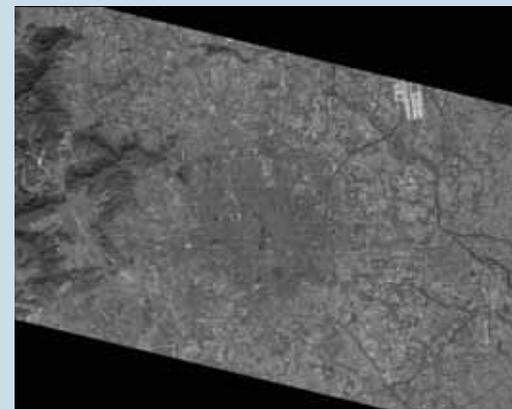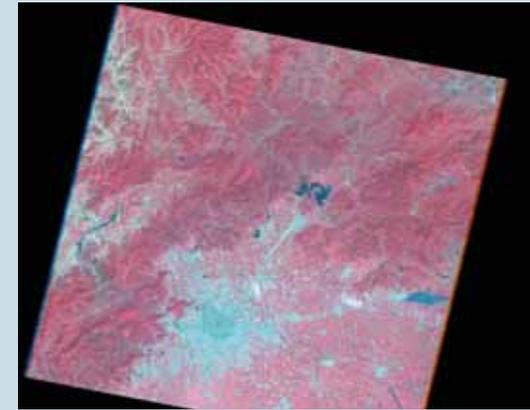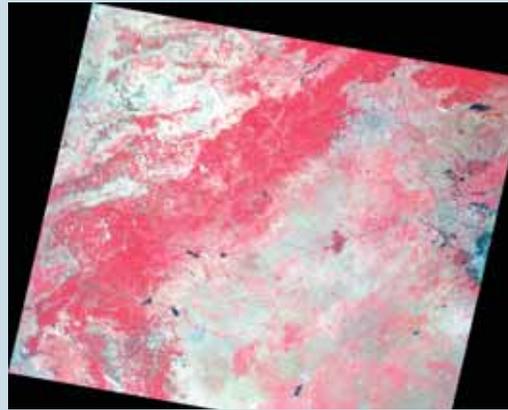
HJ1B 30 m resolution

Landsat 30 m resolution

CBERS 20 m resolution

**TERRA-ASTER
15 m resolution**

**ALOS-PRISM
2.5 m resolution**
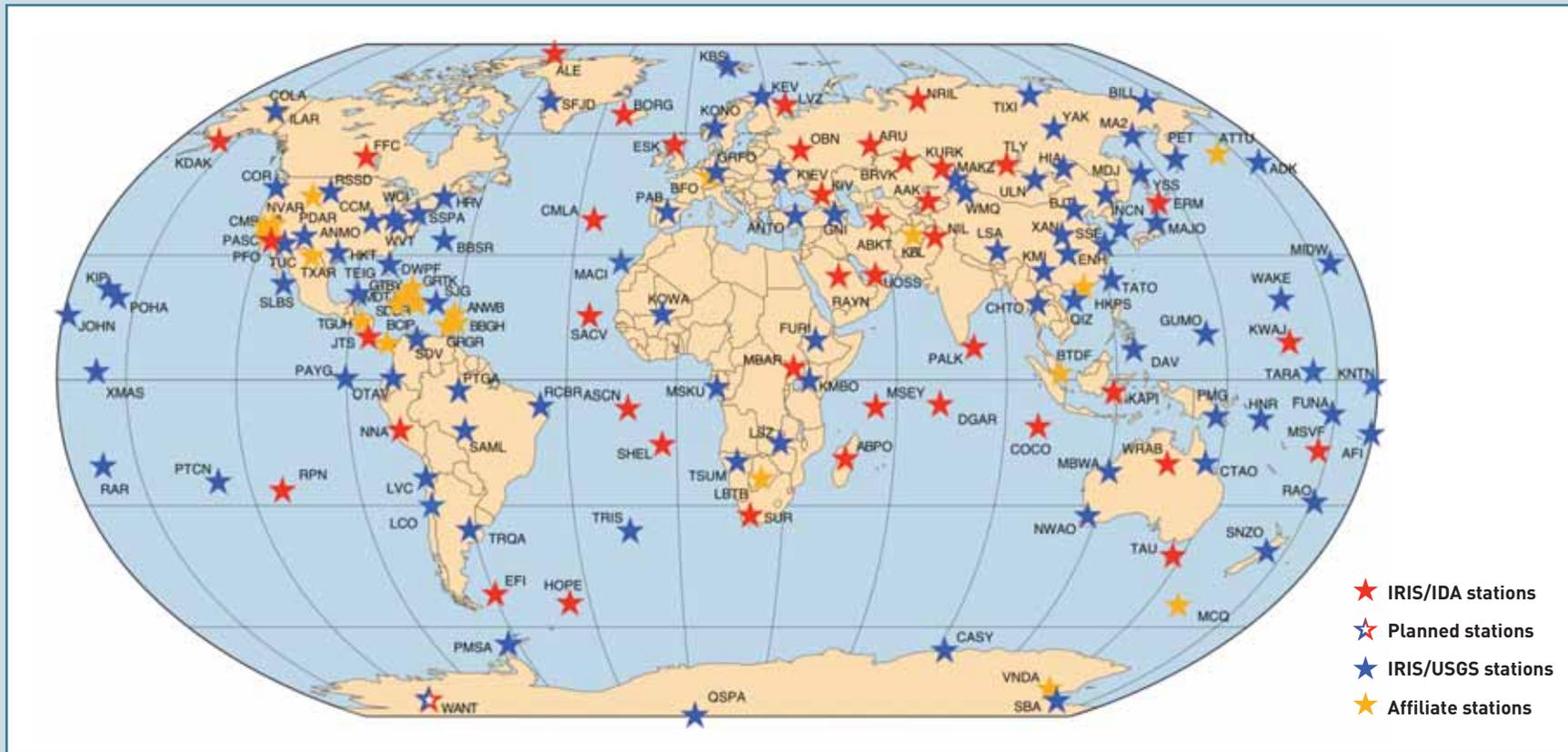
EARTHQUAKES: THE GLOBAL SEISMOGRAPHIC NETWORK

THE GLOBAL SEISMOGRAPHIC NETWORK (GSN) consists of over 150 stations sited from the South Pole to Siberia, and from the Amazon basin to the sea floor of the northeast Pacific Ocean. It cooperates with over 100 host organizations and seismic networks in 59 countries worldwide. The participating seismological and geophysical sensors are connected to one another via telecommunications. All GSN data are freely and openly available via the Internet both in real time and from archival storage at the IRIS Data Management System posted at www.iris.edu.

Seismic waves recorded after they have travelled thousands of kilometres through the Earth's interior bear significant information about the tectonic plates, the mantle and core that underlie them. Researchers use GSN data extensively to construct and revise three-dimensional models of the Earth's interior. These models, in turn, are used to accurately locate earthquakes and large explosions.

Source: GSN.

ON-SITE VALIDATION: THE GEO-WIKI

THE GEO-WIKI consists of a global network of volunteers working to improve the quality of global land cover maps. Since large differences occur between existing global land cover maps, current ecosystem and land-use science lacks the accurate data needed for crucial purposes, such as determining how much additional agricultural land may be available to grow crops in Africa. Volunteers are asked to review hotspot maps of global land cover disagreement and to determine, based on what they actually see on existing geo-tagged photos, or based on their local knowledge, whether the land cover maps are correct or incorrect. Their input is recorded in a database, along with uploaded photos, to be used in the future for creating a new and improved global land cover map. For more information, visit www.geo-wiki.org.

Source: J. Sawalha/UNEP.
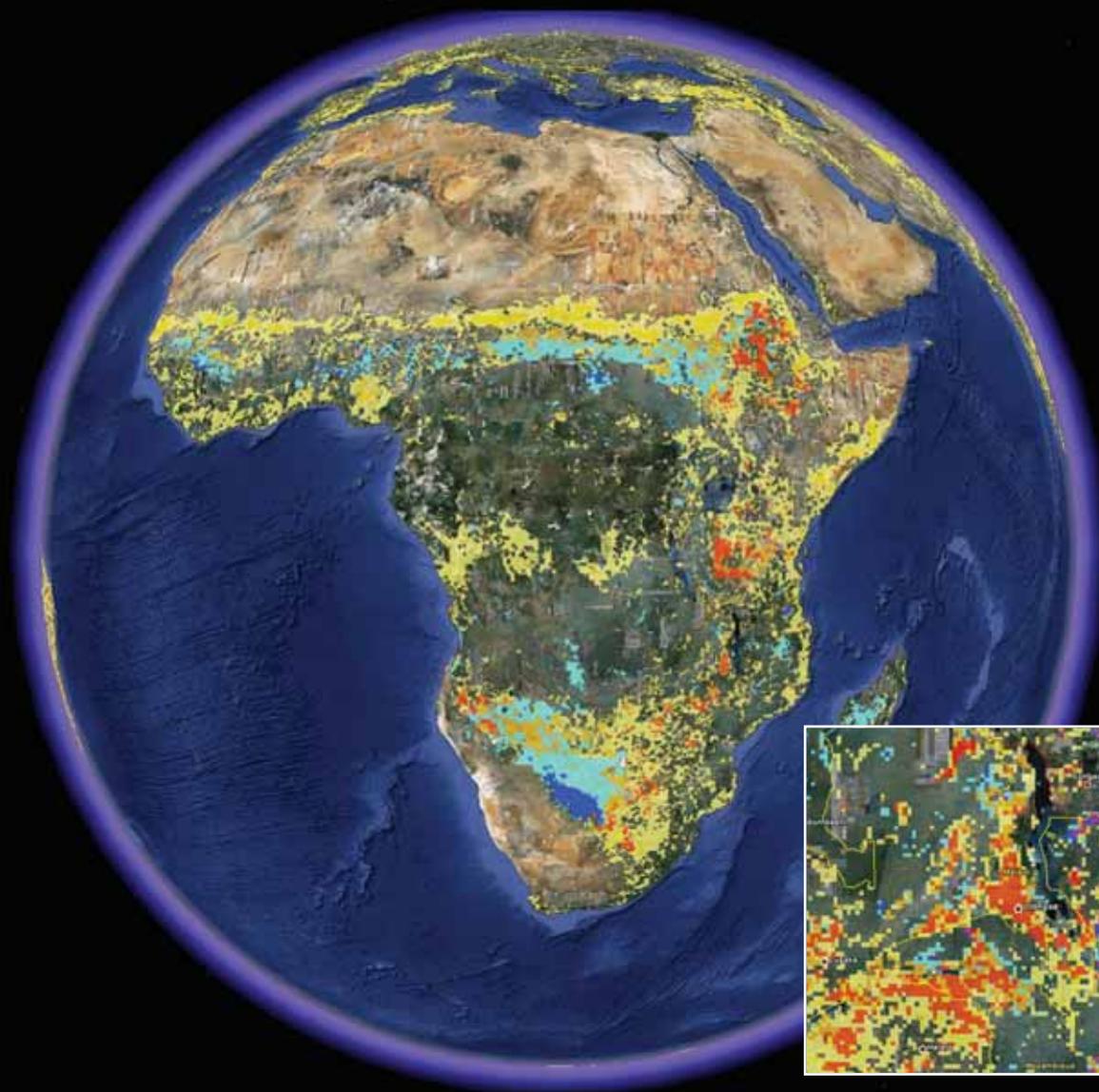
Land cover disagreement

- Cropland disagreement
- High cropland disagreement
- Forest disagreement
- High forest disagreement
- Forest and cropland disagreement
- Forest and high cropland disagreement
- High forest and cropland disagreement
- High forest and high cropland disagreement
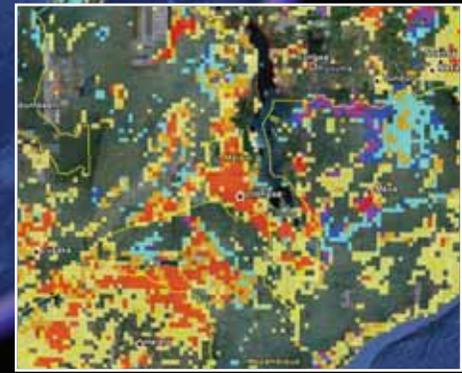
An overall land cover disagreement map over Africa comparing GLC-2000, MODIS and GLOBCOVER satellite land cover products within the Geo-Wiki. Large areas of cropland disagreement are visible in yellow and orange. The inset shows a close-up of part of Malawi, a country with large areas of cropland disagreement.

Validate the land cover of the polygons

Show instructions

MODIS — good / not sure / bad — **Non-woody savannahs**

Correct class

Croplands ▼

GlobCover — ○ ○ ○ — **Mosaic grass or shrub or forest/cropland**

GLC-2000 — ○ ○ ○ — **Cultivated and managed areas**

Problems choosing the right land cover? View your profile and choose simple validation method.

Provide picture URLs (ending with .jpg/.png if available)

The volunteer is asked to determine whether the land cover pixels recorded by the three products in the coloured rectangles correspond to what can be seen on the Google Earth Imagery (cropland in this example).

Possible choices are good, bad or unsure. A revised category can be chosen from a drop-down list. Pressing 'submit' records the validation in a database.

Producing data: the GEO-WIKI 81

On-the-ground photos available in Geo-Wiki to support validation in Malawi. Currently 1,000 geo-tagged photos exist for the entire country, distributed on a grid. Each point contains a photo in each cardinal direction, greatly aiding cropland validation.
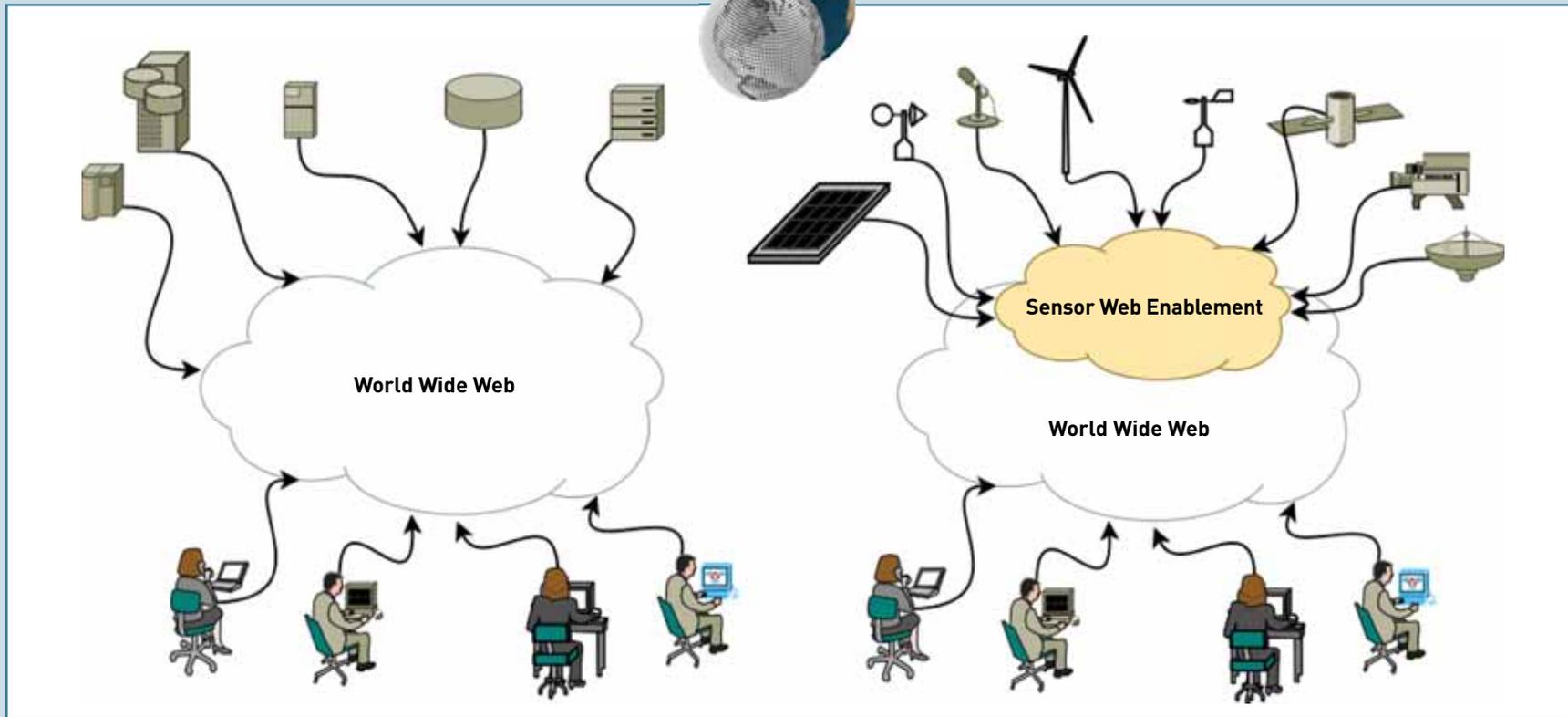
INTEROPERABILITY: THE SENSOR WEB

THE SENSOR WEB CONCEPT aims to improve interoperability between existing sensor systems that were originally designed to stand alone. In this way it will improve the relevance of the spatial and temporal data that they produce and increase the value of these earlier Earth observation investments.

The Sensor Web will provide direct access to the sensors that gather the data rather than just to the resulting data sets. Users of the Sensor Web will be able to provide instructions to the sensors, thus adjusting what they observe and ensuring that the relevant data with the correct spatial and temporal definition are gathered.

The key to success for the Sensor Web will be the development of a set of standardized Internet-based web services. The Open Geospatial Consortium (OGC) is supporting the Sensor Web Enablement (SWE) initiative for open standards, including web service interface descriptions and data mark-up descriptions. These standards are continuously evolving and being improved.

N

0   3.5   7 km

Leopard range
boundaries

Female AS29
50
95

Female AS37
50
95

Female AS57
50
95

Male AS9
50
95

IN SITU OBSERVATION: PEOPLE POWER

CRITICAL ENVIRONMENTAL OBSERVATIONS can only be made by human observers on the ground – often referred to as *in situ* observations. For example, these South African researchers are collecting field data for a biodiversity study. Well-trained *in situ* observers provide high-quality data that are used for research and for calibrating or validating many other kinds of information gathered from remote observation systems.
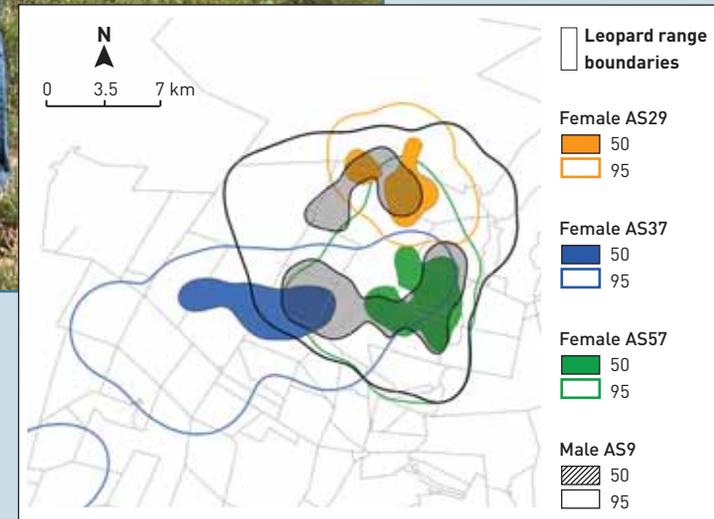
In situ observations are used for numerous studies, including weather, agriculture, ecosystems, biodiversity and many others. In the map above, ground observations have been used to investigate seasonal variation in diet and species richness, and to track the range of individual leopards, illustrating the overlapping boundaries of males and females.

TYPHOON LUPIT

In 2003, the Fourteenth Congress of the World Meteorological Organization (WMO) established The Observing System Research and Predictability Experiment (THORPEX). This international programme seeks to accelerate improvements in the accuracy and utility of high-impact weather forecasts up to two weeks ahead of an event.

Today, 10 of the world's leading weather forecast centres regularly contribute ensemble forecasts to the THORPEX Interactive Grand Global Ensemble (TIGGE) project in order to support the development of probabilistic forecasting techniques. Ensemble probabilistic forecasting is a numerical prediction method that uses multiple simulations, sometimes 20 or more, in a given time frame to generate a representative sample of the possible future states of weather systems.

Within the realm of numerical weather prediction, ensemble probabilistic forecasting is a major new tool for improving early warning of such high-impact events. This is particularly important for predicting severe tropical cyclones, also known as hurricanes and typhoons, which are the most powerful and destructive weather systems on the planet. The photo above shows damage caused by Typhoon Parma in the Philippines in September 2009.

Source: J. Van de Keere/Bloggen.be

Information for decision making: weather 85

TIGGE Ensemble Prediction System

In situ, airborne and satellite observations are used to initialize TIGGE Ensemble Prediction Systems (EPS1, EPS2, etc.). The EPS outputs can in turn be combined to generate weather prediction products. These can then be distributed via regional centres to national centres and end users. Ten of the world's leading weather forecasting centres regularly contribute ensemble forecasts to the TIGGE project. The map below shows how data are transferred from the forecast centres to three archiving centres.

Source: WMO.
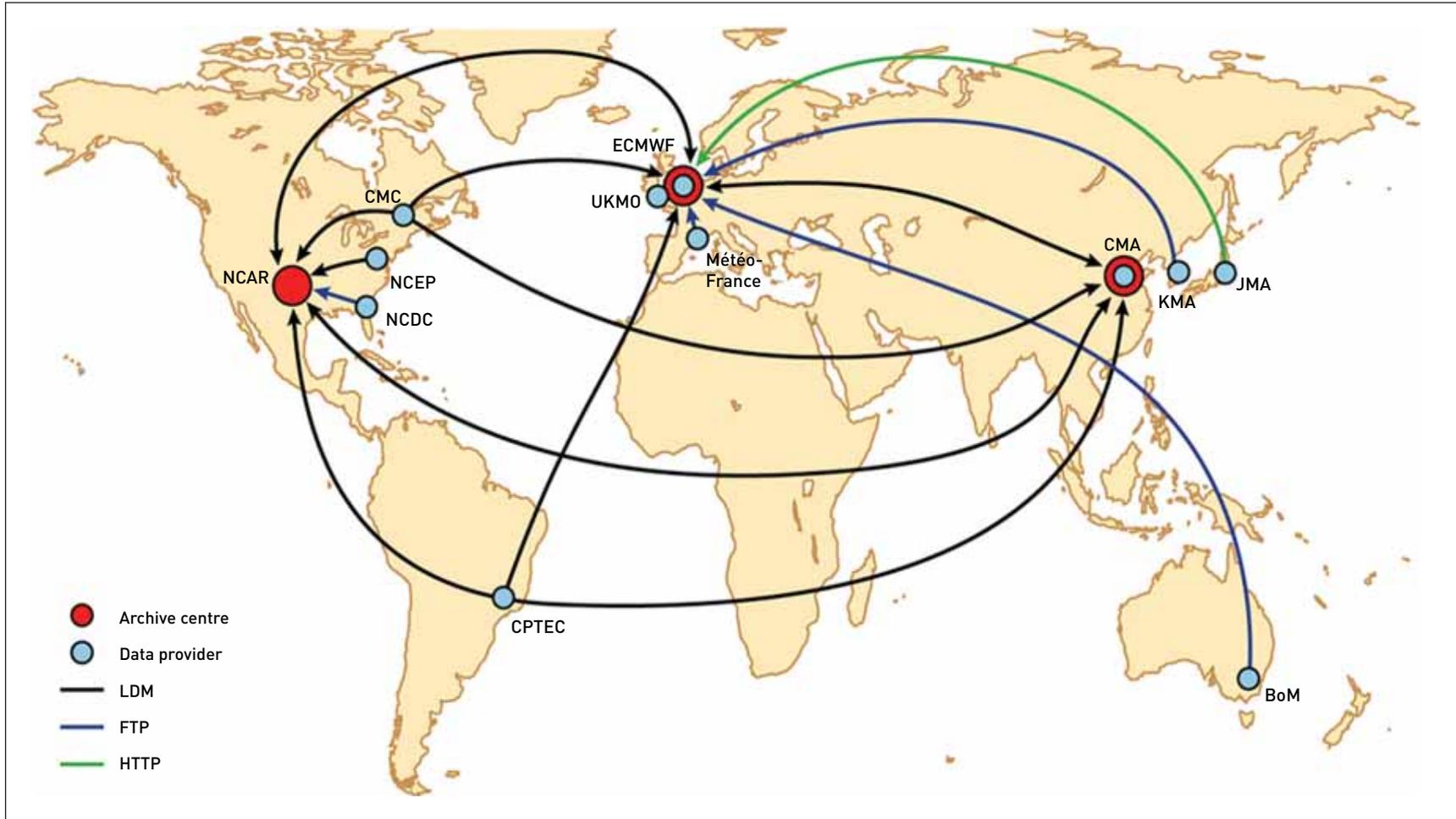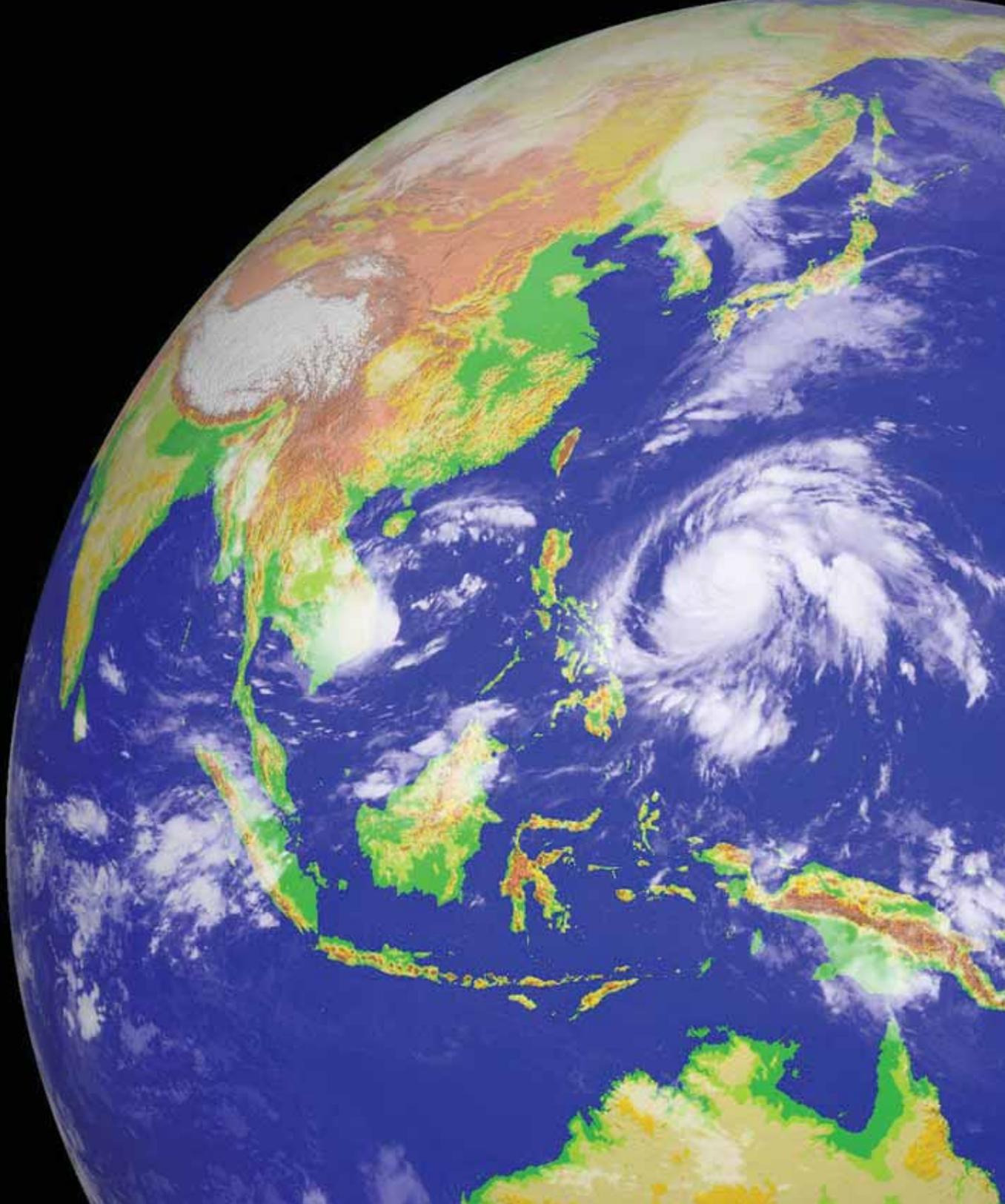
Typhoon Lupit

In October 2009, Typhoon Lupit approached the Philippines from the Pacific Ocean. Forecasters wanted to determine the storm's probable path and whether it would strike the Philippines, adding to the destruction recently brought by Typhoon Parma, or veer off in another direction. This is an example of how TIGGE can help with forecasts of tropical cyclones.

Source: Hurricane Lupit 17 October 2009 MTSAT-1R processed by Japan's National Institute of Informatics.

Information for decision making: weather 87

Forecasting Typhoon Lupit's path

The US/Japan Tropical Rainfall Measuring Mission (TRMM) observed that some of Lupit's towering thunderstorms reached as high as 14 kilometres (more than 8.5 miles), indicating very powerful storms with heavy rainfall threat.

Source: TRMM.

TRMM Precipitation Radar

200km

Light rain   Moderate rain   Heavy rain
15 20 25 30 35 40 45 50 50 55 dBZ
10/17/2009 1629Z LUPIT West Pacific
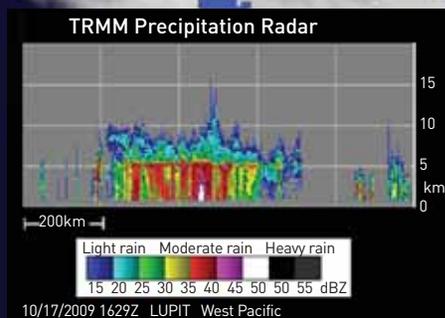
Four-day forecast of Typhoon Lupit's path: 18 October
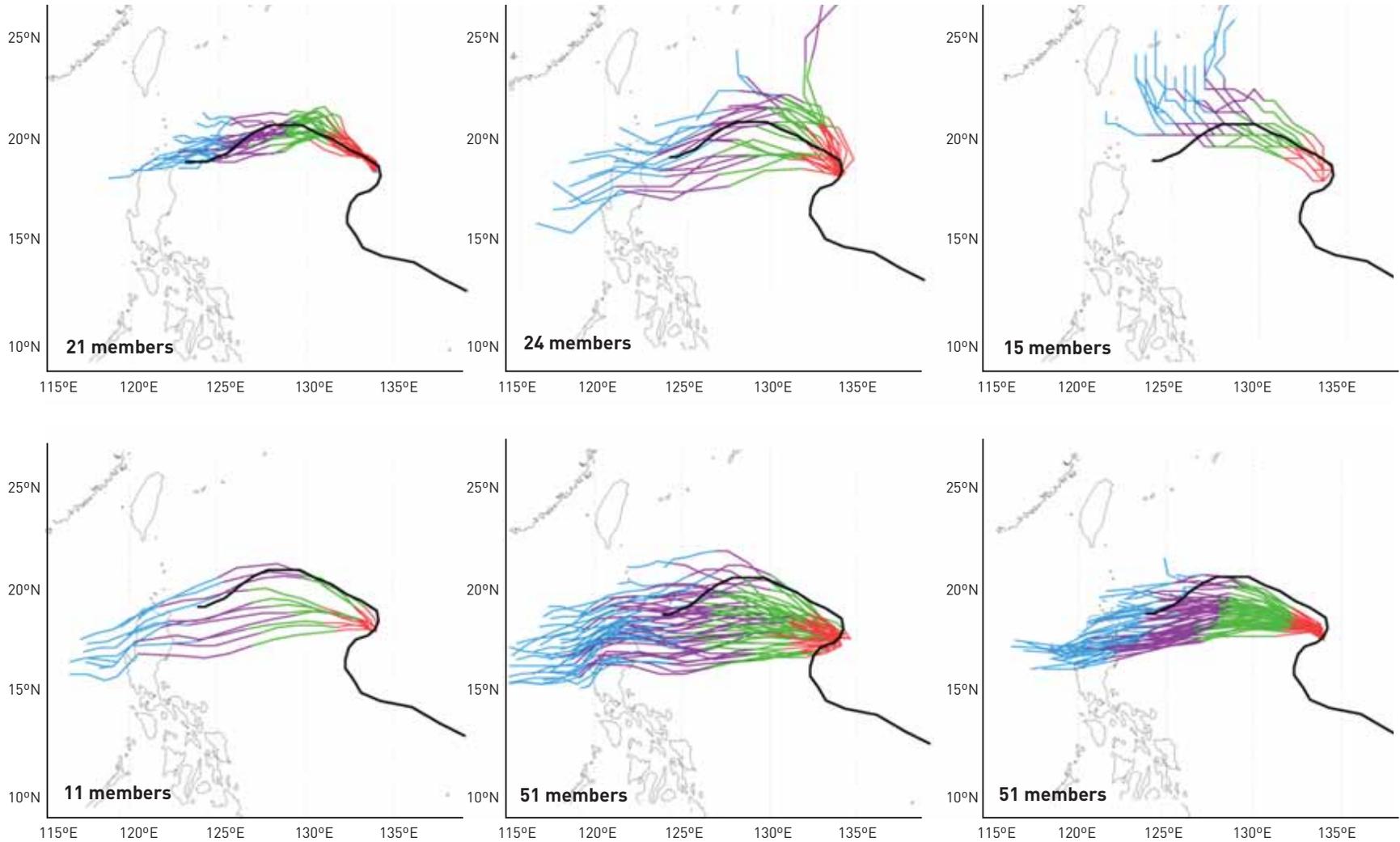
Source: JMA.

Forecast paths of Typhoon Lupit, 18 October 2009, 12:00 UTC, from six of the TIGGE data providers, as displayed on the Japanese Meteorological Research Institute's tropical cyclone forecast website.

The colour changes every 24 hours along each forecast track. The black line is the storm's actual path (as recorded *a posteriori*).

Nine-day forecast of Typhoon Lupit's path: 18 October

These images show the UK Met Office's early forecasts for Lupit (left). Based on these tracks, it was forecast (right) that there was a high probability of the typhoon striking the northern end of the Philippines – but there is also a hint that the hurricane could instead turn toward the northeast.

Ensemble forecast tracks   **Lupit 18 Oct 2009**   Strike probabilities

Colour change each 24 hours in forecast

- T0-24
- T24-48
- T48-72
- T72-96
- T96-120
- T120-144
- T144-168
- T168-192
- T192-216

Probability the storm will pass within 75 miles

- 5-19%
- 20-39%
- 40-59%
- 60-79%
- 80-100%

Source: UK Met Office.

90 Crafting geoinformation
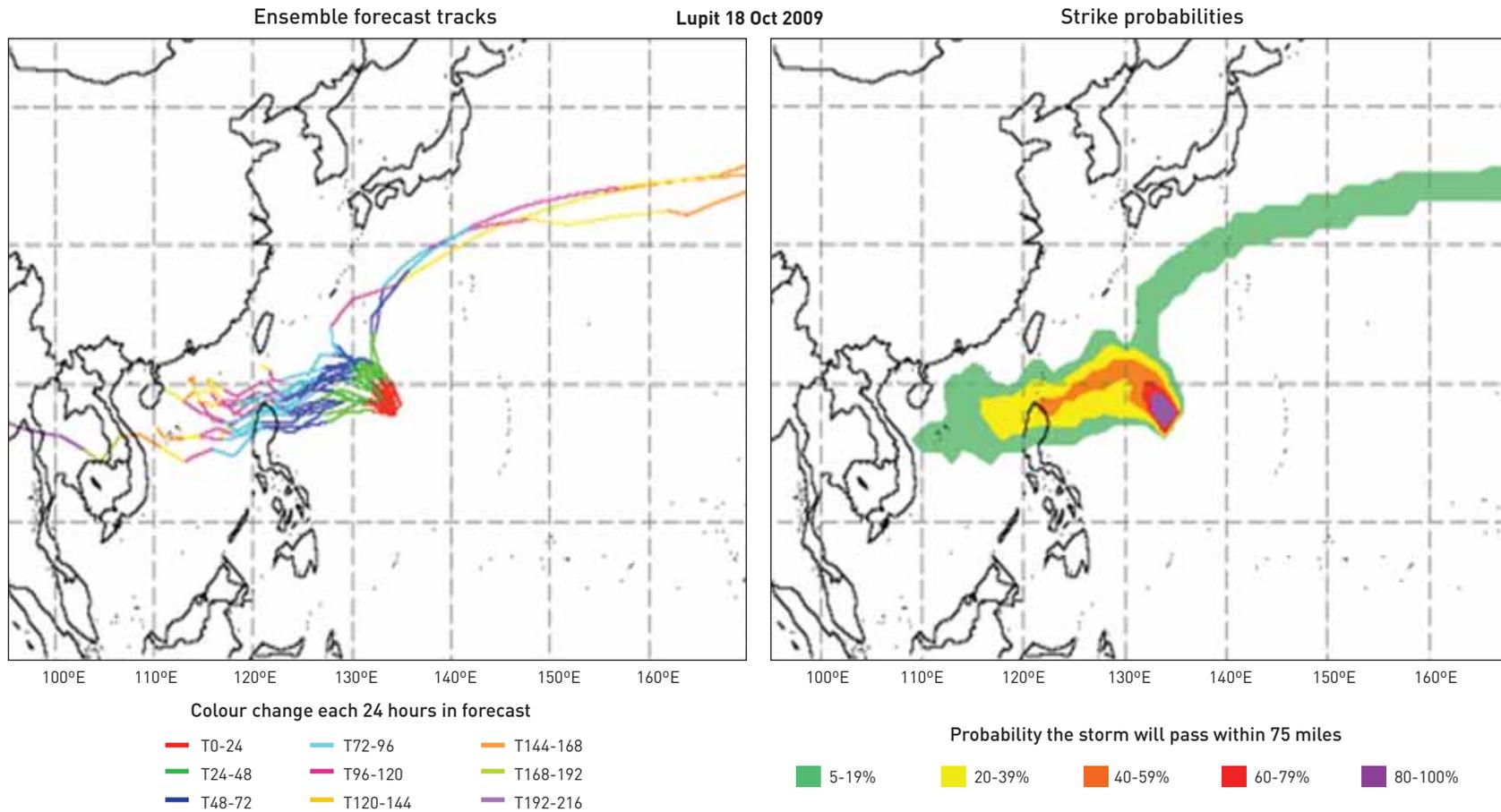
Forecasting Typhoon Lupit's path: 21 October

Later ensemble forecasts showed increasing probability that Lupit would turn north-eastward, as shown on this web site display from the US National Oceanic and Atmospheric Administration (NOAA). Forecast tracks are shown in colour, with the actual track in black. Lupit is shown clearly turning north, sparing the Philippines this time.

Source: NOAA.

21 October 2009 12Z
ECMWF (51) members
UKMO (51 members)
NCEP (21 members)
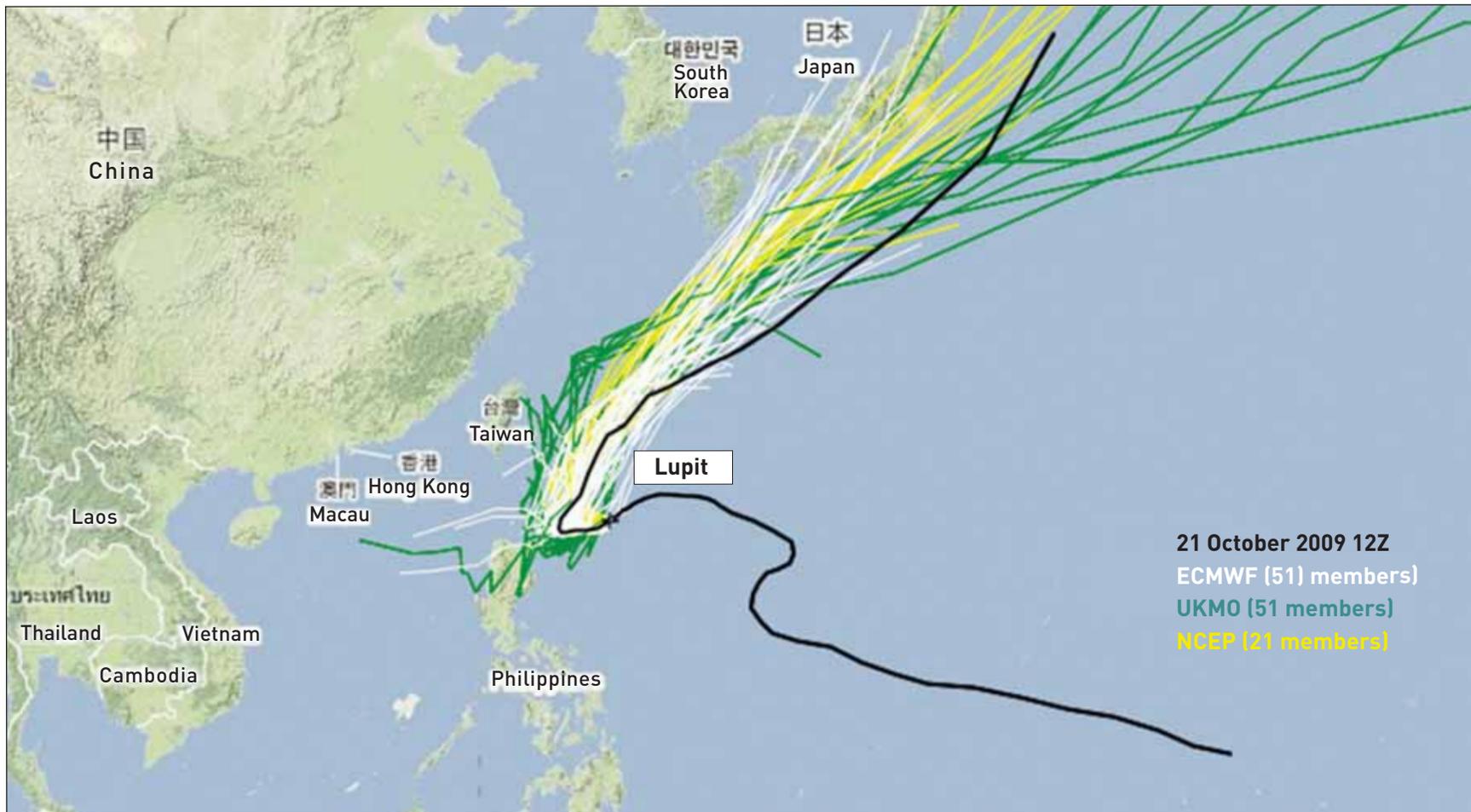
ECOSYSTEM SERVICES

Ecosystems provide many valuable products and services, from food, fuel and fibre to purification of water, maintenance of soil fertility and pollination of plants. To sustain these societal benefits, managers need to fully understand the types, spatial patterns, scales and distributions of the ecosystems under their care. Some of the critical tools they rely on are ecosystem classifications and maps at scales ranging from global to local. The ecosystem mapping activities described in the following pages are being carried out by the US Geological Survey and its partners.

Source: USGS.

Ecosystem structure

An ecosystem can be viewed as a spatial integration of its landforms, climate regime, vegetation and other features that occur in response to the physical environment.

ECOSYSTEM

- Macroclimate
- Topoclimate
- Biota
- Landform
- Surface water
- Soils
- Groundwater
- Bedrock

Source R. Bailey/US Forest Service.

Information for decision making: ecosystems 93
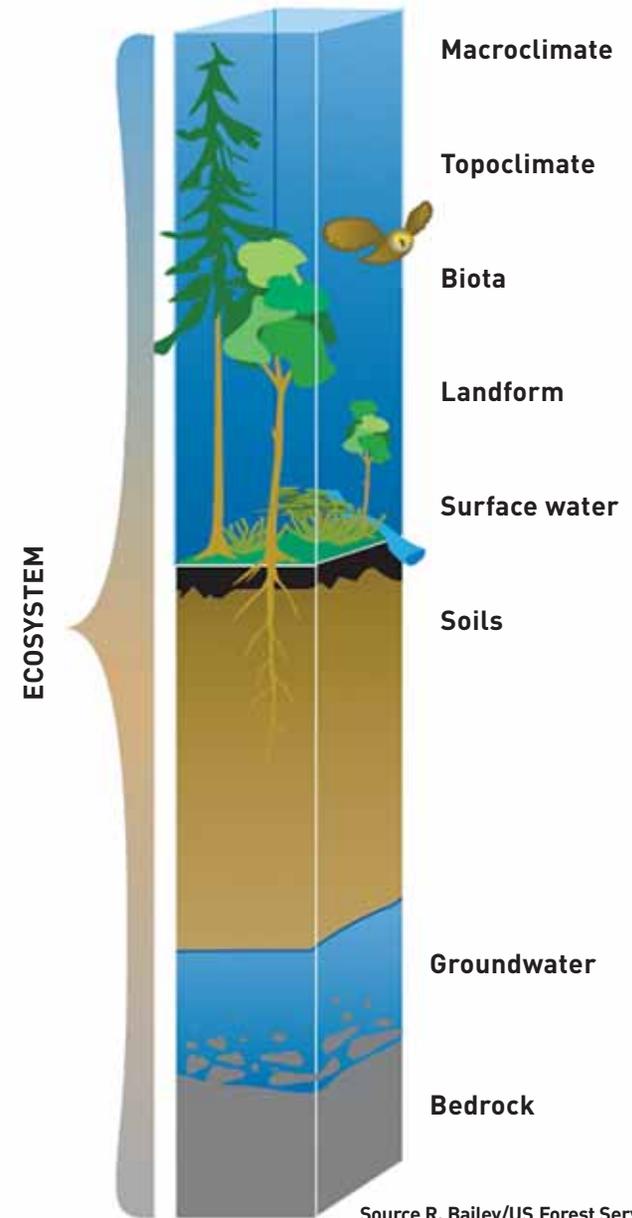
Bioclimate maps

Satellite and *in situ* observations are the building blocks for creating the elements of ecosystem structure. The observations are processed using a range of techniques; for example, bioclimate is modelled from *in situ* and automated weather station observations.

Key environmental data layers are first developed for large regions or continents. They include landforms, geology, bioclimate regions and land cover. These data layers serve as input data into models to map ecosystems.

Source: TNC/NatureServe.

Legend:
- Tropical pluvial
- Tropical pluvial/seasonal
- Tropical xeric
- Tropical desertic/hyperdesertic
- Mediterranean pluvial/seasonal oceanic
- Mediterranean xeric oceanic
- Mediterranean desertic/hyperdesertic
- Temperate hyperoceanic/oceanic
- Temperate xeric
- Boreal hyperoceanic

Legend (left column):
- Moorland/heathland
- Closed steppe grassland
- Grassland
- Barren
- Desert
- Salt pan
- Water
- Montane transitional forest
- Montane flooded forest

Legend (center column):
- Tree cover, broadleaf evergreen forest
- Bamboo dominated forest
- Tree cover, broadleaf deciduous forest
- Mangrove
- Freshwater flooded forest
- Permanent swamp forest
- Temperate evergreen forest
- Temperate mixed forest
- Temperate deciduous broadleaf forest
- Converted vegetation
- Degraded vegetation
- Herbaceous cover
- Shrub savannah
- Periodically flooded savannah
- Closed shrubland
- Sparse herbaceous
- Periodically flooded shrubland

Scale bar: 0 — 500 — 1,000 km / 0 — 250 — 500 miles

Land cover maps

Land cover maps are produced by using statistics to categorize regions in multispectral satellite images as particular land cover types.

Source: TNC/NatureServe.

Towards a global ecosystems map: South America

The ecosystem structure approach to ecosystem mapping involves mapping the major attributes of the physical environment that contribute to the ecosystem's structure. Satellite imagery, field observations and other data are used to characterize the biological and physical environment. These data are then integrated and interpreted in order to present a coherent picture of each ecosystem.

The resulting ecosystem map can be used for a variety of applications, such as climate change assessments, ecosystem services evaluations, conservation applications and resource management.

Source: TNC/NatureServe.

Terrestrial ecosystems
- Forest
- Flooded forest
- Savannah
- Flooded savannah
- Shrubland
- Flooded shrubland
- Grassland
- Desert
- Barren
- Salt
- Water
- Converted

Towards a global ecosystems map: United States of America

The methodology for producing ecosystems maps using Earth observation data has been implemented for several continental regions and a global ecosystem map is in development.

Source: USGS.

Terrestrial ecosystems

- Forest and woodland ecosystems
- Herbaceous ecosystems
- Shrubland ecosystems
- Steppe/savannah ecosystems
- Woody wetland ecosystems
- Herbaceous wetland ecosystems
- Sparsely vegetated ecosystems
- Water
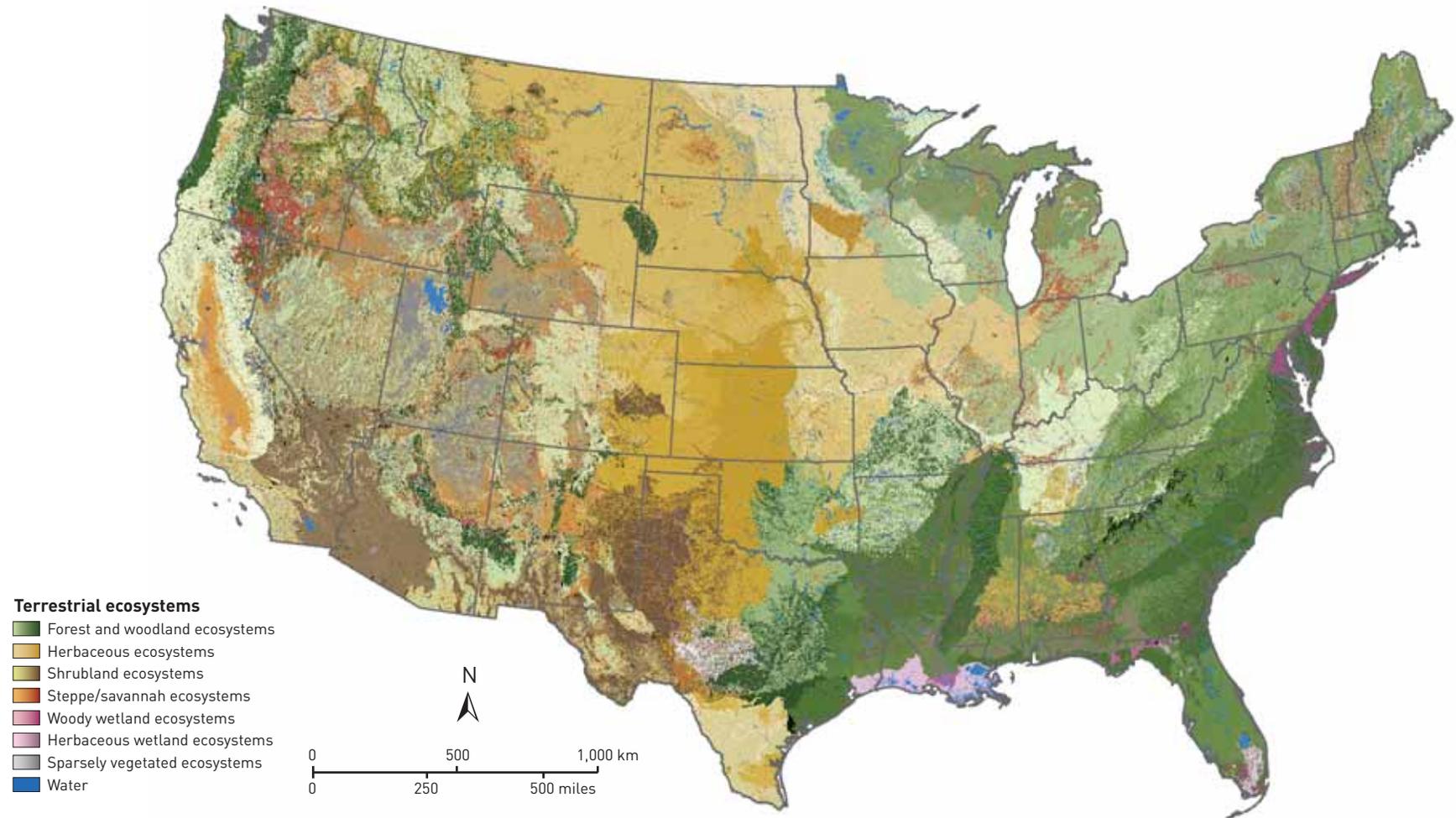
Towards a global ecosystems map: Sub-Saharan Africa

Sub-Saharan ecosystems

- African temperate dune vegetation
- African tropical freshwater marsh (dembos)
- Antostema-Alstoneia swamp forest
- Baikiaea woodland and savannah
- Bushmanland semi-desert scrub and grassland
- Central Congo Basin swamp forest
- Central Indian Ocean coastal forest
- Drakensberg grassland
- Dry Acacia woodland and savannah
- Dry Acacia-Terminalia-Combretum woodland and savannah
- Dry Combretum-mixed woodland and savannah
- Dry miombo
- Eastern Africa Acacia woodland
- Eastern Africa Acacia-Commiphora woodland
- Eastern Africa bushland and thicket
- Etosha salt pans
- Gabono-Congolian mesic woodland and grassland
- Gariep desert
- Guineo-Congolian evergreen rainforest
- Guineo-Congolian littoral rainforest
- Guineo-Congolian semi-deciduous rainforest
- Guineo-Congolian semi-evergreen rainforest
- Indian Ocean mangroves

- Kalahari camel thorn woodland and savannah
- Limpopo mopane
- Lower Karoo semi-desert scrub and grassland
- Lowveld-Limpopo salt pans
- Makarenga swamp forest
- Moist Acacia (-Combretum) woodland and savannah
- Moist highveld grassland
- Namaqualand Hardeveld
- Namibia-Angola mopane
- North Sahel steppe herbaceous
- North Sahel treed steppe and grassland
- Pro-Namib semi-desert scrub
- Southern Indian Ocean coastal forest
- Southern Kalahari dunefield woodland and savannah
- Southern Namib Desert
- Southern Namibian semi-desert scrub and grassland
- Sudano-Sahelain herbaceous savannah
- Sudano-Sahelain shrub savannah
- Sudano-Sahelain treed savannah
- Upper Karoo semi-desert scrub and grassland
- Wet miombo
- Zambezian Cryptocepalum dry forest
- Zambezi mopane
- Zululand-Mozambique coastal swamp forest

Source: USGS.

FOOD SECURITY

The GEO Global Agricultural Monitoring Community of Practice is leading the effort to develop a global agricultural monitoring system of systems. Based on existing national and international agricultural monitoring systems, this comprehensive network will improve the coordination of data and indicators on crop area, soil moisture, temperature, precipitation, crop condition, yield and other agricultural parameters. The end result will be better forecasting of agricultural yields and enhanced food security.

Crop mapping

Probability
0
100
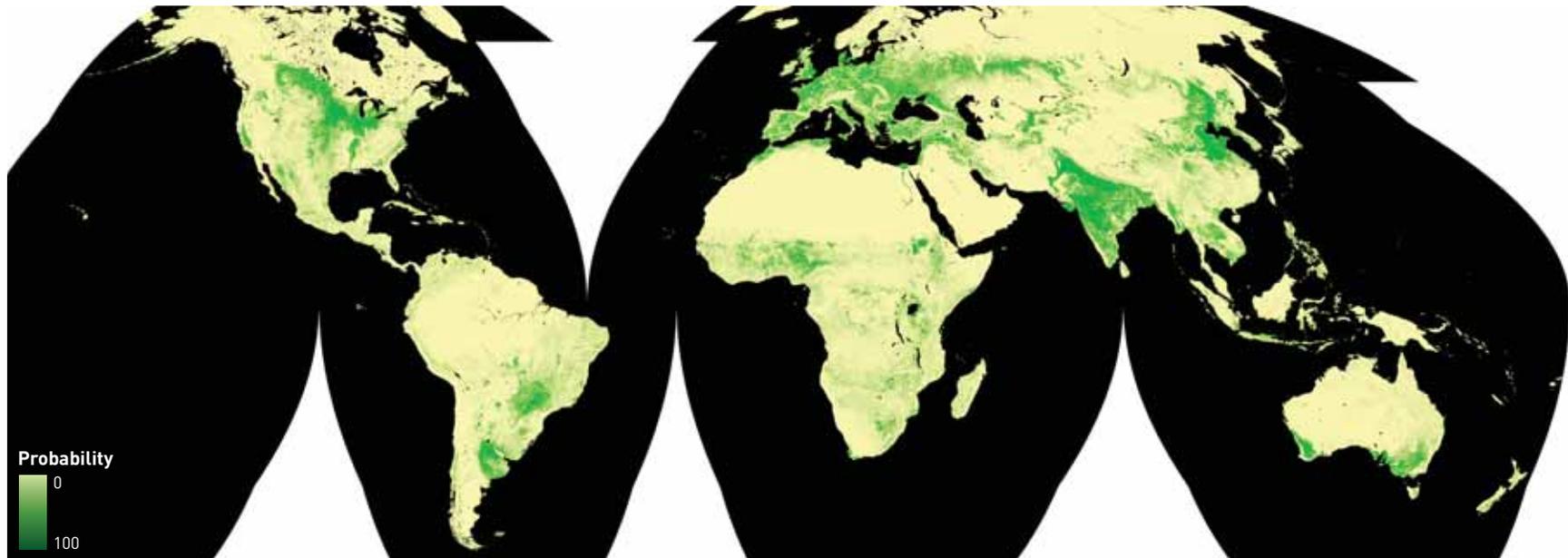
Multiple spatial and temporal scales of Earth observation data are needed for monitoring agriculture because cropping systems vary widely in terms of field size, crop type, cropping intensity and complexity, soil type, climate, and growing season. This global crop land distribution map (top), based on 250 metre resolution data from the MODIS Earth Observing Satellite sensor, is useful for monitoring global vegetation conditions and identifying anomalies.

Source: MODIS.

The image of the Indian state of Punjab (right) is based on 30–65 metre resolution images. Even finer resolutions, down to 6 metres, are used for monitoring at the district and village levels.

Source: AWiFS/NASA.

Crop rotation in Punjab State, 2004-05

- Rice / wheat
- Cotton / wheat
- Maize-based
- Sugar cane-based
- Cotton / other crops
- Rice / other crops
- Other crops / wheat
- Triple cropping
- Other rotations
- Non-agriculture
- District boundary
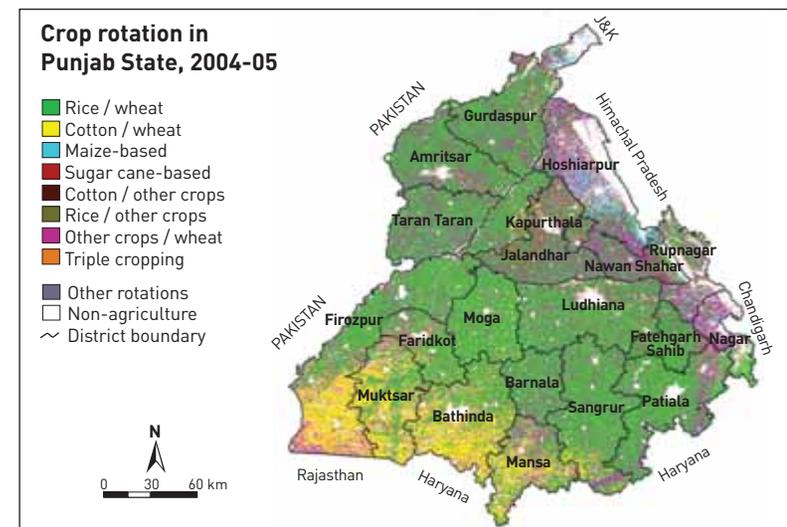
Crop yield models

Crop yield models are a critical tool for decision making on agriculture and food security, and daily weather data are a critical input for these models. These data are gathered by weather stations and coordinated on a global basis. This image depicts zones in Europe that suffered from high temperatures throughout June and July 2010 and where the crop model depicts soil moisture values for spring barley 20 per cent below the average.

Dry and hot regions
Number of days with temperature over 30ºC
in areas with low soil moisture

Number of days
- 1 - 3
- 4 - 6
- 7 - 9
- 10 - 12
- 13 - 15
- 16 - 18
- 19 - 21
- 21 +

Crop analysed: spring barley soil moisture/soil moisture 20% below the average
Period of analysis: 11 June 2010 - 20 July 2010
Data source: MARS agrometeorological database
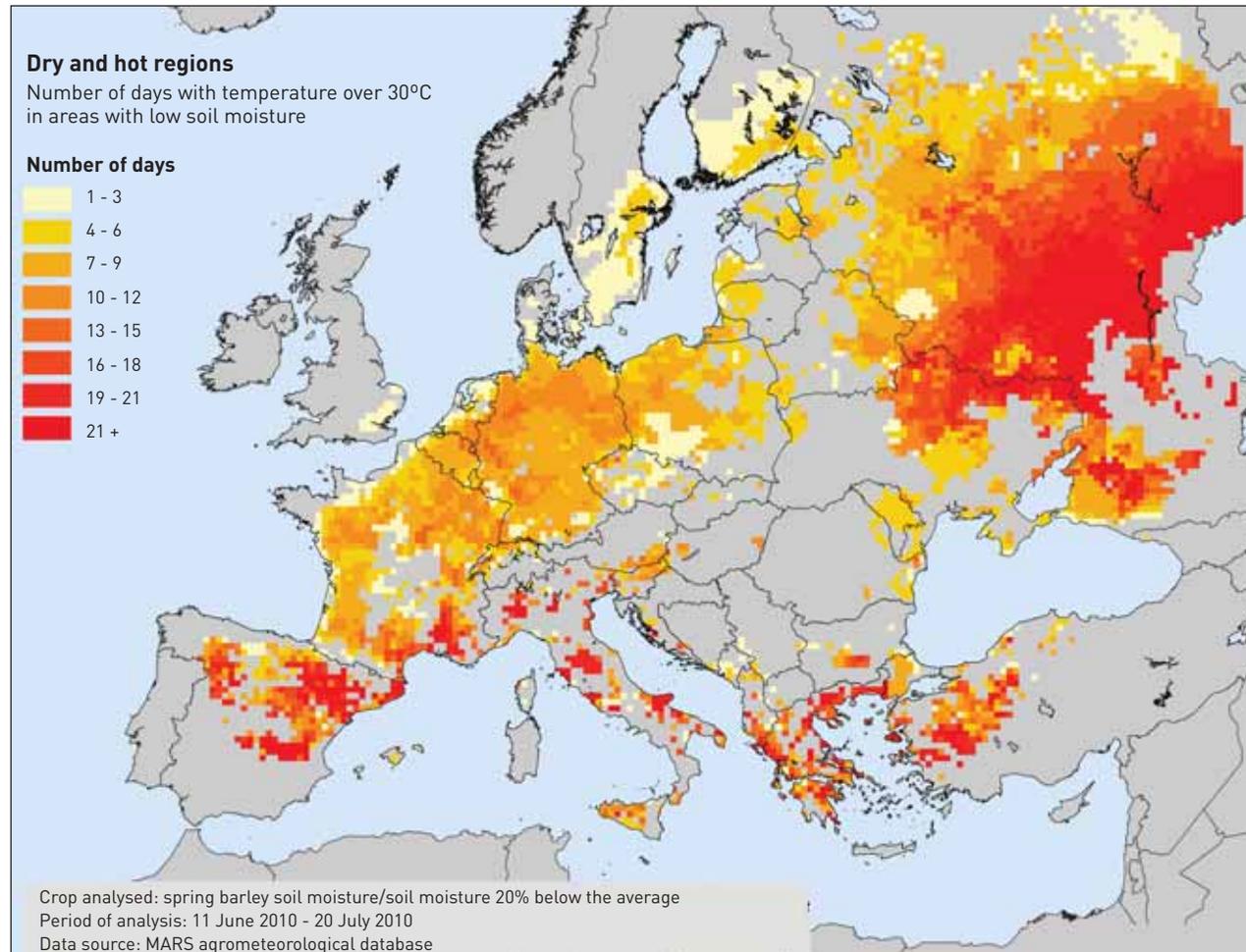
Modelling heat stress

Another example based on observed meteorological data shows areas
where crops are under stress conditions due to consecutive days with high
temperatures.

Number of heat waves
> = 2 consecutive days where TMAX > 30, cumulated values
From 11 June 2010 to 10 July 2010

Number of occurrences
- 0
- > = 1- < 2
- > = 2- < 3
- > = 3- < 4
- > = 4

13/07/2010
Interpolated grid
of 25x25km

Source: National Meteorological Services
Processed by Alterra Consortium on behalf
of AGRI4CAST Action - MARS Unit
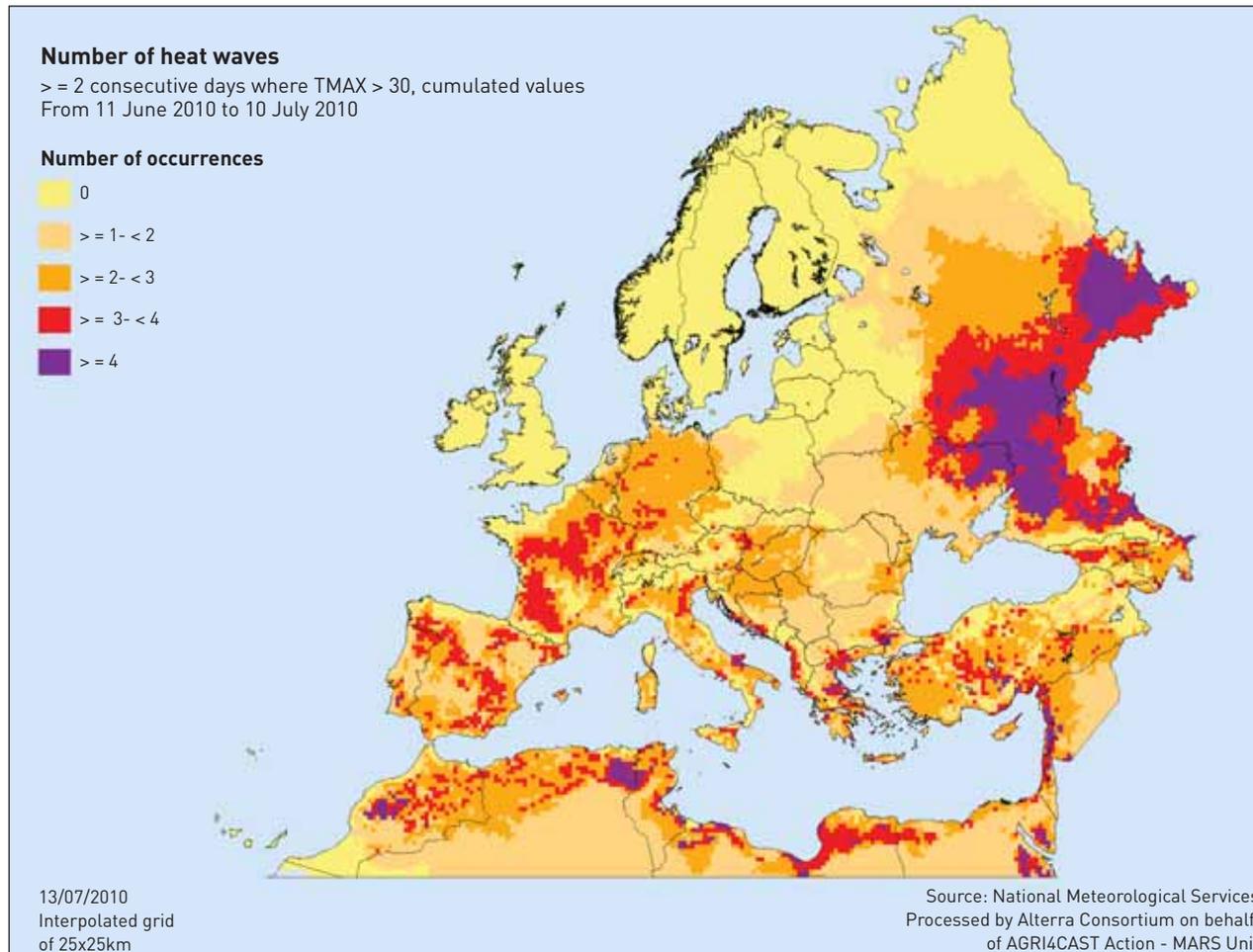
Monitoring agricultural areas

Besides crop models which are used for qualitative forecasts, low-resolution data are used to monitor agricultural areas. Below is an example from the JRC MARS Remote Sensing database. The map displays the results of a cluster analysis of NDVI (Normalized Difference Vegetation Index) values throughout the season from March to June. The NDVI, a "greenness index", is an indicator of green biomass derived from satellite observations and widely used for vegetation monitoring. The diagram displays the early start of the season around the Mediterranean Basin and the winter dormancy of most crops in central Europe.

Clustering: arable land
based on NDVI actual data
SPOT-Vegetation (P) from 1 October to 30 April 2010
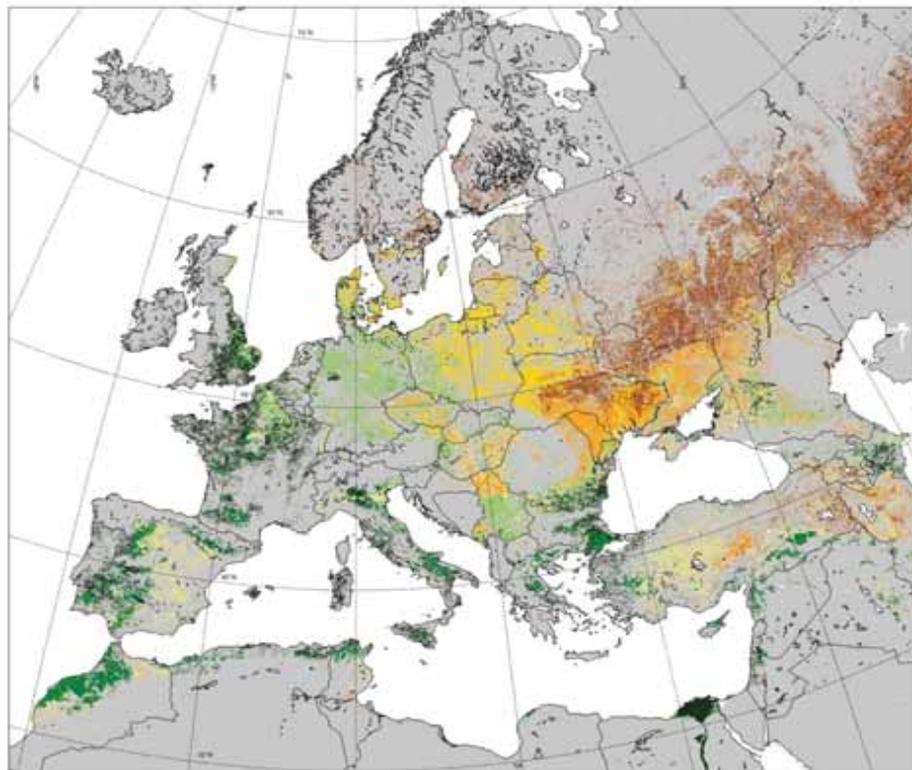
Clusters
- 11%
- 10%
- 14%
- 15%
- 15%
- 14%
- 19%
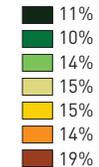
- Masked
- No data

Produced by VITO (BE)
on behalf of the
AGRI4CAST Action
AGRICULTURE Unit
on 02 May 2010

10-daily NDVI [-]

2009/2010
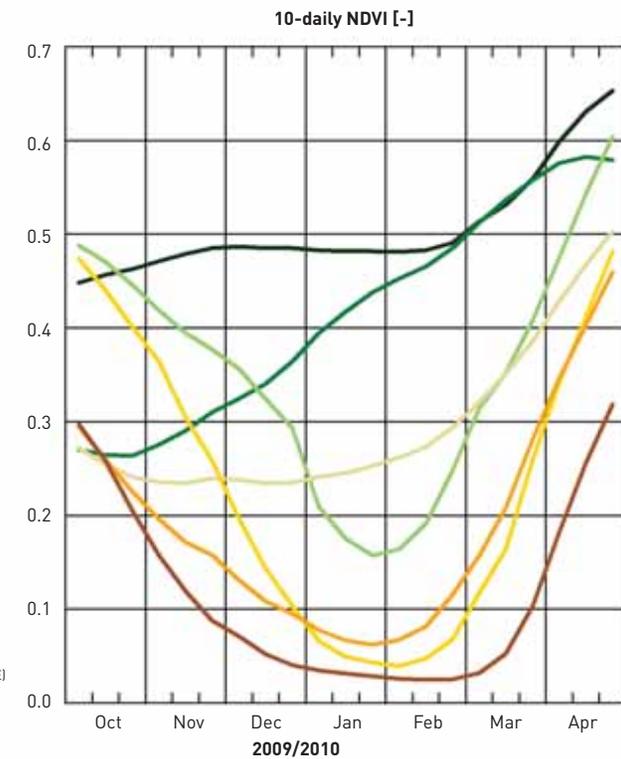
Rainfall estimates

Daily rainfall is also a key input for crop yield models. It is estimated by integrating satellite-derived precipitation estimates with weather-station observations, as presented in the example below from the Famine Early Warning System Network (FEWS-NET) system.

Rainfall estimates 6 - 11 August 2010

Daily totals (mm)

☐	0 - 0.1
☐	0.1 - 1
☐	1 - 2
☐	2 - 5
☐	5 - 10
☐	10 - 15
☐	15 - 20
☐	20 - 30
☐	30 - 40
☐	40 - 50
☐	50 - 75
☐	> 75
☐	No data

6 August 2010

7 August 2010

8 August 2010

9 August 2010

10 August 2010

11 August 2010

Data:
NOAA-RFE 2.0

Famine early warning

Crop water requirement

**Crop WRSI
Grains: 2010-08-1**

- < 50 failure
- 50 - 60 poor
- 60 - 80 mediocre
- 80 - 95 average
- 95 - 99 good
- 99 - 100 very good
- No start (late)
- Yet to start
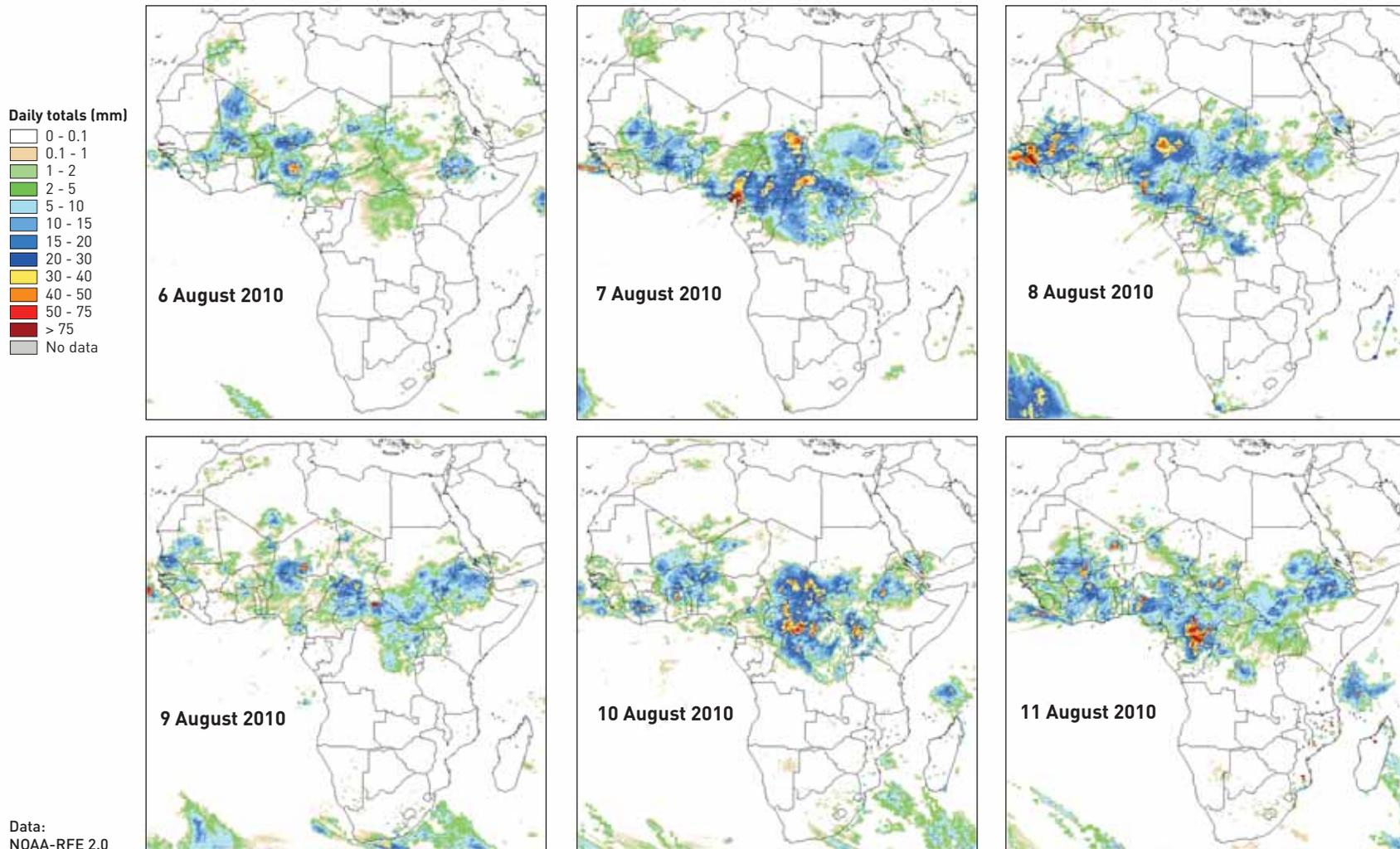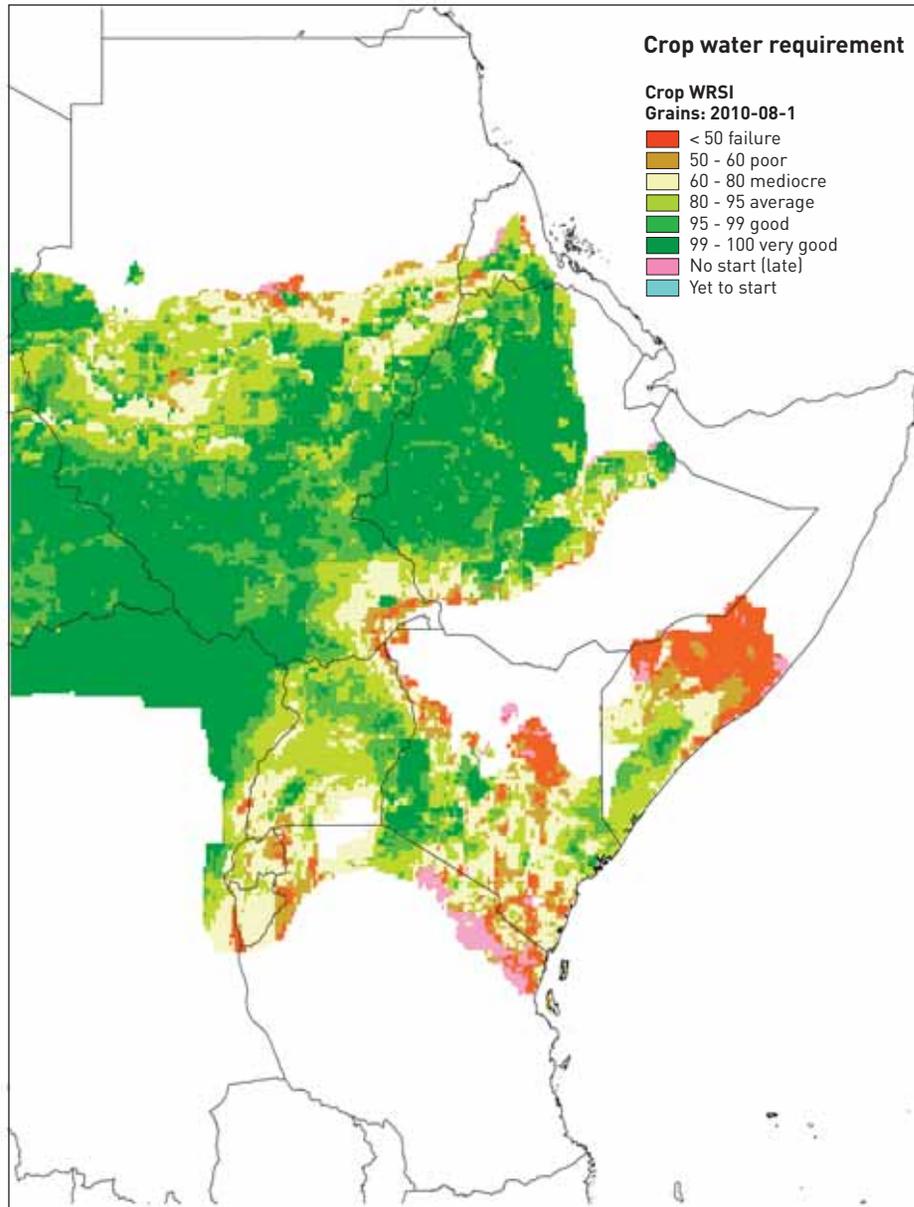
Effective early warning of famine is vital for quickly mobilizing food aid and other support. Areas of maize crop failure due to drought in the Greater Horn of Africa in August 2009 are here indicated in pink and red, based on the Water Requirement Satisfaction Index (WRSI).

Source: FEWS-NET.

Calculating NDVI anomalies

NDVI anomalies can be calculated on a regular basis to identify vegetation stress during critical stages of crop growth. An example below shows how drought effects on crops were tracked during 2010 over Central America using vegetation index data. The image from the Moderate Resolution Imaging Spectroradiometer (MODIS) contrasts the conditions between data collected from 2000 to 2009 (average conditions) and the conditions under the drought of 2010. The brown and red areas on the Mexico–Guatemala border indicate the areas affected by the drought where the vegetation index is lower than average, meaning that less photosynthesis was occurring.

Central America - eMODIS 250m NDVI Anomaly Period 2, 1-10 January 2010
2010 minus average (2001-2008)

NDVI anomaly
	< -0.3
	-0.2
	-0.1
	-0.05
	-0.02
	No difference
	0.02
	0.05
	0.1
	0.2
	> 0.3
	Water
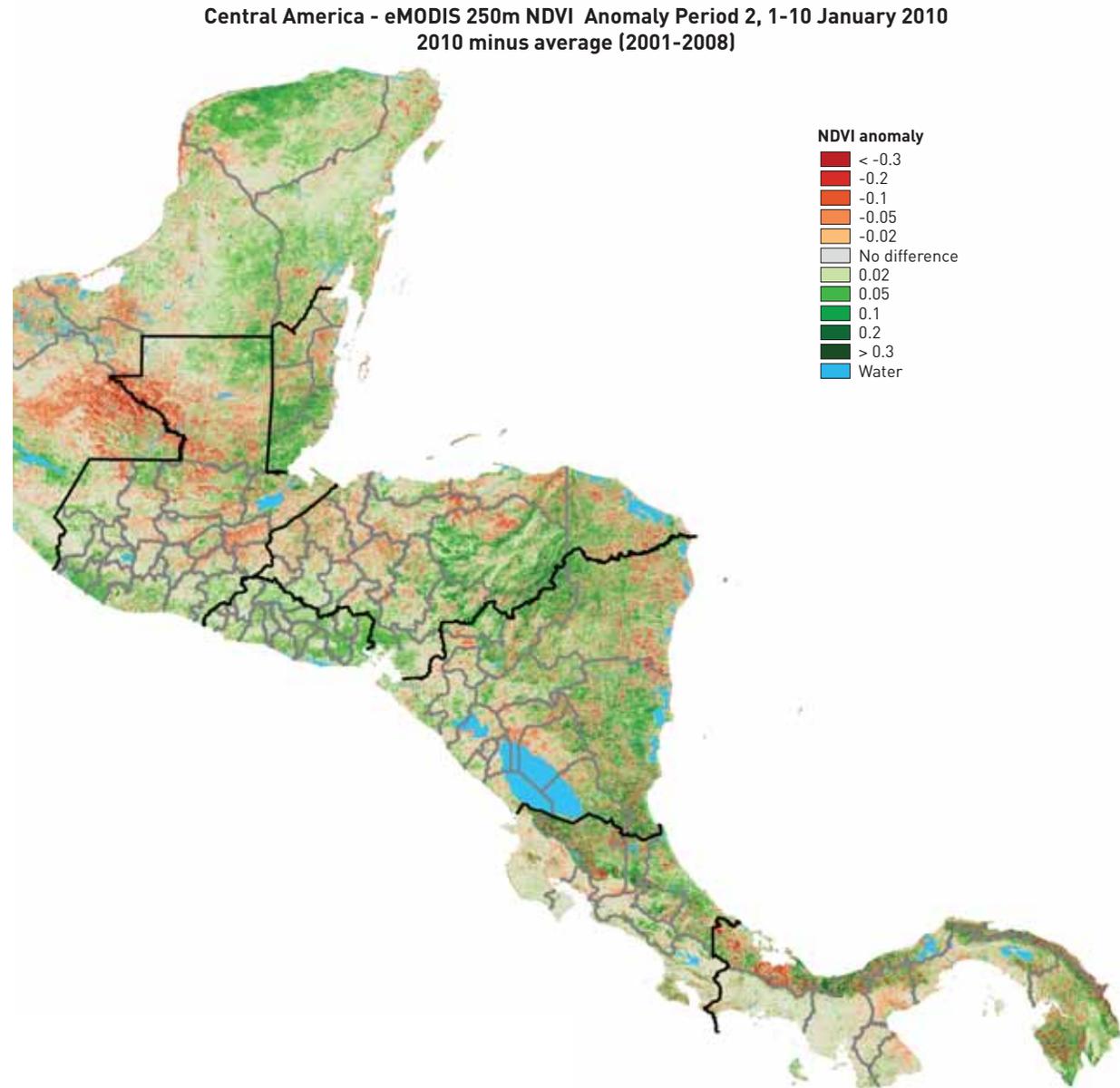
Source: MODIS.

Crop assessment

The timely and accurate assessment of crop condition is a determining factor in the process of decision making in response to crop stress. Crop condition maps and crop growth profile charts of several provinces in China in mid-April 2009, retrieved from the global Crop Watch System, show the crop condition in drought-affected areas relative to the previous year. The crop growth profile charts of three selected provinces illustrate how crop growth responds to drought conditions.

Source: China CropWatch System.

Crop condition in China, April 2009

- Significantly improved
- Improved
- Normal
- Worse
- Significantly worse
- No data

Crop-growing profile - Shandong
- Max 2005-09
- Average 2005-09
- 2009
- 2010

Crop-growing profile - Henan
- Max 2005-09
- Average 2005-09
- 2009
- 2010

Crop-growing profile - Anhui
- Max 2005-09
- Average 2005-09
- 2009
- 2010
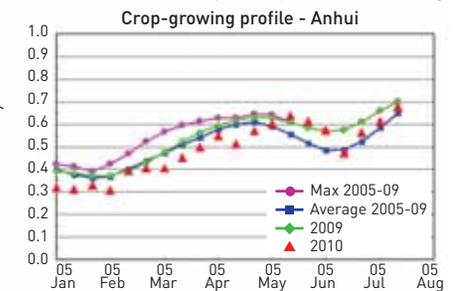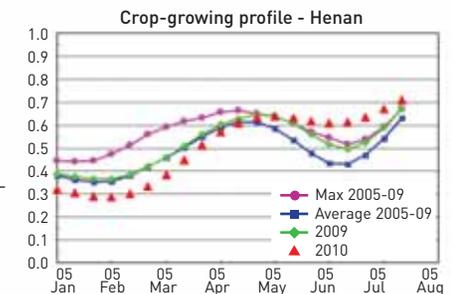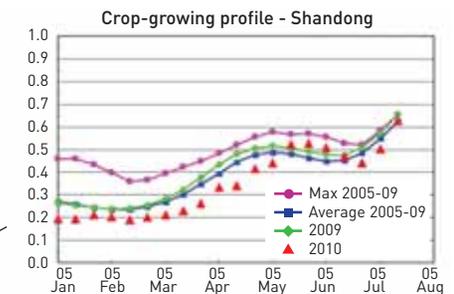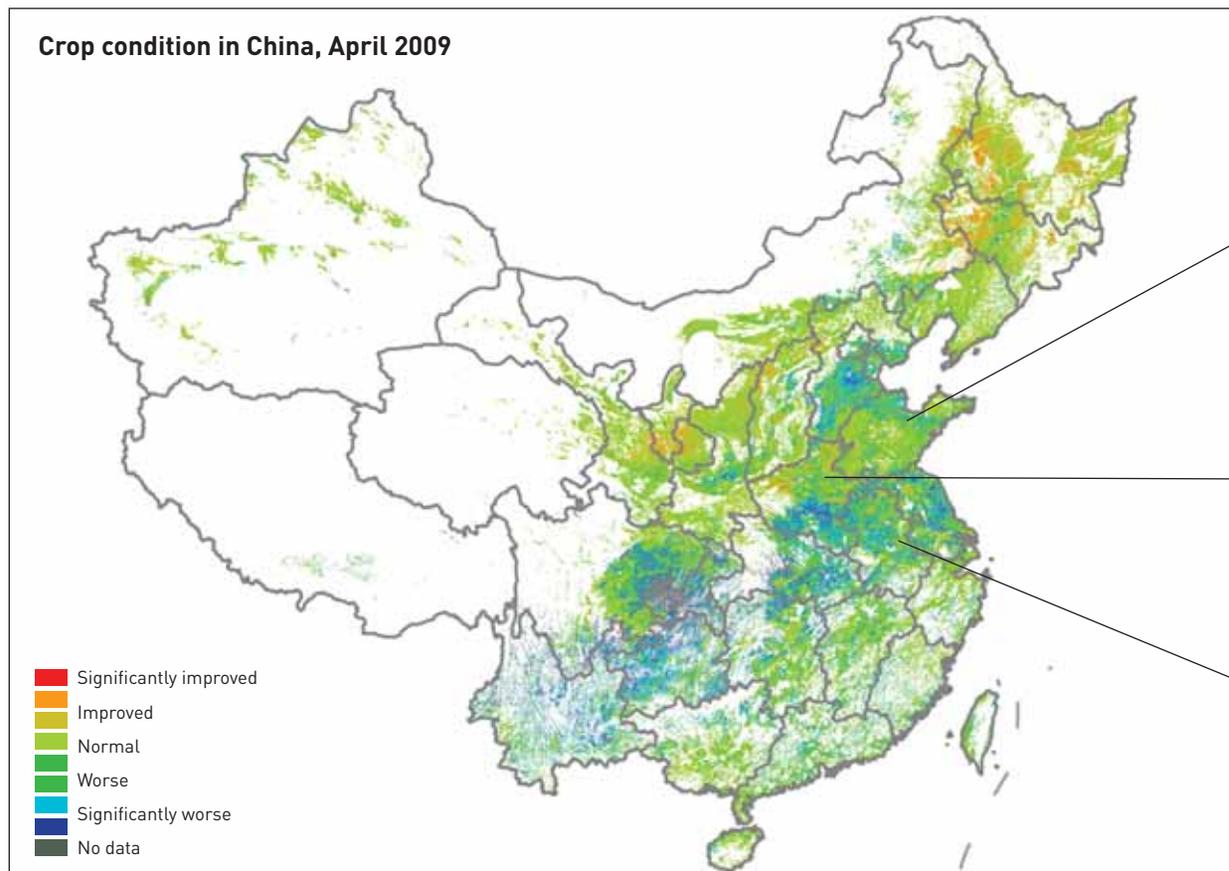
PROTECTED AREAS

Protected areas are often seen as a yardstick for evaluating conservation efforts. While the global value of protected areas is not in dispute, the ability of any given area to protect biodiversity needs to be evaluated on the basis of rigorous monitoring and quantitative indicators.

The GEO Biodiversity Observation Network (GEO BON) African Protected Areas Assessment demonstrates how field observations combined with satellite imaging can be combined to assess the value of protected areas.

Data for 741 protected areas across 50 African countries have been assembled from diverse sources to establish the necessary information system. The data cover 280 mammals (including the African wild dog pictured here), 381 bird species and 930 amphibian species as well as a large number of climatic, environmental and socioeconomic variables.
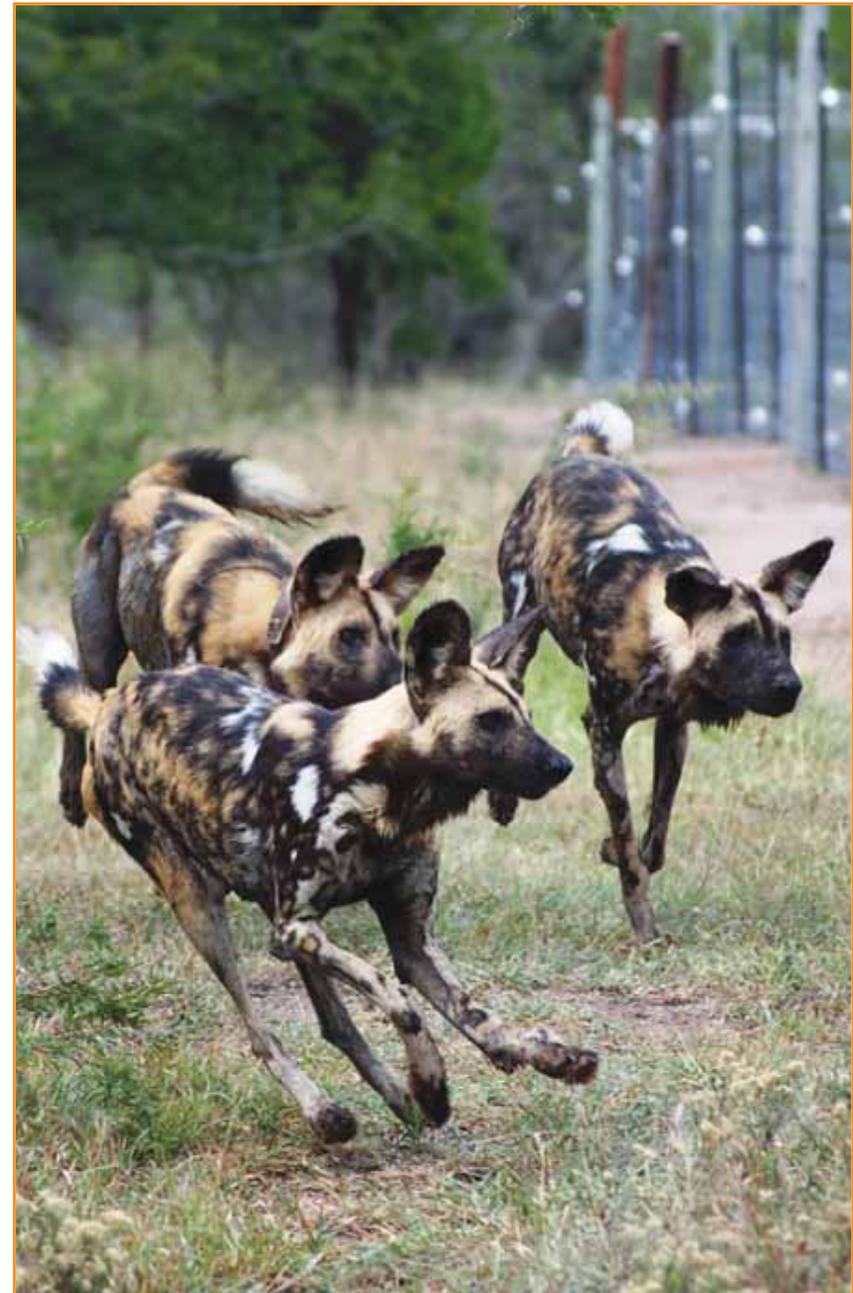
Source: P. Becker and G. Flacke.

Assessing pressures on biodiversity
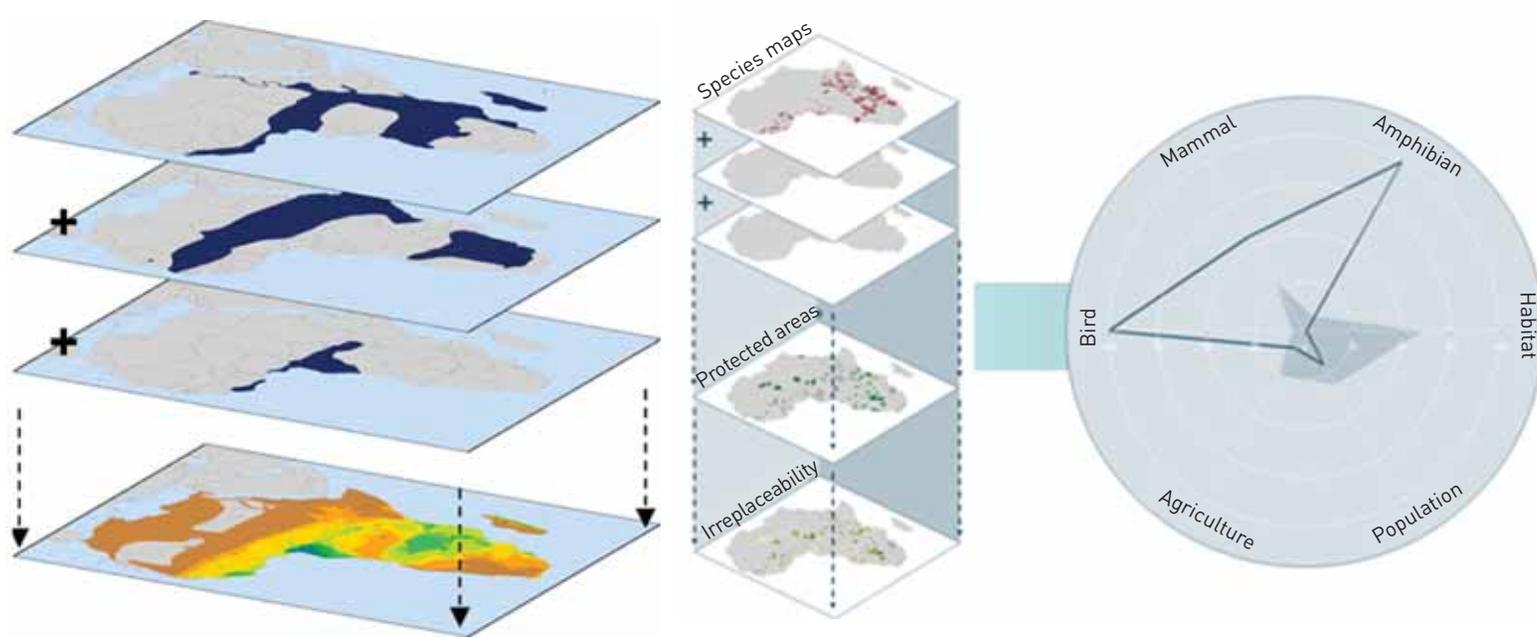
Indicators of Protected Areas Irreplaceability (where the loss of unique and highly diverse areas may permanently reduce global biodiversity) and Protected Areas Threats are developed as practical and simplified estimates of the highly complex phenomenon of biodiversity. They are established using a wide range of geographic, environmental and species data from the World Database on Protected Areas and other sources. The habitat of each protected area is characterized on the basis of its climate, terrain, land cover and human population. The data layers are then integrated and the multiple pressures on biodiversity are assessed.

Protection status

This map shows the protected areas in Africa. The colour code indicates their protection status. The information is gathered from national governments and international agencies and is used by the assessment team as its starting point.

Categories of protected area management

- Ia Science
- Ib Wilderness protection
- II Ecosystem protection and recreation
- III Conservation of specific natural features
- IV Conservation through management intervention
- Convention on wetlands of international importance
- UNESCO World Heritage Convention
- Other national parks

Vegetation index

The following three continent-scale maps have been processed to show the vegetation index, the percentage of land covered by trees and crops, and the land elevation.

Source: NASA.

Vegetation index

0

0.3

0.6

0.9

Cropland and tree cover

Per cent cropland
- 30 – 40
- 40 – 60
- > 60

Per cent tree cover
- < 10
- 10 – 30
- 30 – 60
- > 60
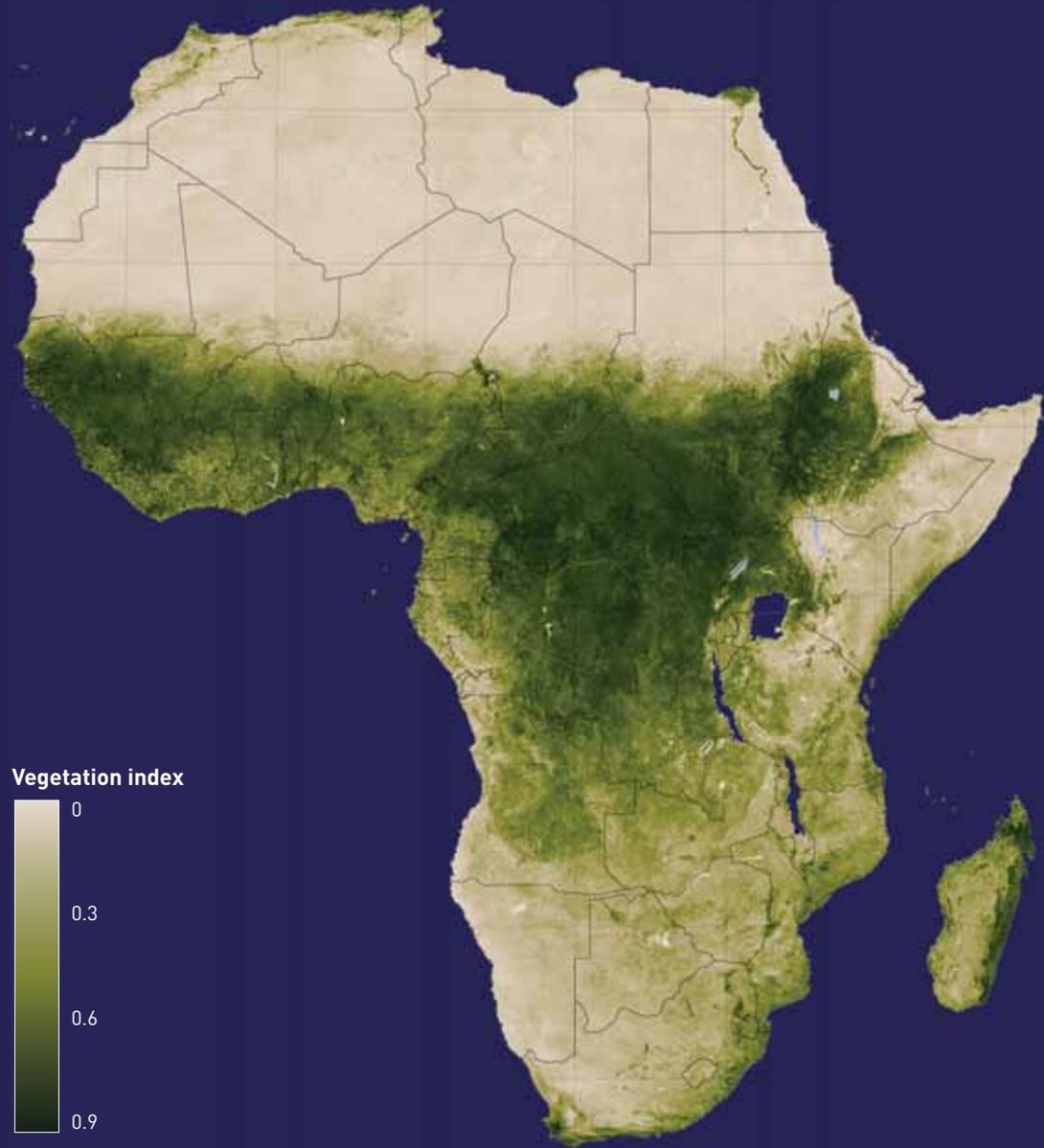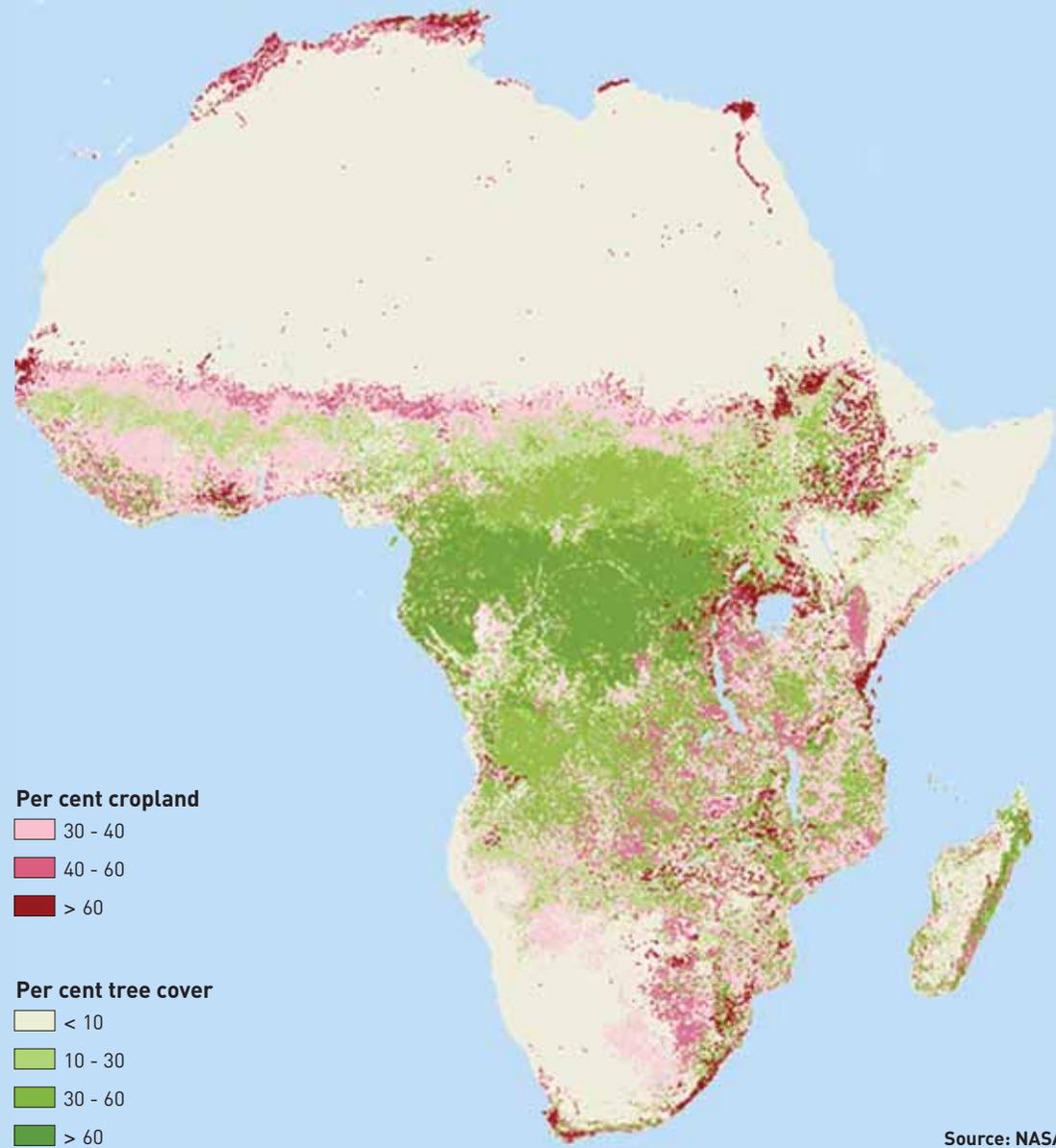
Source: NASA.
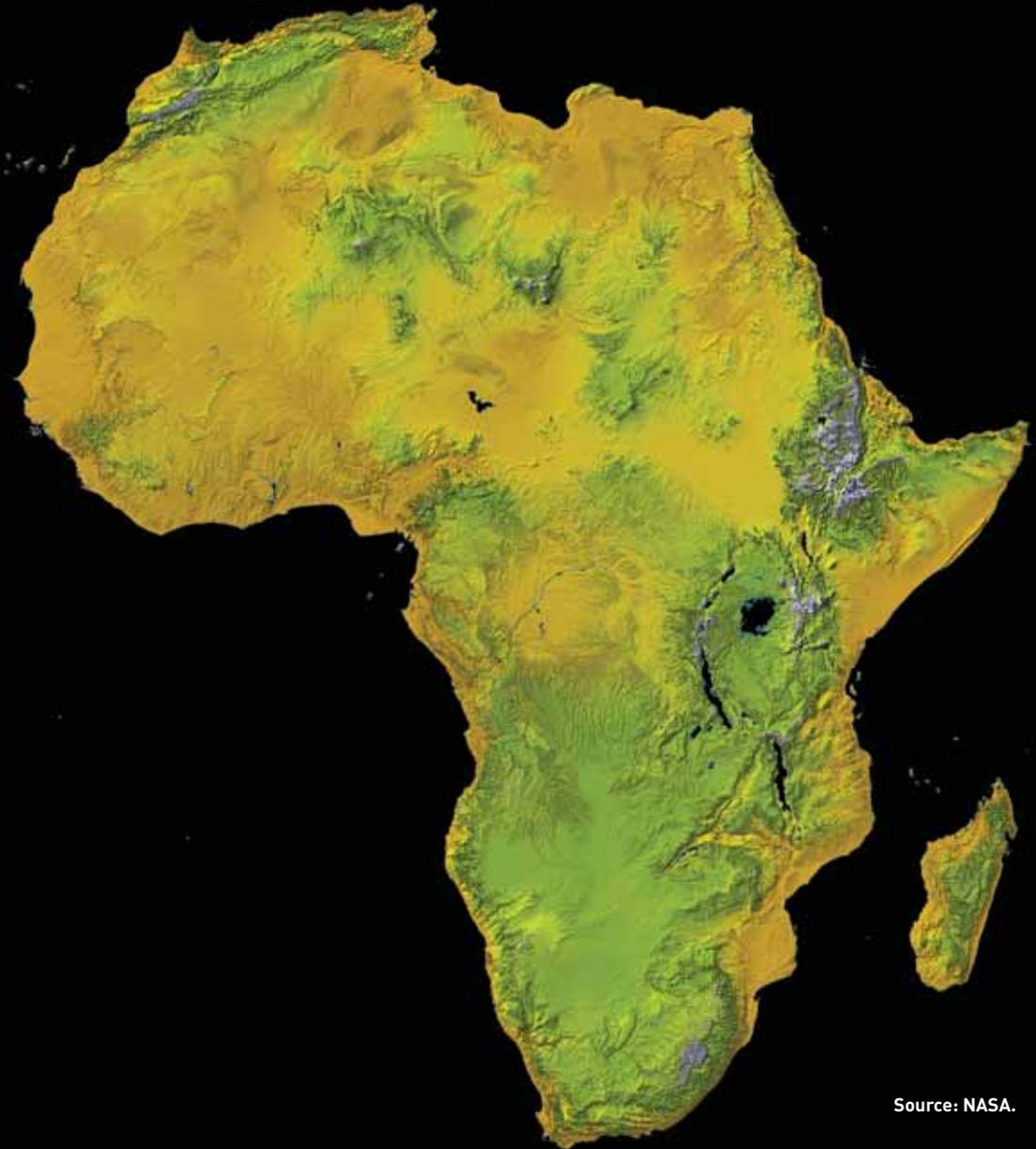
Elevation

Source: NASA.

Assessing protected areas
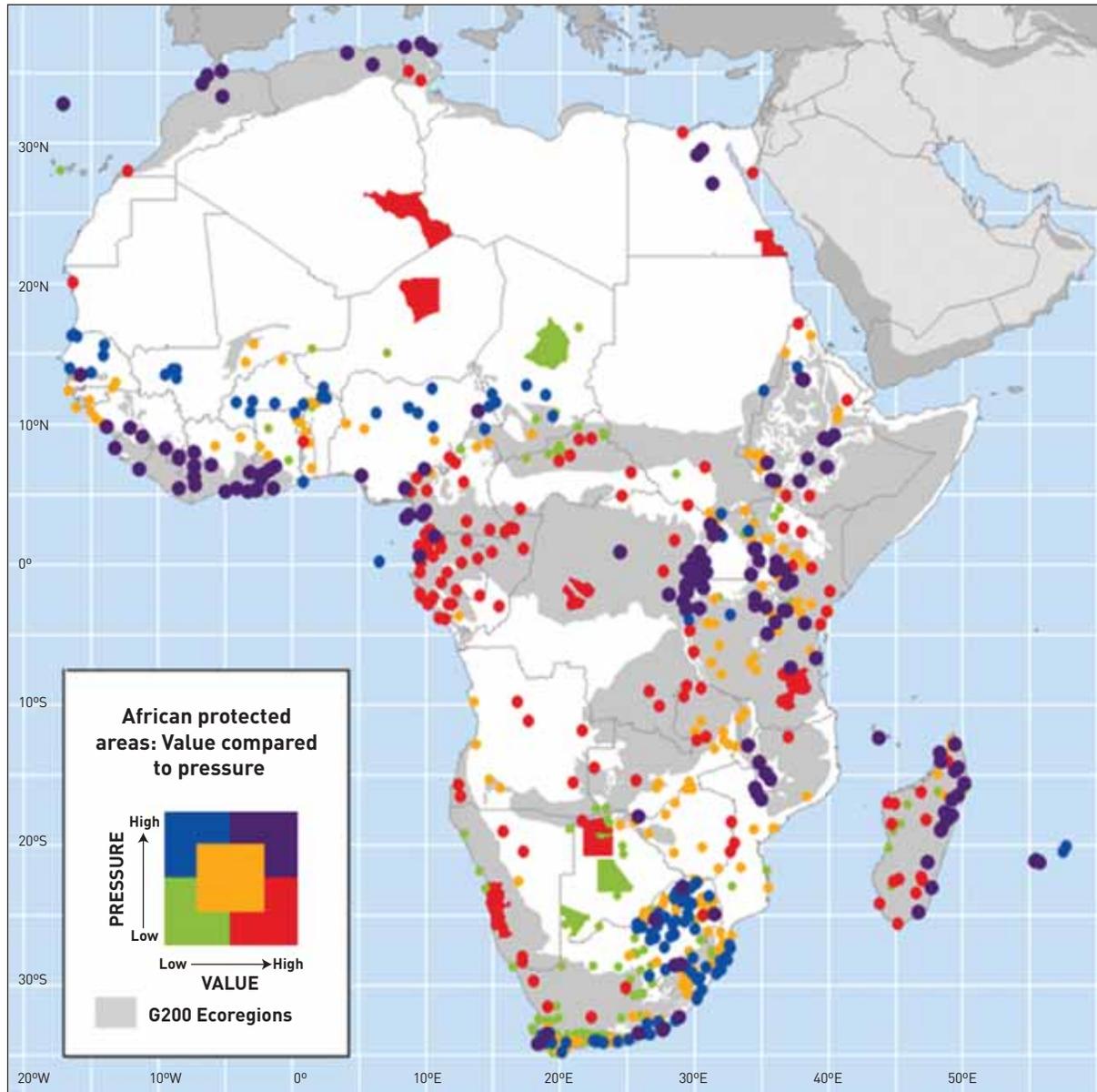
Based on the previous maps of protection status, vegetation coverage, elevation and other variables, indicators have been developed to score each protected area for the value of its biodiversity and the threats that it faces.

Informing decision making

Visual products that can be understood and interpreted by a wide range of end users can also be created and used to inform decision making on conservation actions and funding priorities. For example, protected areas in Ghana (left) can be contrasted with all protected areas in Africa (right) to determine their relative status. The coloured sectors of the graph depict indicators of biodiversity and habitat value (increasing to the right)

and indicators of pressure (increasing to the top). Ghana's protected areas are represented by the square symbols. The upper-right portion of the graphic identifies the protected areas – including several in Ghana – that have high biodiversity value and are also under high pressure.

Source: GEO BON.
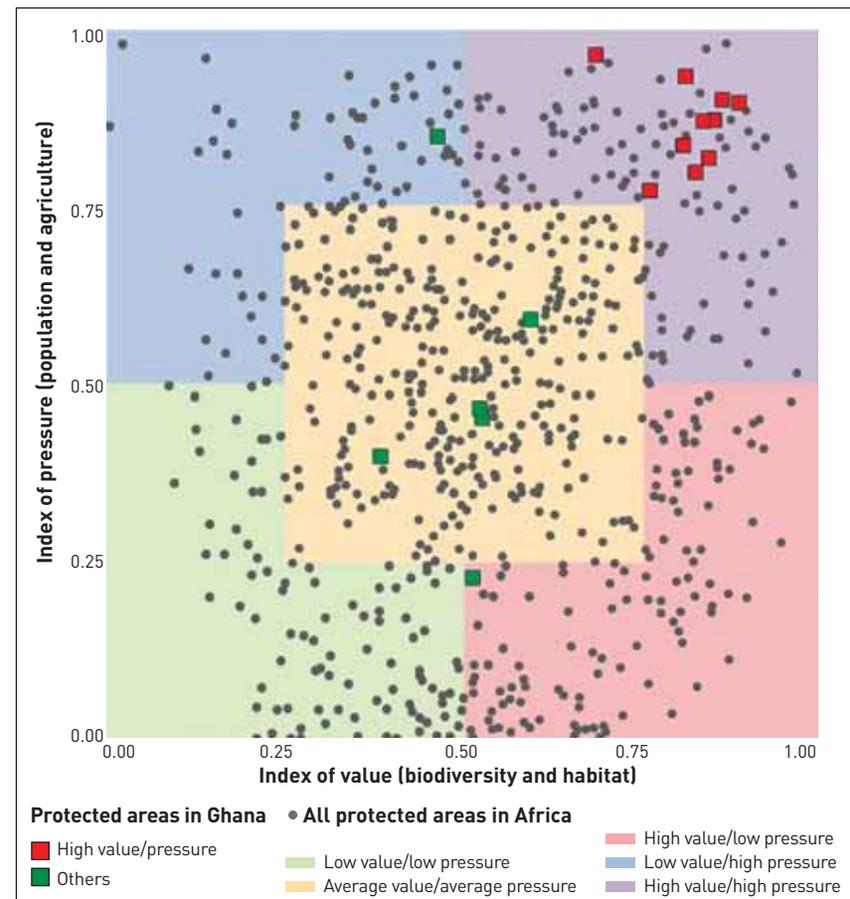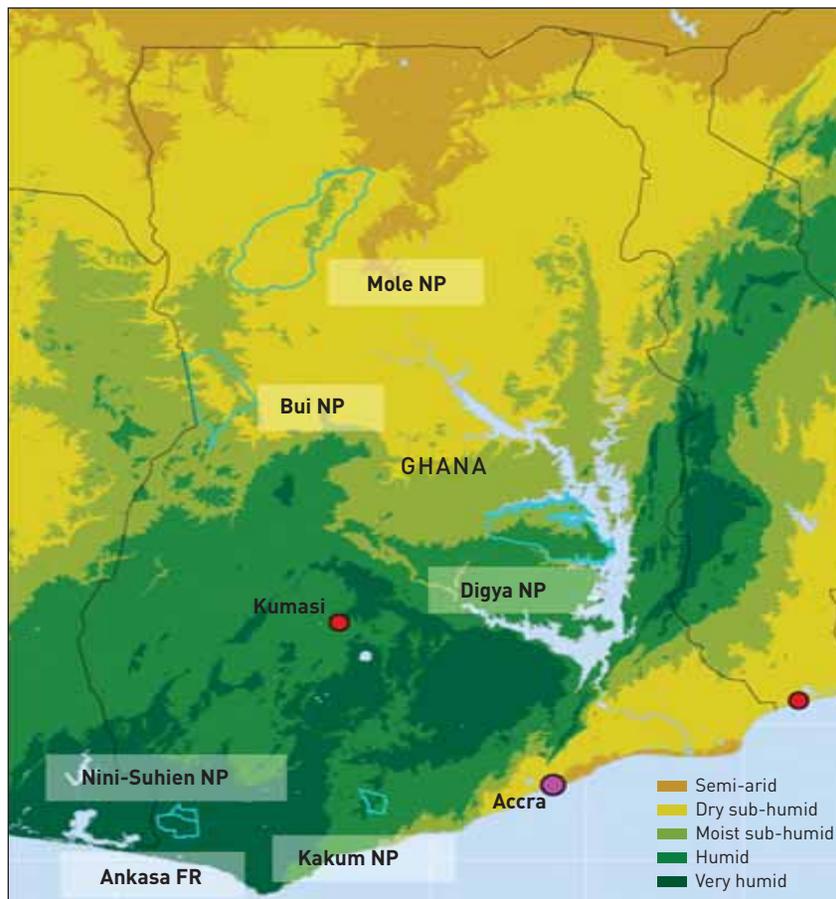
CONCLUSION: GLOBAL CHANGE AND TRENDS

The nine stories in this book have described how geoinformation can be used to support decision making in nine separate societal benefit areas. None of these issues, of course, exists in isolation. They are all interrelated: water supplies affect agriculture, ecosystems affect health, climate affects biodiversity, and so forth. Drawing these linkages together in order to monitor and understand the Earth system as an integrated system of systems is essential for addressing today's complex global challenges.

The Global Earth Observation System of Systems makes it possible to do this by assembling a large number of consistent, validated and interoperable data sets of Earth observations. These diverse data sets can be used to generate a snapshot of the Earth at a given moment in time. This snapshot can serve as a comprehensive baseline against which to measure global change over the years and decades to come. It can provide an essential point of departure for both retrospective analysis and ongoing monitoring.

The individual baselines presented in the following pages include parameters that do not change substantially over short periods of time but are fundamental for understanding global change. These relatively static data sets include elevation, soils and geology. Also featured are data sets for continuously changing variables that must be gathered at regular intervals. These data sets include surface reflectance, temperature, precipitation and vegetation.

The establishment of a comprehensive 2010 baseline for the Earth and its oceanic, atmospheric and terrestrial components would serve as a lasting contribution of the Earth observation community to international efforts to protect and manage the planet for future generations.

Source: NASA.

Topography
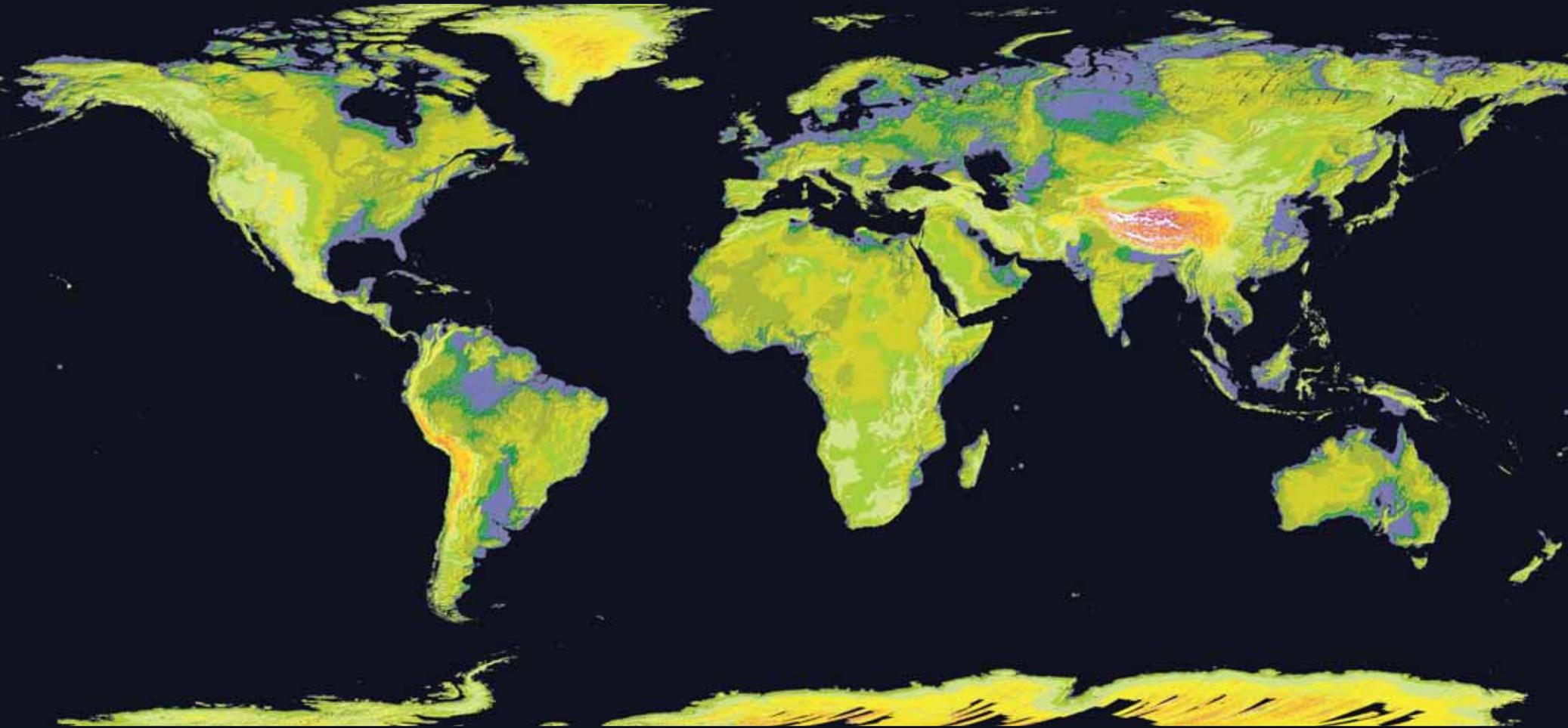
Global digital elevation models (DEMs) are created through the stereo-scopic analysis of multiple satellite images, in this case from the Advanced Spaceborne Thermal Emission and Reflection Radiometer (ASTER).

Digital elevation models are used to extract terrain parameters such as slope, aspect and elevation. They can be used as inputs for flood prediction models, ecosystem classifications, geomorphology studies and water-flow models.

Source: ASTER NASA.

Conclusion: global change and trends 117

The OneGeology initiative is working to make geological maps more widely available. It has assembled maps from geological surveys around the world.

Geological maps are used to identify natural resources, understand and predict natural hazards, and identify potential sites for carbon sequestration.

Source: OneGeology.

Surface reflectance
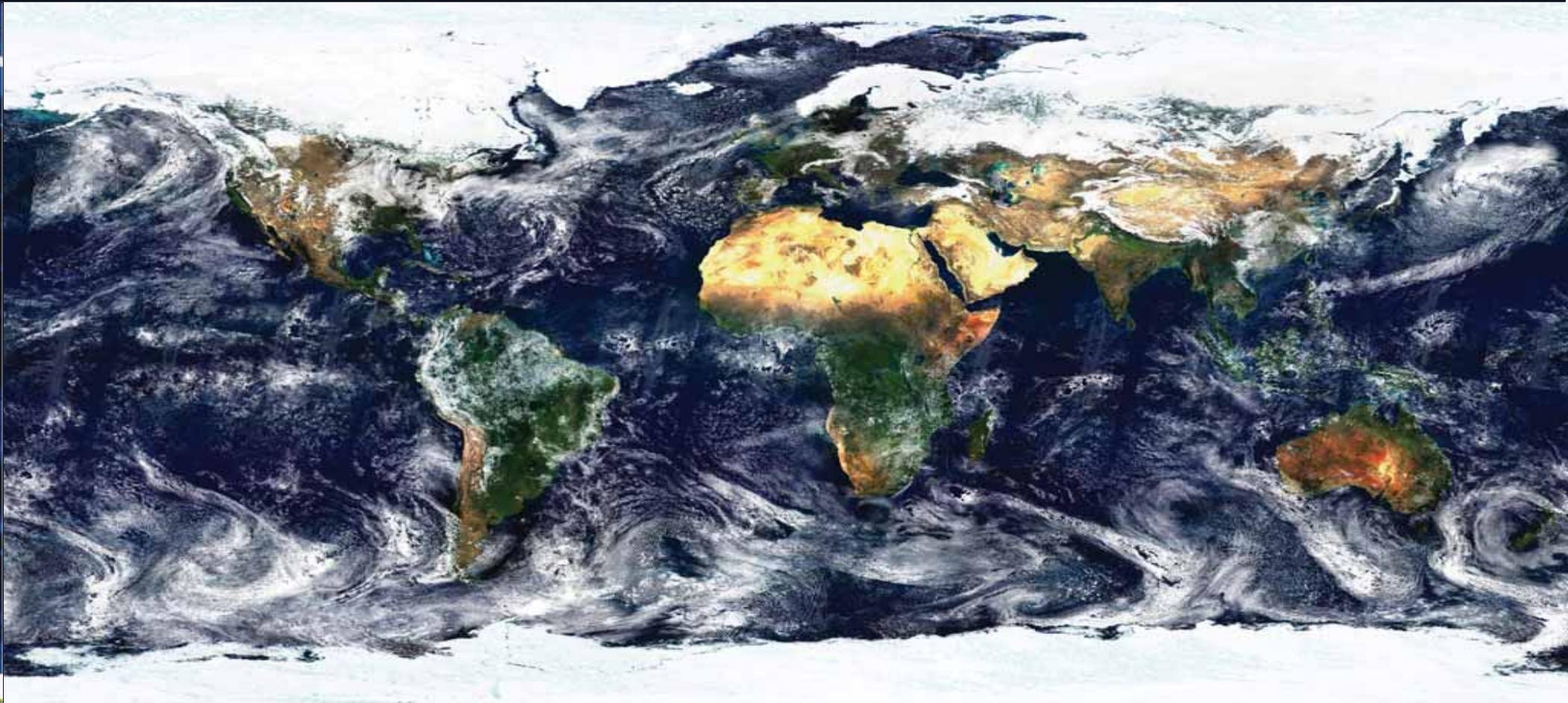
Surface reflectance images such as the map above provide an estimate of the surface spectral reflectance as it would be measured at ground level without the distortion of atmospheric effects. To achieve this, raw satellite data are corrected for the effects of atmospheric gases and aerosols and the positions of the satellite and the sun.

Surface reflectance data can be used for improving land-surface type classification, monitoring land change and estimating the Earth's radiation budget. These data can also serve as building blocks for other processed data such as vegetation indices and land cover classification.

Source: NASA/MODIS.

Vegetation index
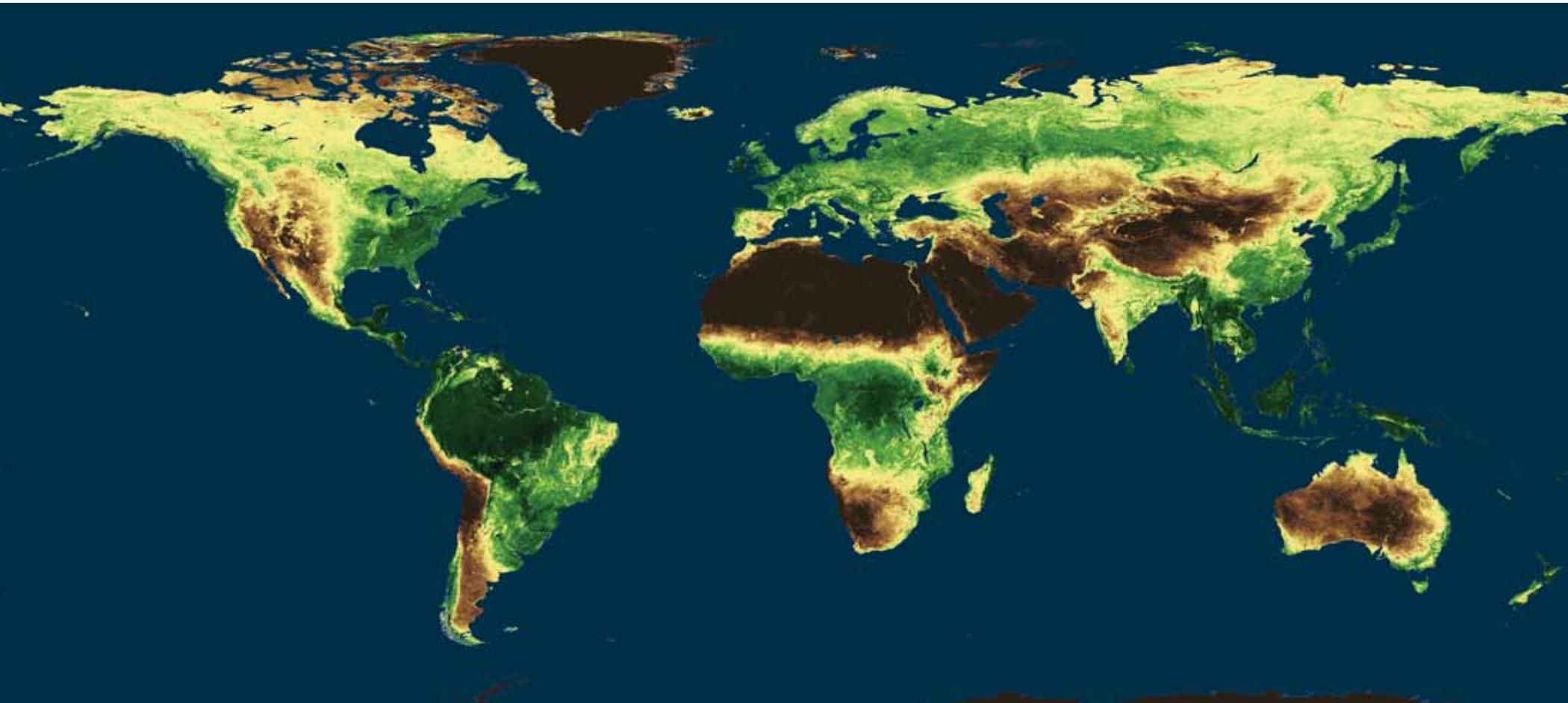
Vegetation indices are created from surface reflectance data. By combining spectral bands that are sensitive to chlorophyll absorption and cellular structure, it is possible to highlight variations in the type and density of forests, fields and crops.

Vegetation index data are used for a wide variety of applications, including agricultural assessment, land management, forest-fire danger assessment and drought monitoring. The data are also used as key inputs for land cover mapping, phenological characterization and many other applications.

Source: ESA/MERIS.

Land cover
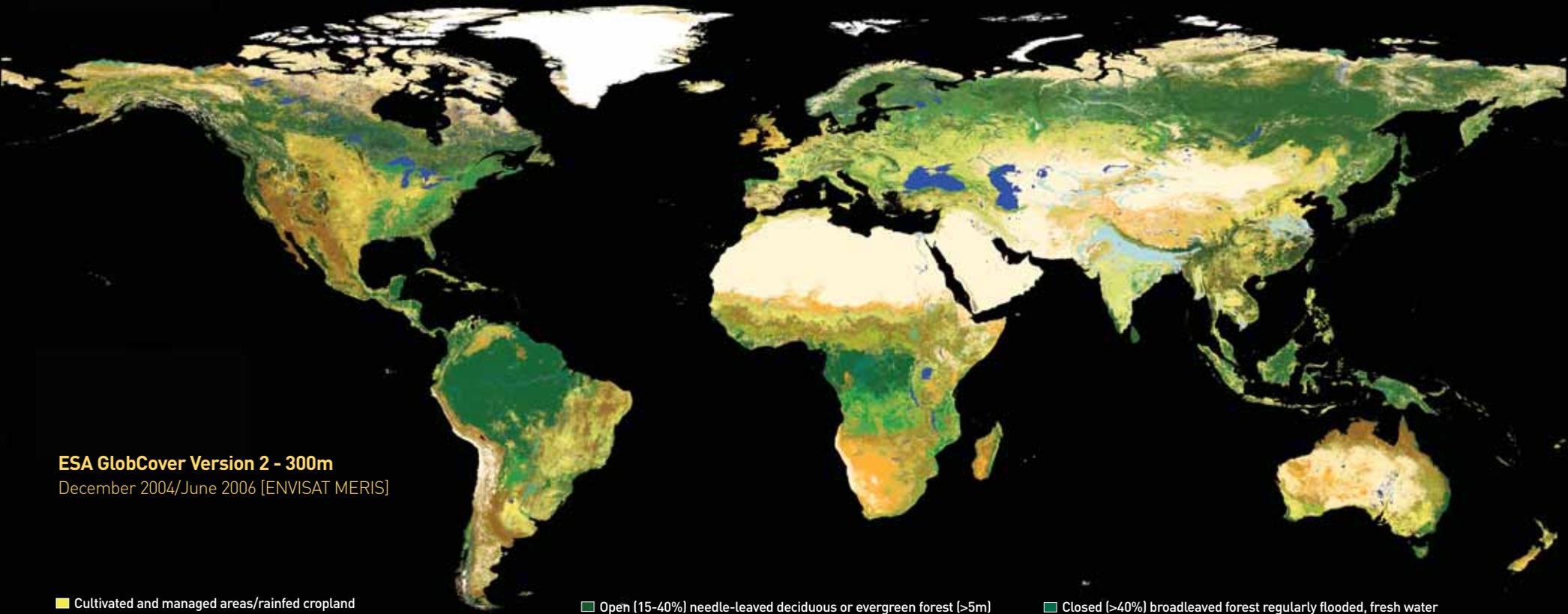
ESA GlobCover Version 2 - 300m
December 2004/June 2006 [ENVISAT MERIS]

- Cultivated and managed areas/rainfed cropland
- Post-flooding or irrigated croplands
- Mosaic cropland (50-70%)/vegetation (grassland/shrubland/forest) (20-50%)
- Mosaic vegetation (grassland/shrubland/forest) (50-70%)/cropland (20-50%)
- Closed to open (>15%) broadleaved evergreen and/or semi-deciduous forest (>5m)
- Closed (>40%) broadleaved deciduous forest (>5m)
- Open (15-40%) broadleaved deciduous forest/woodland (>5m)
- Closed (>40%) needle-leaved evergreen forest (>5m)
- Closed (>40%) needle-leaved deciduous forest (>5m)

- Open (15-40%) needle-leaved deciduous or evergreen forest (>5m)
- Closed to open (>15%) mixed broadleaved and needle-leaved forest
- Mosaic forest or shrubland (50-70%) and grassland (20-50%)
- Mosaic grassland (50-70%) and forest or shrubland
- Closed to open (>15%) shrubland (<5m)
- Closed to open (>15%) grassland
- Sparse (<15%) vegetation
- Closed (>40%) broadleaved semi-deciduous and/or evergreen forest regularly flooded, saline water

- Closed (>40%) broadleaved forest regularly flooded, fresh water
- Closed to open (>15%) grassland or shrubland or woody vegetation on regularly flooded or waterlogged soil, fresh, brackish or saline water
- Artificial surfaces and associated areas (urban areas >50%)
- Bare areas
- Water bodies
- Permanent snow and ice
- No data

Land cover data are produced from relevant data sets such as surface reflectance, temperature, vegetation indices, and other satellite products. Land cover data are created by statistically clustering together pixels with similar spectral and/or temporal patterns and then labelling them accordingly. Large-area land cover data are used for many applications, including change detection studies, agricultural and forest monitoring, and input to global circulation models and carbon sequestration models.

Source: ESA.

Tropical rainfall

Average of ALL AVAILABLE rainfall mm/dd (3B43) 1998 to 2008
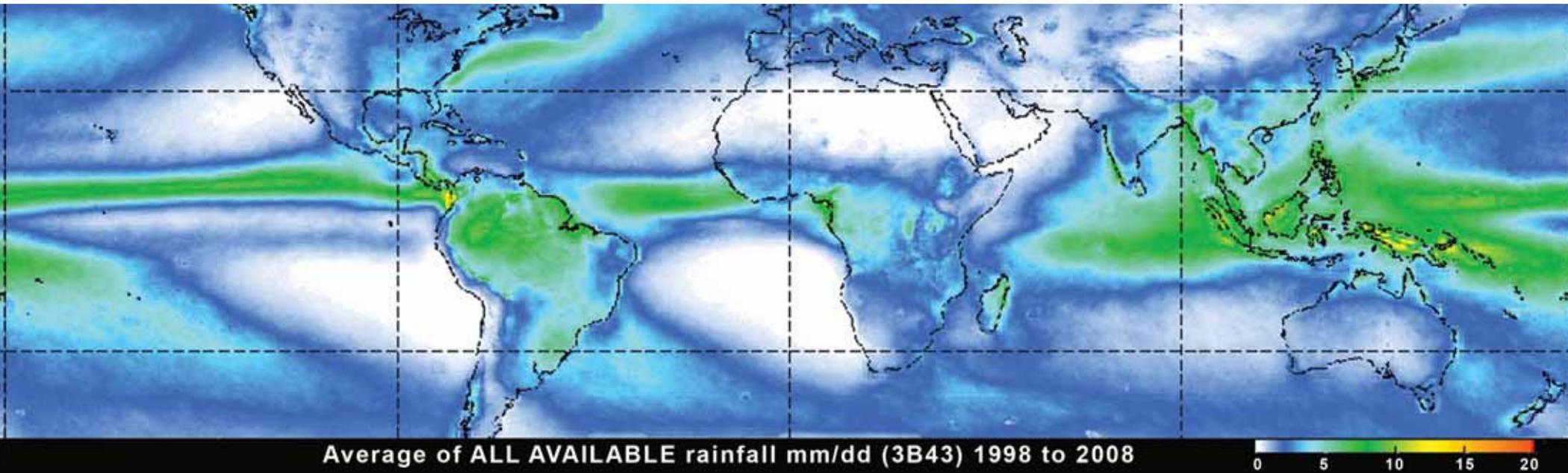
The Tropical Rainfall Measuring Mission (TRMM) is a research satellite designed to increase our understanding of the water cycle. Although rainfall has been measured for more than 2,000 years, it is still not known how much rain falls in many remote areas of the globe, in particular over the oceans. With the TRMM it is now possible to directly measure such rainfall rates. The TRMM satellite carries a passive microwave detector and an active spaceborne weather radar called the Precipitation Radar (PR).

TRMM data enhance the understanding of interactions between the sea, air and land. These interactions produce changes in global rainfall and climate. TRMM observations also help to improve the modelling of tropical rainfall processes and their influence on global circulation. This leads to better predictions of rainfall and its variability at various time scales.

Source: TRMM.

Forest height
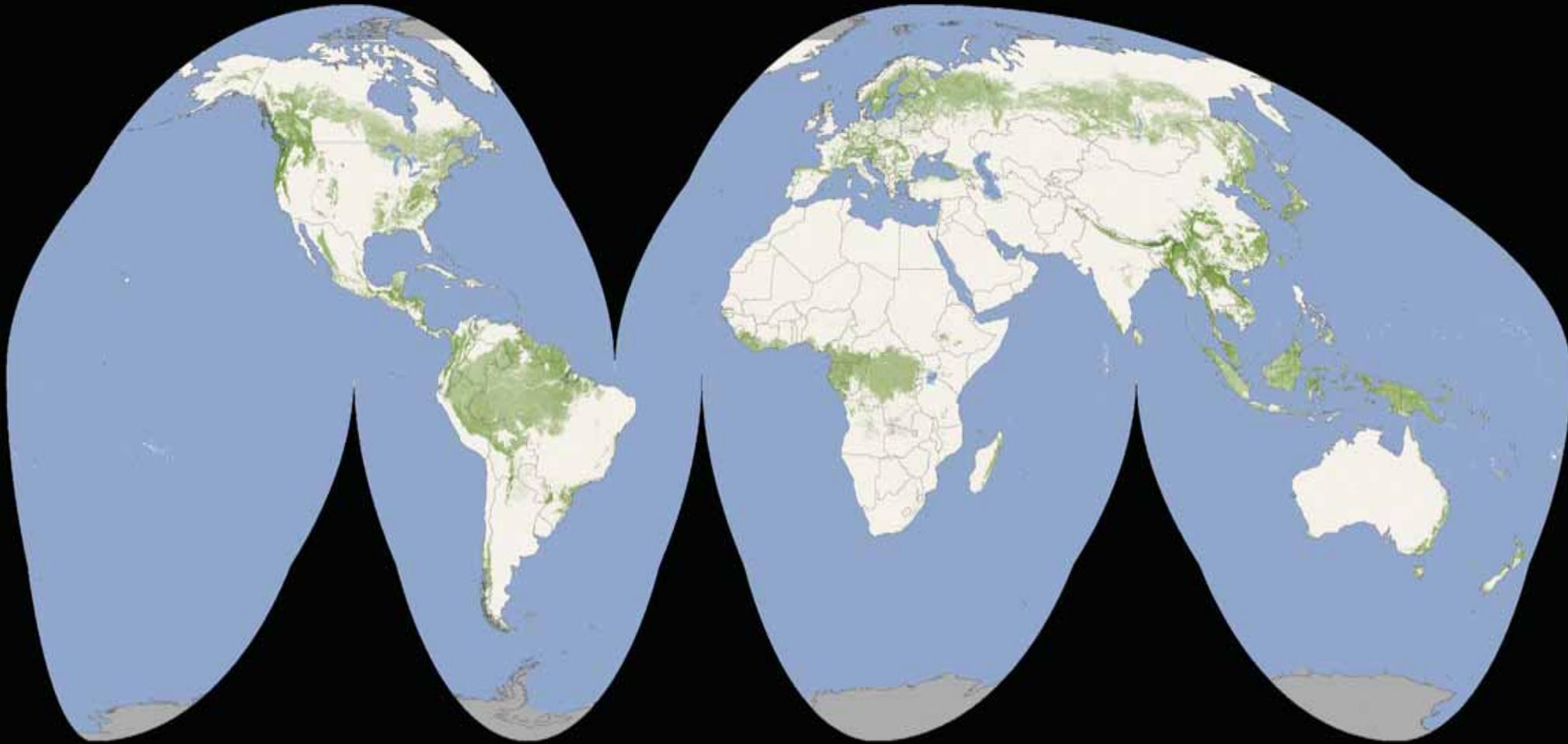
Many data serve as building blocks for more highly processed data sets. These "derived" data sets tend to require a substantial period of time to develop at a satisfactory level of quality.

    Scientists have used a combination of satellite data sets to produce a map that details the height of the world's forests. Data collected by multiple satellites are also being used to build an inventory of how much carbon the world's forests store and how fast carbon cycles through ecosystems and back into the atmosphere.

Sea surface temperature
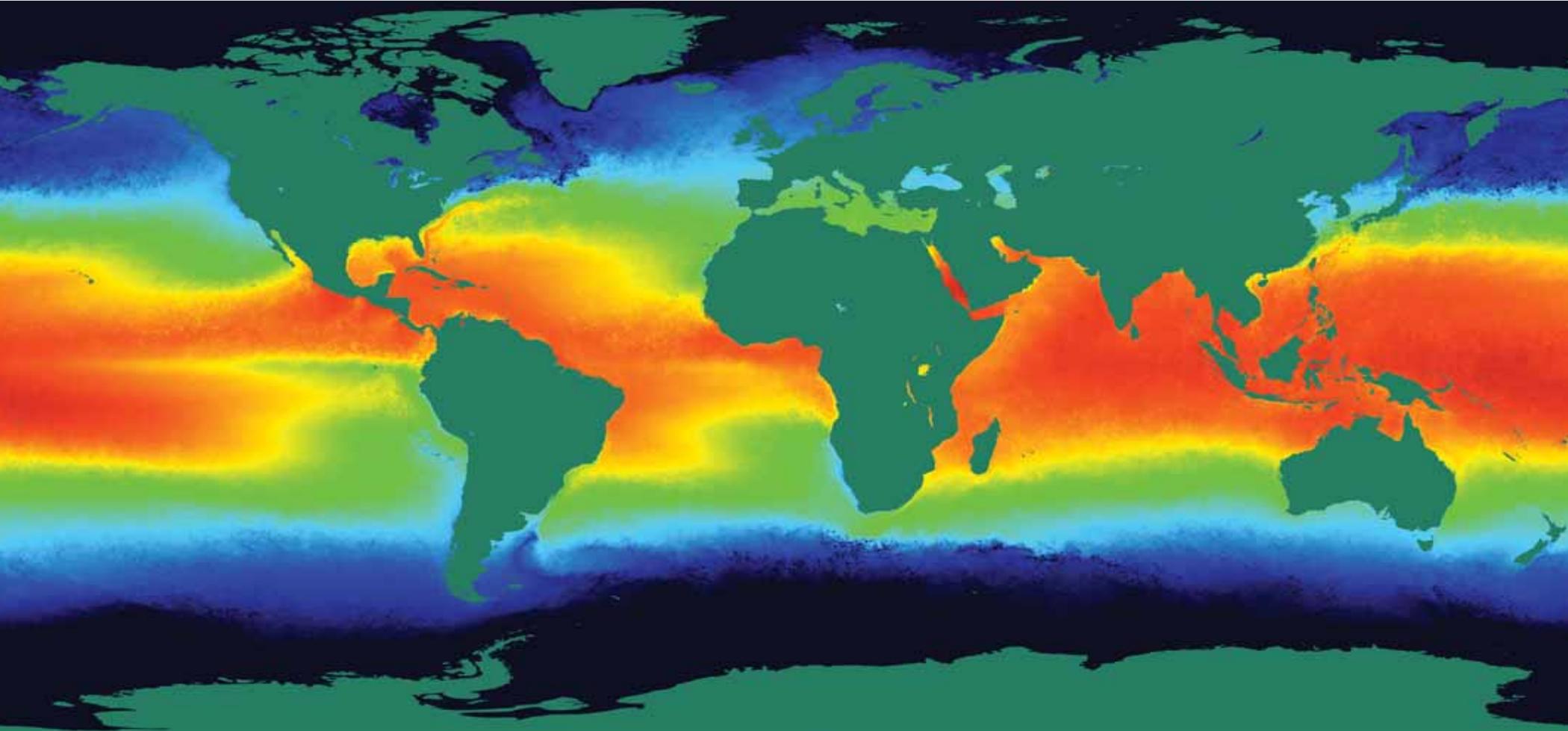
This sea surface temperature (SST) map was created from data collected by the Advanced Along Track Scanning Radiometer. The image is an average of all data available for one year. The colours represent the sea surface temperature, from dark blue (cold) to dark red (warm).

SST measures are used to monitor and predict the El Niño and La Niña phenomena. They are extensively used in hurricane and cyclone prediction and numerical weather and ocean forecasts.

Source: AASTR/ESA.